



**The Performance of Two-Stage Submerged Anaerobic Membrane Bioreactor
(2-sAnMBR) Coupling with Forward Osmosis Membrane (FO)
for Palm Oil Mill Effluent (POME)**

Wiparat Chaipetch

**A Thesis Submitted in Partial Fulfillment of the Requirements for the Degree of
Doctor of Philosophy in Environmental Engineering**

Prince of Songkla University

2023

Copyright of Prince of Songkla University



**The Performance of Two-Stage Submerged Anaerobic Membrane Bioreactor
(2-sAnMBR) Coupling with Forward Osmosis Membrane (FO)
for Palm Oil Mill Effluent (POME)**

Wiparat Chaipetch

**A Thesis Submitted in Partial Fulfillment of the Requirements for the Degree of
Doctor of Philosophy in Environmental Engineering**

Prince of Songkla University

2023

Copyright of Prince of Songkla University

Thesis Title The Performance of Two-Stage Submerged Anaerobic Membrane Bioreactor (2-sAnMBR) Coupling with Forward Osmosis Membrane (FO) for Palm Oil Mill Effluent (POME)

Author Miss Wiparat Chaipetch

Major Program Environmental Engineering

Major Advisor

.....
 (Asst. Prof. Dr. Watsa Khongnakorn)

Examining Committee:

.....Chairperson
 (Assoc. Prof. Dr. Chart Chiemchaisri)

Co-advisor

.....
 (Prof. Dr. Heran Marc)

..... Committee
 (Prof. Dr. Sumate Chaiprapat)

.....Committee
 (Prof. Dr. Heran Marc)

Co-advisor

.....
 (Prof. Dr. Sumate Chaiprapat)

.....Committee
 (Assoc. Prof. Dr. Charongpun Musikavong)

.....Committee
 (Assoc. Prof. Dr. Thaniya Kaosol)

.....Committee
 (Asst. Prof. Dr. Watsa Khongnakorn)

The Graduate School, Prince of Songkla University, has approved this thesis as Partial fulfillment of the requirements for the Doctor of Philosophy Degree in Environmental Engineering

.....
 (Asst. Prof. Dr. Thakerng Wongsirichot)
 Acting Dean of Graduate School

This is to certify that the work here submitted is the result of the candidate's own investigations. Due acknowledgement has been made of any assistance received.

..... Signature
(Asst. Prof. Dr. Watsa Khongnakorn)
Major Advisor

..... Signature
(Miss Wiparat Chaipetch)
Candidate

I hereby certify that this work has not been accepted in substance for any degree,
and is not being currently submitted in candidature for any degree.

..... Signature
(Miss Wiparat Chaipetch)
Candidate

ชื่อวิทยานิพนธ์	ประสิทธิภาพของระบบล้างปฏิกรณ์ชีวภาพเมมเบรนชนิดไร้อากาศแบบสอง ขั้นตอนร่วมกับกระบวนการฟอร์เวิร์ดออสโมซิสในการบำบัดน้ำทิ้งจาก โรงงานสกัดน้ำมันปาล์ม
ผู้เขียน	นางสาววิภารัตน์ ชัยเพชร
สาขา	วิศวกรรมสิ่งแวดล้อม
ปีการศึกษา	2565

บทคัดย่อ

น้ำทิ้งจากโรงงานสกัดน้ำมันปาล์มมีองค์ประกอบของสารอาหารที่หลากหลาย จึงเกิดแนวคิดของการบำบัดน้ำเสียดังกล่าว และการนำสารอาหารที่ได้จากการบำบัดกลับมาใช้ใหม่และกำจัดวิธีการนี้สามารถพัฒนาเทคโนโลยีการบำบัดน้ำเสียเข้าสู่ความยั่งยืนได้ ในการศึกษาได้ใช้ถึงปฏิกรณ์ชีวภาพเมมเบรนแบบไร้อากาศแบบสองขั้นตอนร่วมกับกระบวนการฟอร์เวิร์ดออสโมซิสของเมมเบรนเพื่อบำบัดน้ำทิ้งจากสกัดน้ำมันปาล์ม โดยมีการเปรียบเทียบประสิทธิภาพของเมมเบรนในเชิงพาณิชย์สองชนิดคือเมมเบรน thin film composite membrane (TFC) และ cellulose triacetate membrane (CTA) และใช้โซเดียมคลอไรด์เป็นสารละลายตั้งในความเข้มข้นที่แตกต่างกันคือ 2.0 3.0 และ 4.0 โมลาร์ การใช้วิธีนี้เพื่อต้องการแยกสารอาหารที่เป็นองค์ประกอบในน้ำทิ้งที่ผ่านการบำบัดด้วยระบบล้างปฏิกรณ์ชีวภาพเมมเบรนชนิดไร้อากาศแบบสองขั้นตอน ดำเนินการทดลองในระดับห้องปฏิบัติการโดยควบคุมการเดินระบบแบบต่อเนื่องเป็นเวลา 9 เดือน ด้วยอัตราการระบรทุกสารอินทรีย์ที่ 43 57 และ 99 กิโลกรัมซีโอดีต่อลูกบาศก์เมตรต่อวัน การก่อกำเนิดและสะสมของสารพอลิเมอร์นอกเซลล์ ทำให้มีการยึดเกาะของฟิล์มชีวภาพบนพื้นผิวของเมมเบรน พบว่าในระยะที่สองของการบ่อน้ำเสียเข้าสู่ปฏิกรณ์ ก่อเกิดปริมาณพอลิแซ็กคาไรด์และโปรตีนในชั้นเค้ก โดยอัตราส่วนของพอลิแซ็กคาไรด์ต่อโปรตีนเท่ากับ 0.26-0.28 การเพิ่มขึ้นอัตราการบ่อนสารอินทรีย์ให้สูงขึ้น ทำให้อัตราส่วนสารอาหารต่อจุลชีพในถังเพิ่มสูงขึ้นด้วย ขณะเดียวกันความเข้มข้นของสารพอลิเมอร์นอกเซลล์ และความดันในเมมเบรนเพิ่มสูงขึ้นด้วย กล่าวได้ว่าการเปลี่ยนแปลงค่าความดันระหว่างเมมเบรน ก่อให้เกิดกลไกของการยึดเกาะ การดูดซับ และการดักจับของพอลิเมอร์นอกเซลล์ ที่มีองค์ประกอบคือโปรตีน มาอุดตันในรูพรุนของเมมเบรน อย่างไรก็ตามปฏิกริยาการสร้างมีเทนในถังปฏิกรณ์ถูกยับยั้งโดยแบคทีเรียกลุ่มผลิตกรด เนื่องจากการสะสมของกรดไขมันระเหยง่ายในรูปกรดอะซิติกสูงถึง 30 เปอร์เซ็นต์ และทำการคำนวณอัตราส่วนของการเกิดไฮโดรไลซิสพบว่าสูงถึง 13.76 เปอร์เซ็นต์ ในเฟสสาม และทำให้เกิดการผลิตก๊าซมีเทนลดลง จากการเปรียบเทียบประสิทธิภาพของ

เมมเบรนชนิด TFC กับ CTA พบว่าเมมเบรนชนิด TFC มีผลการซึมผ่านของน้ำได้สูงในกระบวนการฟอร์เวรดออสโมซิส แต่สูญเสียฟลักซ์ของน้ำมากกว่าเมื่อเปรียบเทียบกับเมมเบรน CTA เพราะ CTA เกิดการแพร่กระจายของแคลเซียม ไอออน จึงก่อให้เกิดการเพิ่มขึ้นของชั้นเค้กบนชั้นผิวของเมมเบรน (active layer) นอกจากนี้กระบวนการฟอร์เวรดออสโมซิสสามารถกำจัดสารอาหารในน้ำทิ้งที่ผ่านการบำบัดแบบสองขั้นตอน โดยให้ประสิทธิภาพการกำจัดฟอสฟอรัสและแอมโมเนียได้สูงถึง 90-100 เปอร์เซ็นต์ ดังนั้น กระบวนการฟอร์เวรดออสโมซิสสามารถคัดแยกและนำสารอาหารกลับคืนได้ และลดต้นทุนของสารเคมี และสามารถลดสารอินทรีย์และสารอนินทรีย์ได้ อย่างไรก็ตาม สารอาหารจำพวกไนโตรเจน ฟอสฟอรัส และโปแตสเซียมเป็นปุ๋ยที่สำคัญสำหรับพืช ดังนั้นการผลิตเป็นปุ๋ยน้ำจึงเป็นทางเลือกที่ดี

Thesis Title	The Performance of Two-Stage Submerged Anaerobic Membrane Bioreactor (2-sAnMBR) Coupling with Forward Osmosis Membrane (FO) for Palm Oil Mill Effluent (POME)
Author	Miss Wiparat Chaipetch
Major Program	Environmental Engineering
Academic Year	2022

ABSTRACT

Palm oil mill effluent (POME) contains abundant nutrients. The concept of POME treatment and nutrient recovery/removal applied as a sustainable development of wastewater treatment technologies. Two-stage submerged anaerobic membrane bioreactor (2-sAnMBR) combining with forward osmosis membrane (FO) was used to treatment POME. Two types of membranes including a commercial thin film composite (TFC) and cellulose triacetate (CTA), and different concentration of draw solutions which used NaCl as draw solution that including 2.0M, 3.0M and 4.0M were adopted to investigate the separated of nutrient in the permeate two-stage sAnMBR. In this work, the long-term operational control of the two-stage sAnMBR maintained organic loading rate (OLR) of 43, 57 and 99 kgCOD/m³/day in 9 months continuous operation of lab-scale. The formation and accumulation of extracellular polymeric substances (EPS) cause the adherence of biofilms to surfaces membrane. The phase II of two-stage sAnMBR shown polysaccharide and protein content in the cake layer; the ratio of polysaccharide/protein (C/P) was 0.26-0.28. The increasing of OLR led to high F/M ratio meanwhile the EPS concentrate and transmembrane pressure (TMP) was increased. The evolution of TMP indicated that attachment mechanisms, adsorption, and entrapment of protein EPS occurred in the pores of membrane (clogging). Nevertheless, the methanogenesis activity in sAnMBR was inhibited by acidogenesis bacteria due to the accumulated of volatile fatty acid (VFA) that acetic acid was highest about 30% however the calculation of hydrolysis ratio found up to 13.76% in phase III. A high concentration of VFA can inhibit methanogenesis occurred the rising of OLR causing to low methane yield. TFC membrane exhibited higher water permeability in FO process but more loss of water flux in comparison with CTA; the diffusion of Ca₂⁺ ion in CTA, enhanced a cake layer formed on the membrane's active layer. Furthermore, the efficiency of nutrient removal by FO system reported phosphorus and ammonia up to 90-100% thus FO capability can recover nutrients and reduce chemical costs and it can decrease organic/inorganic substances. Moreover, the nutrients; nitrogen, phosphorus, and potassium were the most important of plant fertilizer so the best way to water fertilizer produce.

ACKNOWLEDGEMENT

First and foremost, to be acknowledged in this thesis is Asst. Prof. Dr. Watsa Khongnakorn, who offered and supported for me during project; she gave me patient, persevere, strength and spirit while encountering all the obstacles while completing this thesis. Under the processing of the edited thesis and wrote manuscript to be succeed, I would like to gratitude Prof. Dr. Heran Marc and the Institute European of Membranes (IEM), University Montpellier, UM2, CNRS, ENSCM, Montpellier, France.

Special thanks and appreciation to the Research and Researchers for Industries (RRI) funds and Tha Chang Palm Oil Industries, Co., Ltd. for their financial support to this research under contract number “PHD58I0056”. I would like to appreciate the Membrane Science and Technology Research Center (MSTRC) and Department of Civil Engineering, Faculty of Engineering, Prince of Songkla University for partial support of this for providing the numerous facilities to accomplish the research successfully. And thankful the Thailand Institute of Scientific and Technological Research (TISTR): Expert Centre of Innovative Materials; (INNOMAT) for supported the materials of membrane.

Successful completion of this research, I am indebted to my parents, husband, friend and my son for their care, support and sacrifices to finish my research successfully

Wiparat Chaipetch

CONTENTS

	Page
ABSTRACT (Thai language)	v
ABSTRACT (English language)	vii
ACKNOWLEDGEMENT	viii
CONTENTS	ix
LIST OF TABLES	x
LIST OF FIGURES	xi
LIST OF ABBREVIATION	xiii
LIST OF PAPERS	xvi
PAPER I Reprint was made permission from the publisher	xvii
PAPER II Reprint was made permission from the publisher	xviii
CHAPTER 1 INTRODUCTION	1
1.1 State of art	1
1.2 Objectives	4
1.3 Scope of work	4
CHAPTER 2 RESULTS AND DISCUSSION	6
2.1 Performances of High Rate Two-Stage AnMBR for Palm Oil Mill Effluent Treatment	6 6
2.2 Fouling Behavior in a High-Rate Anaerobic Submerged Membrane Bioreactor (AnMBR) for Palm Oil Mill Effluent (POME) Treatment	8 8
2.3 Thin film composite forward osmosis membrane for anti-fouling the nutrient from permeates of a two-stage submerged anaerobic membrane reactor (AnMBR)	11 11 11
CHAPTER 3 CONCLUSION REMARK	14
REFERENCES	16
SUPPLEMENTARY DATA OF PAPER I	22
SUPPLEMENTARY DATA OF PAPER II	26
APPENDIX I	30
APPENDIX II	46
APPENDIX III	62
VITAE	85

LIST OF TABLES

	Page
SUPPLEMENTARY DATA OF PAPER I	22
Table S1 Control hydrodynamic in sAnMBR	23
Table S2 The methodology and analyzation of VFA concentration and component	23
Table S3 The concentration of phenolic compound in POME	23
Table S4 Method and analysis of foulant and fouling	24
APPENDIX I	30
Table 1 Characteristics of raw palm oil mill effluent (POME) and inoculum (mean±standard deviation)	33
Table 2 Operating conditions of the anaerobic hydrolytic reactor (HR) and submerged anaerobic membrane bioreactor (sAnMBR) under mesophilic conditions (35°C ±5°C).	34
APPENDIX II	46
Table 1 Characteristics of palm oil mill effluent (POME) after treatment	48
Table 2 EPS substances and fouling parameters evaluated for each OLR	52
Table 3 Summary of FTIR spectra peak assigned for the samples	55
APPENDIX III	62
Table 1 The specification of CTA FO and TFC FO membrane	65
Table 2 Characteristics for FO experiment	73
Table 3 Comparative analysis of nutrient concentration (Na ⁺ , Ca ₂ ⁺ ,	74

LIST OF FIGURES

	Page
CHAPTER 1	
Figure 1 Scope of work	4
CHAPTER 3	
Figure 1 The concluding results	13
SUPPLEMENTARY DATA OF PAPER I	
Figure S1 Step of preparation POME and sludge for feed in the two-stage sAnMBR	25
Figure S2 Collection sample in two-stage sAnMBR	25
SUPPLEMENTARY DATA OF PAPER II	
Figure S1 The particle size of a) POME, b) Sludge, c) Effluent of HR reactor, d) Effluent of AnMBR and e) Completely mixed in AnMBR	27
Figure S2 FTIR spectra peak of (a) virgin and fouled membranes and (b) POME and EPS	28
Figure S3 FESEM of the virgin membrane (a: top surface, b: cross section, c: EDX element), fouled membrane in period I (d: top surface, e: cross section, f: EDX element), fouled membrane in period II (g: top surface, h: cross section, i: EDX element), and fouled membrane in period III (j: top surface, k: cross section, l: EDX element) with thickness scales.	29
APPENDIX I	
Figure 1 Lab-scale diagram of two-stage submerged anaerobic membrane bioreactor (sAnMBR). pHC: pH controller, TC: temperature controller, V1: hydrolytic reactor, V2&V3: anaerobic membrane bioreactor	33
Figure 2 Performance of hydrolysis reactors; a) TCOD, SCOD, and total VFA, b) VFAs and pH, and c) TS, VS, and TSS	37
Figure 3 The COD component in AnMBR system and the COD removal performance	38
Figure 4 COD mass balance for hydrolysis, acidogenesis, and methanogenesis ratio in the AnMBR	39
Figure 5 VFA concentrations and methane yields in AnMBR	40
Figure 6 The fouling rate and SMP concentration in AnMBR	41
APPENDIX II	
Figure 1 A diagram of the lab-scale submerged anaerobic membrane bioreactor (AnMBR)	50

LIST OF FIGURES (CONTINUED)

		Page
Figure 2	EPS characteristic: (a) composition and (b) specific EPS content as a function of HRT	51 51
Figure 3	Flux (a), F/M (b), and EPS (c) profiles compared to TMP during operational periods I, II and III	53 53
Figure 4	CLSM images of cake layer in AnMBR: period I (a,d), period II (b,e), and period III (c,f)	54 54
Figure 5	FTIR spectra of (a) virgin and fouled membranes and (b) POME and EPS in each period	55 55
Figure 6	FESEM of the virgin membrane ((a): top surface, (b): cross section, (c): EDX element), fouled membrane in period I (d): top surface, (e): cross section, (f): EDX element), fouled membrane in period II (g): top surface, (h): cross section, (i): EDX element), and fouled membrane in period III (j): top surface, (k): cross section, (l): EDX element)	56 56 56 56 56 56
Figure 7	AFM image of the (a) virgin membrane, (b) fouled membrane in period I, (c) fouled membrane in period II, and (d) fouled membrane in period III	57 57 57
Figure 8	Behavior of foulants in AnMBR for high-rate POME treatment	58
APPENDIX III		62
Figure 1	FO system diagram	65
Figure 2	The permeate flux versus TFC and CTA in FO filtration process for T-POME treated in different concentration of draw solution (a) 2M NaOH (b) 3M NaOH and (c) 4M NaOH	70 70 70
Figure 3	Nutrient removal efficiencies in FO filtration process with TFC membrane and CTA membrane in loading 1 (L1), loading 2 (L2) and loading 3 (L3)	72 72 72
Figure 4	Cross-section SEM micrographs of (A) CTA-HTI fouled membrane and (B) TFC aquaporin fouled membrane	76 76
Figure 5	SEM micrographs of the top-surface and cross-section modes for TFC virgin membrane and the element component by EDX of membrane	76 76 76
Figure 6	SEM micrographs of the top-surface and cross-section modes for TFC fouled membrane and the element component by EDX	76 76

LIST OF FIGURES (CONTINUED)

	Page
of membrane	76
Figure 7 SEM micrographs of the top-surface and cross-section modes for CTA virgin membrane and the element component by EDX	77
of membrane	77
Figure 8 SEM micrographs of the top-surface and cross-section modes for CTA fouled membrane and the element component by EDX	77
of membrane	77
Figure 9 The most important factors affecting the nutrient removal in the FO process	78
	78

LIST OF ABBREVIATION

AD	Anaerobic digestion
ACP	Amorphous calcium phosphate
AFM	Analyzed by atomic force microscopy
AnMBR	Anaerobic membrane bioreactor
C	Carbon
CH ₄	Methane
CLBR	Covered lagoon bioreactor
CLSM	Confocal laser scanning microscopy
COD	Chemical oxygen demand
CTA	Cellulose triacetate
DS	Draw solution
EPS	Extracellular polymeric substances
EDS	Energy dispersive x-ray spectrometer
FESEM	Field emission scanning electron microscope
FO	Forward osmosis
FOG	Fat, oil and grease
FS	Feed side
FTIR	Fourier transform infrared spectroscopy
HCl	Hydrochloric acid
HNO ₃	Nitric acid
HR	Anaerobic hydrolytic reactor
HRT	Hydraulic retention time
Mg	Magnesium
MLSS	Mixed liquor suspended solids
MLVSS	Mixed liquor volatile suspended solids
MWCO	Molecular weight cut-off
Na	Sodium
NaCl	Sodium chloride
NaHCO ₃	Sodium bicarbonate
O	Oxygen
OLR	Organic loading rates
ORP	Oxidation reduction potential
POME	Palm oil mill effluent
POMS	Palm oil mill sludge
PS	Polysaccharides
PT	Proteins
SCOD	Soluble chemical oxygen demand
SEM-EDX	Scanning electron microscope and energy dispersive x-ray
Si	Silicate
SMP	Soluble microbial products
SRT	Sludge retention time
SS	Suspended Solids

LIST OF ABBREVIATION (CONTINUED)

2-sAnMBR	Two-stage submerged anaerobic membrane bioreactor
TCOD	Total chemical oxygen demand
TFC	Thin-film composite
TMP	Transmembrane pressure
TS	Total solids
TSS	Total suspended solids
VFA	Volatile fatty acids
VS	Volatile solids
VSS	Volatile suspended solids

LIST OF PAPERS

I. W. Chaipetch, W. Khongnakorn, C. Yirong, J. Boonkan and M.Heran. (2022) Performances of High Rate Two-Stage AnMBR for Palm Oil Mill Effluent Treatment. *BioResource*,17(2), 3398-3412.

<https://doi.org/10.15376/biores.17.2.3398-3412>

II. W. Chaipetch, A. Jaiyu, P. Jutaporn, M. Heran and W.Khongnakorn. (2021) Fouling Behavior in a High-Rate Anaerobic Submerged Membrane Bioreactor (AnMBR) for Palm Oil Mill Effluent (POME) Treatment. *Membrane*,11, 649.

<https://doi.org/10.3390/membranes11090649>

PAPER I
Reprint was made permission from the publisher

North Carolina State University is a land-
Grant university and a constituent institution
of The University of North Carolina

Department of Forest Biomaterials

NC STATE UNIVERSITY

College of Natural Resources
Campus Box 8005
Biltmore Hall
Raleigh, NC 27695-8005
919.515.5807
919.515.6302 (fax)

Paper Science & Engineering	919.515.2888
Wood Products	919.515.3181
WP Extension	919.515.5637

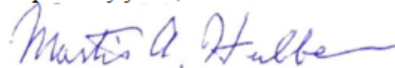
November 8, 2022

To whom it may concern:

Authors who publish in the journal *BioResources* retain copy rights to their work, in whole or in part. This means that the authors automatically have the right to include their work (or any part of it) in a thesis or for other purposes that they may choose. As a courtesy, we just ask that the version published in *BioResources* be cited in such cases.

The journal *BioResources* is provided as a service of North Carolina State University, College of Natural Resources, Department of Forest Biomaterials. The focus of the journal is the science of lignocellulosic materials, related chemicals, and various applications of these. Published articles and other information are available at the journal's website, <https://bioresources.cnr.ncsu.edu/> (alias site: <http://www.bioresources.com>). Authors retain copy rights to everything that is published in the journal.

Respectfully yours,



Martin A. Hubbe, Co-Editor
BioResources
Department of Wood & Paper Science
NC State University
hubbe@ncsu.edu
(919) 513-3022

PAPER II

Reprint was made permission from the publisher

The screenshot shows the article page on the MDPI website. The URL is [mdpi.com/2077-0375/11/9/649](https://www.mdpi.com/2077-0375/11/9/649). The article title is "Fouling Behavior in a High-Rate Anaerobic Submerged Membrane Bioreactor (AnMBR) for Palm Oil Mill Effluent (POME) Treatment". The authors listed are Wiparat Chalpech, Arisa Jaiyu, Panitan Jutaporn, Marc Heran, and Watsa Khongnakorn. The article is categorized as "Open Access Article". The journal is "membranes". The page includes a navigation menu on the left with options like "Submit to this Journal", "Review for this Journal", and "Edit a Special Issue". The article overview section lists "Abstract", "Open Access and Permissions", "Share and Cite", "Article Metrics", and "Order Article Reprints". The article versions, related info links, and more by authors links are also visible. The article is published in Membranes 2021, 11(9), 649.

Open Access Article

All articles published by MDPI are made immediately available worldwide under an open access license. No special permission is required to reuse all or part of the article published by MDPI, including figures and tables. For articles published under an open access Creative Common CC BY license, any part of the article may be reused without permission provided that the original article is clearly cited.

CHAPTER 1

INTRODUCTION

1.1 State of art

The industrial processing of oil palm in Thailand is expanding rapidly that plays significant role in Thailand economy. Thai Office of Agricultural Economics reported Thailand accounted for 3.8% of the global total Palm Oil production in 2021. In the other hand, growth rate of oil palm business led to an important source of wastewater is palm oil mill effluent (POME) and palm oil mill sludge (POMS). The increasing demand for the consumption of edible oils and energy (biodiesel) led to the primary growth of the palm oil industry; thus, it will be causing to higher POME. POME has a highly concentrated pollutant that significantly impacts the environment. In contrast, POME has a high potential for being convert into an alternative renewable energy source. The biological process used to treat POME that shown in anaerobic digestion (AD) which decreases treatment costs by increasing the digestion rate. However, the anaerobic system has an alternative for responding to many research types that classify one and two-stage. In addition, the advantage of two-stage AD for optimal conditions for each group of microorganisms, which higher methane production. Furthermore, the COD removal efficiency is 82-96 percent of AD, leading to increased biogas production and highly CH₄ yield [1,2]. On the other hand, Abdurrahman et al [3] applied AnMBR for POME treatment with a high percentage of COD removal 96.6-98.4 percent for treating POME. The efficiency of AnMBR was higher biogas production that brought to higher CH₄ yield when compared with AD.

Anaerobic membrane bioreactor (AnMBR) is biotechnology reactor that combined both anaerobic digestion and membrane filtration. AnMBR is also applied as an alternative treatment to high strength or hardly biodegradable to obtain the high-water quality and renewable energy as POME. In addition, the advantages of AnMBR are high biomass concentrations, high organic loading rates, excellent effluent quality, low sludge production, a small footprint, and net energy production [4]. Therefore,

integrating anaerobic membrane treatment in the form AnMBR can help to control the growth rate of anaerobic microbial and biomass retention [5] and favors the maintenance of slow growth microorganisms such as methanogens. However, the methanogenic bioreactor can be coupled with a membrane filtration system in a two-stage anaerobic digestion system. The reaction of acidogenesis in the first stage could prevent acidogenesis growth in the methanogenic bioreactor, enhancing sludge properties and filtration performance [6,7,8]. Generally, the external configuration is higher flux, easier cleaning and replacement of membrane but high energy consumption. The submerged configuration or named submerged anaerobic membrane reactor (sAnMBR) is lower energy consumption by placing the membrane module and wastewater into the mixed in reactor. The characterization of fouling phenomena was focused in sAnMBR. Several pieces of research showed the process of decreasing and controlling membrane fouling in AnMBR, including pretreatment of the feed water; improvement of the membrane properties; and optimization of the hydrodynamic conditions by air sparging, liquid recirculation and crossflow [9,10,11]. Moreover, hydrodynamic conditions and increasing of shear stress are the main point in membrane fouling mitigation. Wang et al [12] presented small flocs from sludge caused a high membrane fouling rate. Chen et al [13] and Martin-Garcia et al [14] reported the solid and colloidal organics are adsorbed and biodegraded inside the granular sludge led to less membrane fouling. The effect of coagulation on the aggregation of fine particles to accumulate on the top of the membrane surface (cake layer) due to inertial and gravitational forces [11]. The cake layers can be formed rapidly within 1 hour, making the effluent suspended solids (SS) concentration [15,16,17] which the adsorption, deposition, and accumulation process [18]. The affected factor of fouling in the membrane that was foulant such as sludge, extracellular polymeric substances (EPS), soluble microbial products (SMP), organic and inorganic particles, and the membrane properties, such as structural properties and membrane surface properties (e.g., surface roughness and surface functional groups, etc.).

Forward osmosis membrane (FO) is the separation system by a semi-permeable membrane that operating based on osmotic pressure; low and high osmotic pressure in feed solution and draw solution, respectively. FO has been used for treat the various

complex wastewater and wastewater reclaim the for recovery. The several advantage of FO; operates at very low pressure, simply adequate to circulate the fluids, and the natural osmotic pressure in the draw solution pulls water through the membrane, leaving solids and foulants behind in the concentrated feed solution. Different materials were used for FO membranes. Cellulose triacetate (CTA) is the most commonly used material for FO systems. The characteristics of CTA were found to be highly resistant to chlorine and mostly unsusceptible to the adsorption of mineral and fatty oils, including petroleum [19]. CTA is less sensitive to thermal, chemical, and biological degradation. New generation, a commercial thin-film composite (TFC) membrane was reported superior to CTA [20]. TFC membrane consist with a thin, selective polyamide active layer on a porous supporting layer that presented higher water permeability, good solute rejection to sodium chloride and stability at broader pH 2-12 while it can be found at pH 3-8 in CTA membrane. The hydrophilic nature of cellulose renders these membranes readily wettable. Thus, CTA membranes can simultaneously achieve high water permeability and excellent fouling resistance [21]. The higher resistant to biodegradation and hydrolysis for TFC than CTA [22,23]. In addition, thin and highly porous supporting layer of CTA and TFC membranes which caused to reduce the ICP encountered in FO applications [24,25].

From the literature reviews above, this research aims to contribute to the development of two-stage sAnMBR technology to study how different loadings of organic and constant solid retention time will affect biological activities in two-stage sAnMBR. The performance of this system was examined in terms of COD removal, CH₄ yield, VFA and biogas production and their composition through the continuous treatment of POME and the important factor that show performance of sAnMBR filtration and fouling mechanisms. Furthermore, two-stage sAnMBR coupled with FO system was conducted in lab scale. FO process was studied of effecting in the different membrane materials and draw solution on the FO fouling. The widely use fir TFC and CTA membranes was used in FO system and the identification of factors that it can be caused to fouling mechanisms by comparing the performance of filtration. The performance of material filtration consists of salt rejection rate, water flux and reverse solute flux. The key-point of fouling mechanisms was discussed the influence of soluble

microbial products (SMP), extracellular polymeric substances (EPS) and the membrane properties, such as structural properties and membrane surface properties (e.g., surface roughness and surface functional groups etc.) was measured on AnMBR. Fouling of membrane can be broadly classified into backwashable or reversible and non-backwashable or irreversible which based on the adhesive strength of particles to the membrane surface. The physical and mechanical cleaning process can be removed a reversible foulants such as filter back flushing, ultrasonic, rotary or vibratory shear enhanced. On the other hand, this process cannot eliminate the irreversible foulants which have to use the chemical method for removing irreversible foulants [26-30].

1.2 Objective

1.2.1 The effects of organic loading rate increasing on two-stage sAnMBR performance.

1.2.2 The comparison and identify of the factors that is causing to particles fouling and nutrient rejection of TFC and CTA membrane in different draw solution concentration and loading.

1.2.3 The optimum concentrate of NaCl in 2, 3 and 4 M for draw solution in FO process

1.3 Scope of work

POME wastewater and sludge samples were collected from a covered lagoon bioreactor (CLBR) in the Surat Thani palm oil factory, At the beginning, wastewater and seed sludge were added to the reactor in a 1:1 (v/v) proportion. Then, two-stage anaerobic bioreactor that it consisted of an anaerobic hydrolytic reactor (HR) and submerge anaerobic membrane bioreactor (sAnMBR). Step of preparation POME and sludge for feed in the two-stage sAnMBR shown in **Supplementary data of paper I (Figure S1 and Figure S2)**. However, this inoculum has been acclimatized after step feeding with 10% of POME concentration during four weeks in order to enhance sAnMBR's startup success. Lastly, FO experiment was set up to treated the permeate from Two-stage sAnMBR with CTA and TFC membrane in the different of draw

solution concentration 2M, 3M and 4M in different OLR feeding. The scope of work in **Figure 1**.

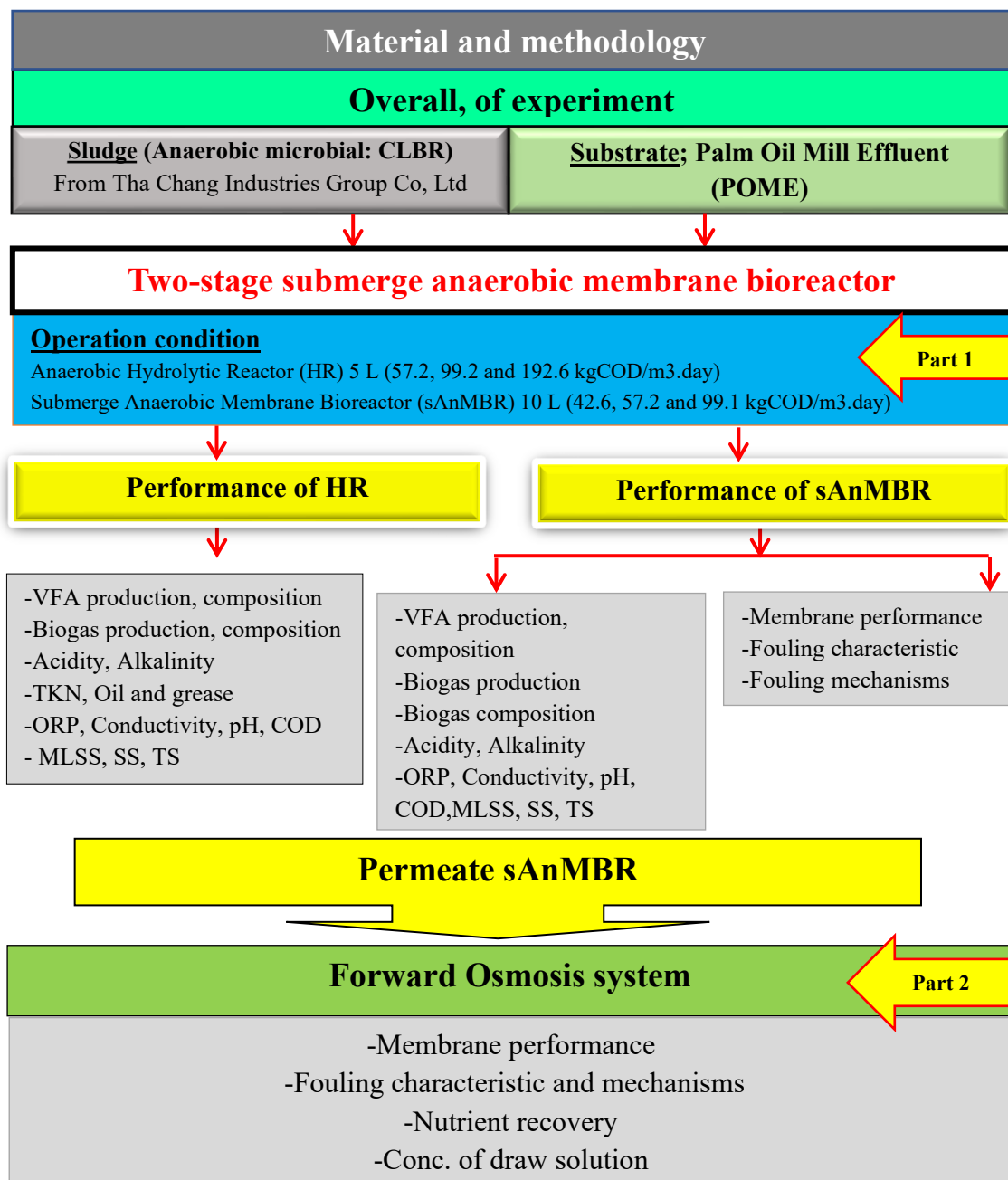


Figure 1 Scope of work

CHAPTER 2

RESULT AND DISCUSSION

2.1 Performances of High Rate Two-Stage AnMBR for Palm Oil Mill Effluent Treatment

Two-stage submerged anaerobic membrane bioreactor (2-sAnMBR) was used as alternative method for treating palm oil mill effluent (POME) from Tha Chang Palm Oil Industries, Co., Ltd., Surat Thani in Thailand which studied of the performances of treatment. The POME and sludge were prepared before feed in the tank shown in **Figure S1**. It consisted of an anaerobic hydrolytic reactor (HR) 5 L and submerge anaerobic membrane bioreactor (sAnMBR) 10 L which made of polysulfone hollow fibers with a 0.025 m² area. The POME was fed in HR with different loading (L1, L2 and L3) 43, 57 and 98 kgCOD/m³.day. While the effluent from HR was taken for treatment in sAnMBR in 43, 57 and 99 kgCOD/m³.day with internal recirculation rate from buffer tank in 1.8, 2.8 and 5.5 L/day that shown in **Figure S2**. The PSf hollow fibers were fixed only at the bottom and operated in an outside-in flow under a vacuum pressure in the range of 0.15–0.25 bar, which was supplied by a peristaltic pump. The TMP at the head of the module was measured by the vacuum pressure gauge. However, the operating pH of HR and sAnMBR were kept constant at 4.3± 0.3 and 7.2 ± 0.2, respectively with adjustment of 2 M HCl or NaHCO₃ solution. The ORP and pH were recorded daily in both HR and 2-sAnMBR tank. Samples were collected three times per week to analyze the TCOD, SCOD, TSS, TS, VS, VSS, and alkalinity, following the standard methods. Moreover, the VFA components and biogas was analyzed also. The volume of biogas production was measured via a gas counter and the composition of the biogas was measured via gas chromatography. The operating conditions of HR and sAnMBR was kept at mesophilic condition (35±5°C). Surface morphology, roughness and the major functional groups of biopolymers in the membrane foulants was analyzed at the end of operation period. In case control the fouling by hydrodynamic; (i) gas sparking, (ii) increase OLR and (iii) recirculation liquid in sAnMBR shown in **Table S1**.

The effected of increasing of OLR in HR for L1, L2 and L3 found the TCOD of the influent was increased. In contrast, hydrolysis processing occurred that led to the SCOD of the influent tended to be slightly increased. Kim et al. [31] reported the increasing of SCOD through solubilization or breaking down the larger molecules into smaller molecules or both in the digestion. The results can demonstrate the activity of microbes convert the organic compounds into volatile acids, as shown by the rising in the total VFAs. In case VFA concentration and composition was analyzed by titration method and gas chromatography that show in **Table S2**. Moreover, the increasing of total volatile fatty acids that can support the growth of acidogenesis microorganisms (L2 in HR). However, in L2 can showed the process of hydrolysis and acidogenesis that convert the organic compound (TCOD) to carbon dioxide and hydrogen. The main

of VFAs was found in term acetic acid (26%), followed by propionic acid (20.2%) however, effected of the rising OLR was enhanced the VFA conversion rate, but appeared in only L1 and was slowly decreased in L2 and L3 in all type of VFA. The increasing VFA contents was correlated with SS decreased and VS contents were relatively stable, so it can be reasoned that the reducing the SS, i.e., fibers changed to VS, in form VFAs. This was confirmed by the stable SCOD in the effluent of the HR; the metabolism of hydrolysis and acidogenesis is rapid that change the organic compound to intermediary product in term VFA. Generally, several research found HR does not remove COD but converts the polymers into monomers or simpler forms of organic compounds. However, poorly methane content about 1% of produced gas in its. It is confirmed this cased it be good for support the methanogens in sAnMBR because of the capability of hydrolysis process was effective.

The average COD removals of sAnMBR were 74%, 66%, and 63% for L1, L2 and L3, respectively. The effected of OLR increasing led to TCOD rising a slight linear trend. The 23.9% and 34.7% of the TCOD removed with membrane filtration process. Moreover, incomplete biodegradation of the VFA when OLR was higher, which occurred the product from the hydrolysis process liked the hydrolysate form in the sAnMBR. It was corresponding with the highest of hydrolysis ratio to 13% in L3 that obtained from the calculation from TCOD and SCOD data when compared to L1 and L2 (0.87% and 0.72%, respectively). The COD proportions in L3 showed that the acidogenesis ratio 46.09% and methanogenesis ratio 40.15% were limited by the residue hydrolysis ratio when compare with L1 and L2 that as similarly observed in Cheng et al [32]. Hence, the POME treatment with high OLR and SS content could improve the COD removal *via* biological process and membrane filtration of the sAnMBR. However, the increase of the OLR should be sure that it cannot affected to the failure of process which result of OLR in sAnMBR performance can summarized it should not exceed $50 \text{ kgCOD.m}^{-3}.\text{day}$.

Main point to be awareness of process in biogas production is the accumulation of VFA that higher OLR can be led to decreasing of CH_4 yield. The average methane production in sAnMBR was increased from 15.4 L/d (66%) to 19.8 L/d (69%) from L1 to L2 and methane production decreased from 19.8 to 16.1 L/d (76%) with an OLR of $99 \text{ kgCOD.m}^{-3}.\text{day}$ in L3. However, In L3 it was slightly declined due to the higher OLR bring to collected of VFAs in system. VFA production rate increased was related with the average methane production reduced that it seemed to COD removal slightly decreased. The major species of VFAs were acetic acid (30.7%) and followed of propionic acid (18.2%) that related several research found that acetic acid being the major component and butyric acid being the minor one. Mostly of both species of VFAs was easily to converting to CH_4 that positive effected. In the other hand, it excessive amount led to negative effect with biogas production because of the inhibition the methanogenic activity. Because of the acetic acid is easily transforming to methane, then presenting a positive effect. The same reason with occurred the propionic acid in process led to negative impact on the biogas yield due the inhibition it causes to acetolactic methanogens. However, the ratio of propionic acid and acetic acid no more than 0.7 owing to inhabitation of methane yield also.

The operate of sAnMBR process was kept a constant of SRT and decreased of HRT (3.3, 2.5 and 1.5 day) but the MLSS is not increased that it found between 36.7 - 39.5 g/L in each loading. Because of the process was not operated until stable because it was highly fouling rate when operated in 90 days then caused to high pressure which effected to membrane leak therefore have to end of filtration and clean membrane (**Table S3**). The fouling rate was increased 0.15-0.19 kPa/day in L1 and highly in 0.18-0.22 kPa/day in L2 and L3. The protein and polysaccharide concentration were analysed in supernatant were 6.4, 6.7, and 7.3 g/L and. 9.7, 11.2, and 11.4 g/L for L1, L2 and L3, respectively. The results from polysaccharide concentration in the filtration process can leached easily than protein then indicated that the high molecular weight of proteins makes them hardly degradable. Thus, it can attach to the membrane surface which resulted in pore blocking and rose the fouling rates that presented by Sara and George and Mota et al [33, 34]. In this filtration process, SMP followed the same trend as the fouling rate that was supported protein, polysaccharide, MLSS, SCOD, TCOD and VFA were the part of impact parameters on fouling rate. The permeability used as a fouling performance indicator for the fouling rate show in **Table S3**. VFAs produced led to inhibition the degradation process in sAnMBR due to it still found in permeate that like a HR effluent and affected to rising the fouling rate.

In conclusion that the coupling process with biological process and filtration process in two-stage sAnMBR had performance more than 70% for COD removal. The higher hydrolysis ratio led to VFA increased and inhibition the degradation process however, higher 0.7 of propionic acid to acetic acid ratio caused to failure anaerobic process. Moreover, the evident of the high loading rate caused to high fouling rate with significant parameter in term VFAs, MLSS, protein and polysaccharide etc.

2.2 Fouling Behavior in a High-Rate Anaerobic Submerged Membrane Bioreactor (AnMBR) for Palm Oil Mill Effluent (POME) Treatment

Membrane fouling was major operational challenge in AnMBR which several researchers was designed the method to operate for prevent the foulant and the parameters relates. sAnMBR was operated with fouling protection from OLR and solid contents increasing with the internal recirculation in L1, L2 and L3 was 1.8, 2.8 and 5.5 L/d, respectively and gas sparging (1.25 L/h) in this studied. Fouladitajar et al [35] found the method of gas sparging to enhance permeate flux and reduce fouling resistances in the membrane surface. The fabricated polysulfone (PSf) hollow fiber membrane was used for POME treatment by sAnMBR. The cake layer and bulk suspension were characterized by FTIR, CLSM, roughness, and field emission scanning electron microscopy (FESEM) coupled with energy dispersive X-ray

spectrometer (EDS) to observe and evaluate the fouling under high-rate conditions to understand the fouling composition and mechanisms over a long operation period.

The flux was obtained at 2.00, 2.04, 2.02 LMH in periods I, II and III, respectively which the maximum time in filtration was operated in 90 days in each loading due to the increasing of fouling rate caused to end of operation (not the steady state) and beginning of the next load until the end of process. The average of MLSS concentrations during periods I, II, and III were 39.51 ± 2.49 , 38.04 ± 1.12 , and 36.71 ± 1.17 g/L, respectively. The main factor which led to decreased of MLSS in the sAnMBR because of the biomass in the system was lost with the cleaning membrane process which the membrane module was taken out from the reactor for chemical cleaning between each period [36]. In contrast, occurred the rising thickness of cake layer on hollow fiber membrane surfaces when increasing OLR found 12.80, 20.1 and 29.35 g/L of MLSS in periods I, II, and III, respectively under the particle size of sample in sAnMBR and sludge were 56.06 and 41.64 μm (**Figure S1**). The increasing of viscosity of the supernatant came from the accumulation of SS in the sAnMBR. However, the increasing of recirculation rate that followed the loading rate was intended to avoid clogging and accumulation of solids on both of the surface and pore membrane.

The average EPS concentration was approximately in 166.02, 177.27, and 193.15 mg/L for periods I, II, and III, respectively. The large fraction of EPS in term protein at 77–79% which was not correlated with biomass concentration but EPS content increased and may have promoted sludge aggregation [37,38] when the OLR increasing. The previously study presented that protein had a low first-order kinetics constant (k) when compared with polysaccharide. Huang et al [34] reported the effect of SRT on biomass concentration in sAnMBRs was insignificant and surface modification can control of foulant and fouling rate because of shown different SMP. Moreover, higher membrane fouling rate may occurred with higher carbohydrate and protein concentrations in SMP at longer SRT [39]. Increasing of SRT can support protein rather than polysaccharide in the biomass [34]. The filtration process in sAnMBR shown 0.26–0.28 of polysaccharine/protein (C/P) ratio which was according to [21,35]. Moreover, the effected of the increasing load caused to high microorganism concentration due to C/P ratio rising. Generally, the increasing of OLR led to F/M ratio highly while SMP and EPS generated, resulting in a low of sludge filterability and filtration index down [40]. Moreover, high biomass concentration and higher cake resistance on membrane surface which in turn accelerated fouling. [41]. In the other hand, this case was removed the membrane module to clean up when highly fouling rate so a portion of the biomass was washed out that effected to biomass concentration no higher.

The control TMP in this experiment lower than 0.3 bar to prevent leaking and lacerating of membrane. The Critical flux control and internal recirculation were used for increase shear stressed so low clogging of foulant. In case found the first stage TMP was decrease that was meaning just to begin filtration system that virgin membrane so

it may be less of solid accumulation on membrane. The primary factor causing clogging as the accumulation rate of solids so internal recirculation in sAnMBR was intended to avoid plugging. The operation of each period was stopped in 90 days with the permeate flux was as low as 1.85 L/m²/h. The filtration in sAnMBR process found TMP was nearly equal during start-up system and gradually increased (highly to 0.25 bar) due to the resistance of membrane increase when the solid clogging on surface membrane. The foulant attached on membrane was washed out by recirculating biogas (gas sparging) from sAnMBR at 1.25 ± 0.25 L/hr can decreased clogging. The average F/M ratio was increased 2.0-5.5 when increase the OLR while MLSS critical concentration presented 40 g/L, it caused to strongly attached cake layer on the membrane surfaces.

CLSM images illustrated the increasing spatial distribution of a thick cake layer and the accumulation of microorganisms and EPS (in the form of protein and polysaccharide) that resulted in irreversible fouling of different membranes. Moreover, increasing of loading rate in sAnMBR led to the thickness and the specific EPS also increased. The resulted of CLSM image confirm that protein more easily attached on the membrane surface than polysaccharide which shown in highly thickness of gel layer due to the charge of the membrane surface, leads to pore blockages. In addition, the protein EPS was accumulated in the biomass granule and membrane surface. Cake layer on membrane surface and gel layer in CLSM image were formed to show the biomass content, causing biofouling, especially by proteins. [42] reported the peaks from FTIR spectra were caused by the formation and release of biomass products on membrane surfaces which supported the fouled membranes had peaks at 1638 cm⁻¹ and 1400 cm⁻¹ that corresponded to protein EPS in amide I and amide II functional group, which was also observable in zone B of the EPS (**Figure S2**). However, the peak at 1231 cm⁻¹ that was P=O in POME which disappeared in EPS, but it was observed at low intensity on the fouled membrane surfaces. The period II shown strong and high spectra which correlated to the higher concentration of biomass in sAnMBR that was obstacles lead to flux declines.

The elemental composition of the foulant on the top surface and cross-section was analyzed with FESEM images that shown the formed cake layer in the ultrafiltration hollow fibers in sAnMBR. The fouled membrane according to EDX was presented the intensive peaks C and O elements indicate the possible presence of bio-foulant (EPS) covered and interacted with organic compounds from POME ingredients on the membrane surfaces [43]. The decline of C of fouled membrane in 70.8, 70.2 and 64.9 wt.% due to increasing the OLR indicated that microorganisms in the anaerobic degradable which preferred to digest carbohydrates rather than proteins [44]. The differences in the elemental composition of the virgin and fouled membranes collected from period I, II and III were observed Na, Mg, and Si present in the fouled membranes show in **Figure S3**. After treatment processes with sAnMBR indicated the preliminary chemical compound was depleted and replaced with the feed solution compound (POME) that led to fouling membrane [45]. In addition, inorganic compound (Mg and Si) on the fouled membranes was increased caused by OLR rising, while it interacted with biomass on membrane surfaces caused to high biofouling rate. Therefore, both of

the organic and inorganic compound lead to the formation cake layer on surface membrane. AFM image can be supported the FESEM image which shown the higher fouling when rising OLR. The average roughness values of the virgin 44.77 nm and fouled membranes from period I, II, and III were, 50.08, 60.58, and 75.80 nm, respectively. The rising of roughness confirmed the trend of pore plugging or fouling of membrane surfaces. The end of operation in each phase led to removed cake layer with clean process caused to increase in roughness when OLR higher.

2.3 Thin film composite forward osmosis membrane for anti-fouling the nutrient from permeates of a two-stage submerged anaerobic membrane reactor (AnMBR)

The experiment presented the efficiency of the FO process to treat the nutrient from the effluent from two-stage sAnMBR (feed solution in FO) by used commercial CTA and TFC membrane. The comparison and identification of the factors that caused to particle fouling (SMP and EPS) and mechanisms fouling. At the end of each FO filtration run the efficiency of nutrient removed in permeate and characteristics of membrane was analyzed in term; phosphorus, COD, ammonium etc. NaCl was applied as draw solutions (DS) at difference concentrate (2M, 3M and 4M) due to the high osmolality of sAnMBR effluent and the filtration process operated with different loading by changing the flow rate at 43, 57 and 99 kgCOD/m³/day as L1, L2 and L3, respectively. Furthermore, the SEM-EDS images recorded surface and cross-section morphology of membrane in form of thickness cake layer of both membrane because of shown arrangement of nutrients clusters and confirms the recovered solids contain phosphorus, potassium and magnesium. Surface and cross-section morphology. The FO module cell consisted of 15 cm length, 10 cm wide, and 0.3 cm depth in both permeate and feed sides of the membrane. The CTA and TFC were cut for each 10 x 5 cm with an effective area (A_m) was 50 cm². The draw solution flow was conducted in co-current mode with a velocity at 0.70 cm/s by a peristaltic pump (EYELA MP-3N, Japan). The pressure was monitored by a pressure transducer (TR-PS2W, Lutron, Taiwan) in both the feed side (FS) and the draw side (DS). The hydrophilic layer in CTA and TFC membrane was analyzed with surface contact angle that summarized 64 and 75°, respectively. The concentration of sodium (Na⁺), calcium (Ca²⁺), magnesium (Mg²⁺), potassium (K⁺) and phosphate (PO₄³⁻) were digested HNO₃ (5%) and determined by inductively coupled plasma–optical emission spectroscopy analysis (Avio 500 ICP-OES, PerkinElmer, USA).

TFC membrane exhibited higher water permeability but more loss of water flux in comparison with CTA in different DS. Wang et al. [46] found the effected of increasing DS concentration (ranged from 0.5 to 5 M) to water fluxes increased with FO process that can supported in NaCl (higher 2.0 to 4.0 M) which enhancing water flux (CTA: 9.2, 11.5 and 17 LMH) and (TFC: 9.8, 16.2 and 14.1 LMH). Higher salinity DS source can efficiently improve the water flux of TFC and CTA in FO membrane also has greater potential flux with higher operation temperature. Meanwhile, CTA membrane had lower water permeability and water flux when compared with TFC that

the accumulated salinity in the feed side came from the recirculation concentrate to feed that led to reduction effective of osmotic pressure and reducing the water flux [47]. The main reason of the increasing water flux is the upper flow rate (L1-L3) of DS (NaCl) can collect more effective osmotic pressure at the support layer because of permeate dilution quickly [48]. However, TFC-FO in 4M of L3 received gradually declined at 14.1 with the salt concentration increasing (recirculation process). Thus, resulted confirm the high efficiency filtration in term the flux of TFC membrane rather than CTA membrane.

However, after 240 mins of FO filtration process, appeared the trend of permeate fluxed of both membrane at three loading was gradually declined as expected from increased osmotic pressure and high driving force from salt concentrate [47]. The permeate flux of loading 1 to loading 2 at 2M, 3M and 4M of DS shown CTA membrane was slowly decreased about 0.31 LHM but it rising in loading 3 more than 0.70 LHM. On the other hand, the permeate flux of TFC membrane in loading 3 had less value than the lowest loading 1 to 0.35, 0.81 and 1.25 LMH in 2M to 4M of NaCl, respectively. Thus, the rising DS concentrate in L1-L3 was stronger effect for both permeates water flux and increased reverse draw solute fluxes [48, 49] that shown the high efficiency in the 3M.

The concentration of COD, ammonia, and phosphorus in the feed solution showed that varies from 37.52-55.06, 30.49-81.06 and 6.086-16.321 mg/L, respectively at different phases (L1 to L3). The efficiency of COD removal in form TFC was varied from 53%, 62% and 73% respectively. One hundred percent of ammonia removal efficiency of TFC in L2 after that slightly down to 78% in L3 which caused the salinity of sodium ions leaked from the draw solution. Driver et al. and Loeb et al. [50,51] found the increase of pH (8.0-9.5) and Ca/P ratio in FO process is the one cause which led to the enhance precipitation of the form of amorphous calcium phosphate (ACP) from phosphate, calcium, magnesium and ammonia. However, reducing of the effective osmotic pressure relative with the accumulation of phosphate salts led to Ca^+ and Mg^+ salts increased and water flux decreased.

The efficiency of COD removal in CTA membrane was 20%, 20% and 39%, respectively. Nevertheless, it also the same both ammonia and phosphorus removal efficiency that found at 100% in L2 and after that slowly down to 91% and 88% in L3 which might be possibility that the salinity leaked from the draw solution [52]. The rejection of the FO membrane led to potassium ion (K^+) in the feed being enriched because positive charge of K^+ may also diffuse into the DS. On the other hand, the phosphorus concentrates gradually increased with loading higher but it can maintain the efficiency removal to 100% in L1 and L3 of TFC and 99%, 100% and 88% in L1-L3 of CTA, respectively which can regard as very high phosphorus removal.

SEM micrographs imaging in the top-surface and cross-section modes in fouled TFC and CTA membrane shown arrangement of nutrients clusters and EDS analysis confirms that the recovered solids contain phosphorus, potassium and magnesium (TFC: 13.3, 5.1 and 10.7; CTA: 4.3, 0.1 and 1.5, respectively). The active layer of

membrane shown foulant of sludge meanwhile also found NaCl in support layer [48]. The incorporation of organic matter and precipitation of magnesium in the solids on the surface membrane can identified accumulation of nutrient in the solids; C, O₂ and Mg⁺ on the top-surface membrane. The possibility of diffusion of organic matter from the feed side to DS led to a slightly foul in the draw side. The positive charge of potassium ion in L1, L2 and L3 shown that increased L1 to L2 and decrease in L3 of both membranes indicated the trend of pore plugging and fouling of membrane surfaces [41-43]. The summarization of negative charge in CTA membrane caused to easily fouling layer than TFC membrane although the efficiency of ammonia and phosphorus removal as the same trend in L2. Moreover, the rising DS concentrate led to permeates water flux and reverse draw solute fluxes increased.

CHAPTER 3

CONCLUDING REMARK

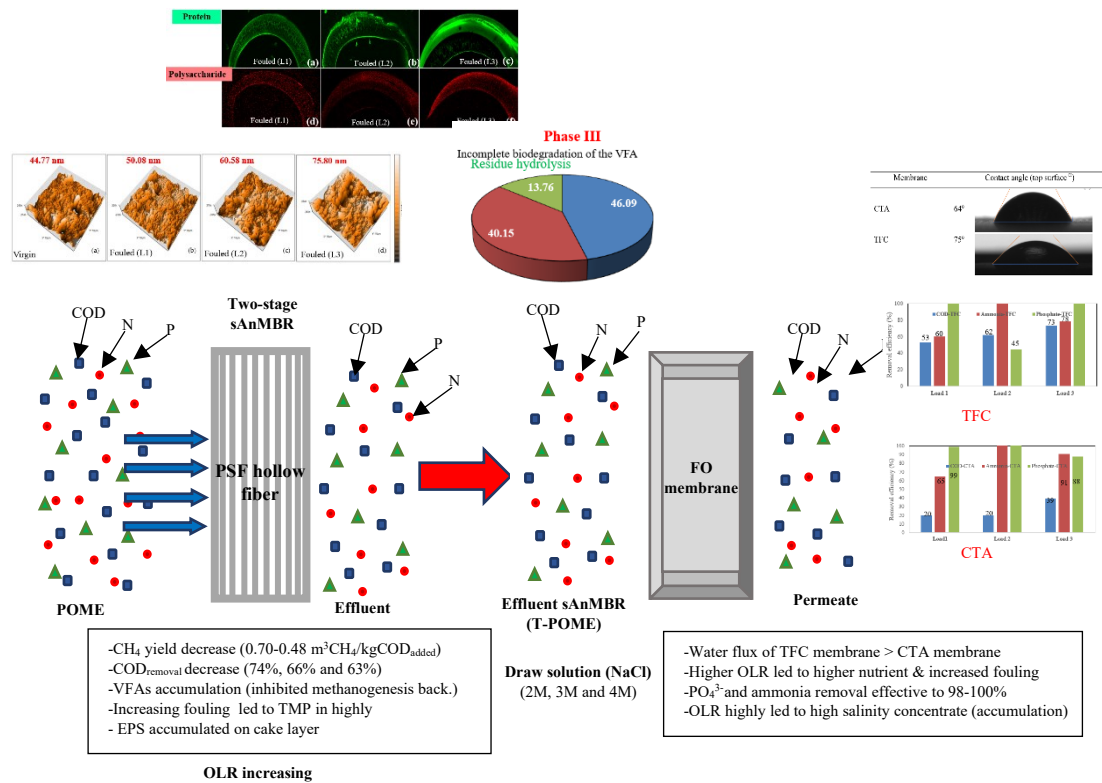


Figure 1 The concluding results

The results obtained from this work were summarized in **Figure1**, the POME treated by the two-stage submerge anaerobic membrane bioreactor with forward osmosis membrane in different of organic loading rate (OLR) that it was operated in long operation period. They create violent hydrodynamic turbulence in two-stage sAnMBR processing, led to minimizing fouling and enhancing biogas production. However, fouling mechanisms were investigated, providing the following;

a) The growing cake layer, which it affected by increasing OLR led to high MLSS in a two-stage anaerobic reactor. The rising biofilm formation on the membrane surfaces caused increased TMP and EPS accumulation on the cake layer, so removing protein from EPS fouling was more difficult.

b) The precipitation of inorganic compounds, silica, and phosphorus, also occurred in the sAnMBR system. The process of high OLR led to the high performance of VFA and COD removal of more than 70% and found the propionic and acetic acid production higher than 0.7 that one factor in failing down of AnMBR.

Finally, FO processing found the accumulation of salt from DS (NaCl) and highly of organic loading rate (L1-L3) that led to rising of salt concentrate (Na^+) in the permeate water. However, T-POME treated with FO process could be found high effective PO_4^{3-} and ammonia removal with 90-100% that a good signal for recovery nutrients and reduced chemical cost for operation. The TFC shown high efficiency removal when compared with CTA because of the diffusion of Ca_2^+ ion in CTA, enhanced the overpass for EPS network; a cake layer formed on the membrane's active layer.

Reference

- [1] Y.J. Chan, M.F. Chong, C.L. Law. Biological treatment of anaerobically digested palm oil mill effluent (POME) using a Lab-Scale Sequencing Batch Reactor (SBR). *Environ. Manage.* 91(2010) 1738-1746.
<http://dx.doi.org/10.1016/j.jenvman.2010.03.021>.
- [2] M. Khemkhao, S. Techkarnjanaruk, C. Phalakornkule. Simultaneous treatment of raw palm oil mill effluent and biodegradation of palm fiber in a high-rate CSTR. *Bioresour. Technol.* 177(2015) 17–27.
<https://doi.org/10.1016/j.biortech.2014.11.052>.
- [3] N.H. Abdurrahman, Y.M. Rosli, N.H. Azhari. “Development of a membrane anaerobic system (MAS) for palm oil mill effluent (POME) treatment”. *Desalination.* 266(2011) 208–212. <https://doi.org/10.1016/j.desal.2010.08.028>.
- [4] H.J. Lin, W. Peng, M.J. Zhang, J.R. Chen, H.C. Hong, Y. Zhang. A review on anaerobic membrane bioreactors: applications, membrane fouling and future perspectives, *Desalination.* 314(2013) 169-188.
<http://dx.doi.org/10.1016/j.desal.2013.01.019>.
- [5] A.L. Smith, L.B. Stadler, N.G. Love, S.J. Skerlos, L. Raskin. Perspectives on anaerobic membrane bioreactor treatment of domestic wastewater. *Bioresour. Technol.* 122(2012) 149–159 <http://dx.doi.org/10.1016/j.biortech.2012.04.055>.
- [6] V.T. Mota, F.S. Santos, C.S.A. Míriam. Two-stage anaerobic membrane bioreactor for the treatment of sugarcane vinasse: Assessment on biological activity and filtration performance. *Bioresour. Technol.* 146(2013) 494–503.
<https://doi.org/10.1016/j.biortech.2013.07.110>.
- [7] J.Y. Joo, C.H. Park, G.B. Han. Optimization of two-phased anaerobic sludge digestion using the pressurized ultra- filtration membrane with a mesh screen (MS-PUFM). *Chem. Eng.* 300(2016) 2028.
<http://dx.doi.org/10.1016/j.cej.2016.04.078>.
- [8] A. Saddoud, S. Sayadi. Application of acidogenic fixed-bed reactor prior to anaerobic membrane bioreactor for sustainable slaughterhouse wastewater treatment. *Hazard. Mater.* 149(2007) 700-706.
<http://dx.doi.org/10.1016/j.jhazmat.2007.04.031>.
- [9] P. Le-Clech, V. Chen, T.A.G. Fane. Fouling in membrane bioreactors

- used in wastewater treatment. *Member. Sci.* 284 (2006) 17–53.
<https://doi.org/10.1016/j.memsci.2006.08.019>.
- [10] C.C.V. Chan, P.R. Bérubé, E.R. Hall. Shear profiles inside gas sparged submerged hollow fiber membrane modules. *Member. Sci.* 297 (2007) 104–120.
<https://doi.org/10.1016/j.memsci.2007.03.032>.
- [11] T. Li, A. Wing-Keung Law, Y. Jiang, A. K. Harijanto, A.G. Fane. Fouling control of submerged hollow fibre membrane bioreactor with transverse vibration. *Member. Sci.* 505 (2016) 216–224.
<http://dx.doi.org/10.1016/j.memsci.2016.01.003>.
- [12] F. Wang, J. Chen, H. Hong, A. Wang, H. Lin. Pollutant removal and membrane fouling in an anaerobic submerged membrane bioreactor for real sewage treatment. *Water Sci Technol* (2014) 69 (8): 1712–1719.
<https://doi.org/10.2166/wst.2014.080>
- [13] C. Chen, W. Guo, H.H. Ngo, S.W. Chang, D. Duc Nguyen, P. Dan Nguyen, X.T. Bui, Y. 543 Wu. Impact of reactor configurations on the performance of a granular anaerobic 544 membrane bioreactor for municipal wastewater treatment. *International Biodeterioration 545 & Biodegradation.* 121 (2017) 131–138.
<https://doi.org/10.1016/j.ibiod.2017.03.021>.
- [14] I. Martin-Garcia, M. Mocosch, A. Soares, M. Pidou, B. Jefferson. Impact on reactor 561 configuration on the performance of anaerobic MBRs: Treatment of settled sewage in 562 temperate climates. *Water Res.* 47 (2013) 4853–4860. 563
<https://doi.org/10.1016/j.watres.2013.05.008>
- [15] X. Ren, H.K. Shon, N. Jang, Y.G. Lee, M. Bae, J. Lee, K. Cho, I.S. Kim. Novel membrane bioreactor (MBR) coupled with a nonwoven fabric filter for household wastewater treatment. *Water Res.* 44 (2010) 751–760.
<http://dx.doi.org/10.1016/j.watres.2009.10.013>.
- [16] J. Xiong, D. Fu, R.P. Singh. Self-adaptive dynamic membrane module with a high flux and stable operation for the municipal wastewater treatment. *Membr. Sci.* 471 (2014) 308–318. <https://doi.org/10.1016/j.memsci.2014.08.001>.
- [17] J. Xiong, D. Fu, R.P. Singh, J.J. Ducoste. Structural characteristics and Development of the cake layer in a dynamic membrane bioreactor. *Sep. Purif. Technol.* 167 (2016) 88–96. <http://dx.doi.org/10.1016/j.seppur.2016.04.040>.

- [18] C.H. Lee, P.K. Park, W.N. Lee, B.K. Hwang, S.H. Hong, K.M. Yeon, H.S. Oh, I.S.Chang. Correlation of biofouling with the bio-cake architecture in an MBR. *Desalination* 231 (2008) 115–123. <http://dx.doi.org/10.1016/j.desal.2007.10.026>.
- [19] K. Lutchmiah, A.R.D. Verliefde, K. Roest, L.C. Rietveld, E.R. Cornelissen. Forward osmosis for application in wastewater treatment: A review. *Water Res.* 58(2014) 179-197. <https://doi.org/10.1016/j.watres.2014.03.045>.
- [20] C. Klaysom, T.Y. Cath, T. Depuydt, I.F.J. Vankelecom. Forward and pressure retarded osmosis: potential solutions for global challenges in energy and water supply. *Chem. Soc. Rev.* 42(2013) 6959-6989. <http://dx.doi.org/10.1039/c3cs60051c>.
- [21] J.R. McCutcheon, M. Elimelech. Influence of membrane support layer hydrophobicity on water flux in osmotically driven membrane processes. *Membr. Sci.* 318 (2008) 458–466. <https://doi.org/10.1016/j.memsci.2008.03.021>
- [22] W. Luo, F.I. Hai, W.E. Price, W. Guo, H.H. Ngo, K. Yamamoto, L.D. Nghiem. High retention membrane bioreactors: challenges and opportunities. *Bioresour. Technol.* 167 (2014) 539–546. <https://doi.org/10.1016/j.biortech.2014.06.016>
- [23] J.H. Choi, K. Fukushi, K. Yamamoto. Comparison of treatment efficiency of submerged nanofiltration membrane bioreactors using cellulose triacetate and polyamide membrane. *Water Sci. Technol.* 51 (2005) 305–312. <https://doi.org/10.2166/wst.2005.0650>
- [24] T.Y. Cath, A.E. Childress, M. Elimelech. Forward osmosis: principles, applications, and recent developments. *Membr. Sci.* 281 (2006) 70–87. <https://doi.org/10.1016/j.memsci.2006.05.048>
- [25] S. Zhao, L. Zou, C.Y. Tang, D. Mulcahy. Recent developments in forward osmosis: opportunities and challenges. *Membr. Sci.* 396 (2012) 1–21. <https://doi.org/10.1016/j.memsci.2011.12.023>
- [26] A. Abdelrasoul, H. Doan and A. Lohi. Fouling in Membrane Filtration and Remediation Methods, Mass Transfer - Advances in Sustainable Energy and Environment Oriented Numerical Modeling. (2013). DOI: 10.5772/52370.
- [27] G. Gompper, M. Lässig, U. Schwarz. Jülich. Particles at Membranes and Interfaces. vorgelegt von Sabyasachi Dasgupta aus Kolkata, India. (2014). der Universität zu Köln.

- [28] D. Feng, J.S.J. Van Deventer, C. Aldrich. Ultrasonic defouling of reverse osmosis membranes used to treat wastewater effluents. (2006). *Separation and Purification Technology* 50(3):318-323. DOI:10.1016/j.seppur.2005.12.005
- [29] W. Shi, M.M. Benjamin. Effect of shear rate on fouling in a Vibratory Shear Enhanced Processing (VSEP) RO system. (2011). *Fuel and Energy Abstracts* 366(1):148-157. DOI:10.1016/j.memsci.2010.09.051
- [30] J. Kim, C. Park, T. H. Kim, M. Lee, S. Kim, S. W. Kim, J. Lee. Effects of Various Pretreatments for Enhanced Anaerobic Digestion with Waste Activated Sludge. (2003). *Biosci. Bioeng.*, 95, 271–275. [https://doi.org/10.1016/S1389-1723\(03\)80028-2](https://doi.org/10.1016/S1389-1723(03)80028-2)
- [31] M. Said A.W. Mohammad, M.T. Mohd Nor, S.R. Sheikh Abdullah and H. Abu Hasan. Chemical cleaning of fouled polyethersulphone membranes during ultrafiltration of palm oil mill effluent. (2014). *Membrane Water Treatment*, 5(3). 207-219. DOI: <http://dx.doi.org/10.12989/mwt.2014.5.3.207>
- [32] H. Cheng, Y. Li, G. Guo, T. Zhang, Y. Qin, T. Hao, Y-Y. Li. Advanced methanogenic performance and fouling mechanism investigation of a high-solid anaerobic membrane bioreactor (AnMBR) for the co-digestion of food waste and sewage sludge. *Water Res.* (2020). DOI: 10.1016/j.watres.2020.116436
- [33] S. Arabiand and G. Nakhla. Impact of protein/carbohydrate ratio in the feed wastewater on the membrane fouling in membrane bioreactor. (2008). *Membrane Science* 324(1):142-150. DOI:10.1016/j.memsci.2008.07.026.
- [34] V. T. Mota, F. S. Santos and M. C. S. Amaral. Two-stage anaerobic membrane bioreactor for the treatment of sugarcane vinasse: Assessment on biological activity and filtration performance. (2013). *Biores. Tech.* 146, 494-503. DOI: 10.1016/j.biortech.2013.07.110
- [35] A. Fouladitajar, F. Z. Ashtiani, H. Rezaei, A. Haghmoradi, A. Kargari. Gas sparging to enhance permeate flux and reduce fouling resistances in cross flow microfiltration. (2014). *Industrial and Engineering Chemistry*,20(2), 624-632. <https://doi.org/10.1016/j.jiec.2013.05.025>
- [36] W. Chaipetch, A. Jaiyu, P. Jutaporn, , M. Heran, W. Khongnakorn. (2021). Fouling behavior in a high-rate anaerobic submerged membrane bioreactor (AnMBR) for palm oil mill effluent. *Membranes* 11(9), 1-15.

DOI: 10.3390/membranes11090649

- [37] L. Chen, P. Cheng, L. Ye, H. Chen, X. Xu, L. Zhu. Biological performance and fouling mitigation in the biochar-amended anaerobic membrane bioreactor (AnMBR) treating pharmaceutical wastewater. *Bioresour. Technol.* 2020, 302, doi:10.1016/j.biortech.2020.122805.
- [38] Z. Zhang, J. Qiu, R. Xiang, H. Yu, X. Xu, L. Zhu. Organic loading rate (OLR) regulation for enhancement of aerobic sludge granulation: Role of key microorganism and their function. *Sci. Total Environ.* 2019, 653, 630–637, doi:10.1016/j.scitotenv.2018.10.418.
- [39] Z. Huang, S.-L. Ong, H. Y. Ng. Submerged Anaerobic Membrane Bioreactor for Low-Strength Wastewater Treatment: Effect of HRT and SRT on Treatment Performance and Membrane Fouling. 2011. *Water Research* 45(2):705-13. DOI:10.1016/j.watres.2010.08.035
- [40] D.C. Banti, M. Mitrakas, P. Samaras. Membrane Fouling Controlled by Adjustment of Biological Treatment Parameters in Step-Aerating MBR. *Membranes* 2021, 11, 553. <https://doi.org/10.3390/membranes11080553>
- [41] L. Yin, L. Haining, C. Li, Z. Kaisong. The ratio of food-to-microorganism (F/M) on membrane fouling of anaerobic membrane bioreactors treating low-strength wastewater. *Desalination.* 297(3), 2012, 97-103. <https://doi.org/10.1016/j.desal.2012.04.026>
- [42] Y. Kaya, A.M. Bacaksiz, H. Bayrak, I. Vergili, Z.B. Gönder, H. Hasar, G.Yilmaz. Investigation of membrane fouling in an anaerobic membrane bioreactor (AnMBR) treating pharmaceutical wastewater. *Water Process Eng.* 2019, 31, 100822, doi:10.1016/j.jwpe.2019.100822.
- [43] G. Matar, G. Gonzalez-Gil, H. Ma, S. Nunes, P. Le-Clech, J. Vrouwenvelder, P.E. Saikaly. Temporal changes in extracellular polymeric substances on hydrophobic and hydrophilic membrane surfaces in a submerged membrane bioreactor. *Water Res.* 2016, 95, 27–38, doi:10.1016/j.watres.2016.02.064.
- [44] S. C. Chanika, K. Akom, S. Kattinat. Utilization of Palm Oil Mill Effluent for Bio-Extract Production: Physical, Chemical and Microbial Properties, and Application to Growth of Chinese Kale. *Science & Technology Asia.* 26(3), 2021,142-155. doi: 10.14456/scitechasia.2021.53

- [45] F. Meng, S. R. Chae, A. Drews, M. Kraume, H.S. Shin and F. Yang. Recent advances in membrane bioreactors (MBRs) membrane fouling and membrane material. *Water Res.* 43, 1489-1512. <http://doi.org/10.1016/j.watres.2008.12.044>.
- [46] Z. Wang, J. Zheng, J. Tang, X. Wang, Z. Wu. A pilot-scale forward osmosis membrane system for concentrating low-strength municipal wastewater: performance and implications. (2016). *Sci. Rep.* 6, 21653.
- [47] L. Huang, D-J. Lee, J-Y. Lai. Forward Osmosis Membrane Bioreactor for Wastewater Treatment with Phosphorus Recovery. *Bioresource Technology* (2015), <http://dx.doi.org/10.1016/j.biortech.2015.09.045>
- [48] N.C. Nguyen, S.S. Chen, H.Y.Y and N.T. Hau. Application of forward osmosis on dewatering of high nutrient sludge. (2013). *Bioresour. Technol.* 132, 224-229.
- [49] B. Kim, S. Lee, S. Hong. A novel analysis of reverse draw and feed solute fluxes in forward osmosis membrane process. 352 (2014), *Desalination* 128–135.
- [50] J. Driver, D. Lijmbach, I. Steen. Why recover phosphorus for recycling, and how? (1999). *Environ. Technol.* 20, 651–662.
- [51] S. Loeb, L. Titelman, E. Korngold, J. Freiman. Effect of porous support fabric on osmosis through a Loeb-Sourirajan type asymmetric membrane. (1997) *Membr. Sci.* 129, 243–249.
- [52] X. Lu, C. Boo, J. Ma. M. Elimelech. Bidirectional diffusion of ammonium and sodium cations in forward osmosis: role of membrane active layer surface chemistry and charge. (2014) *Environ. Sci. Technol.* 48, 14369–14376.

Supplementary Data of paper I

Performance of a High Rate Two-Stage Anaerobic Membrane Bioreactor (AnMBR) for the Treatment of Palm Oil Mill Effluent

Wiparat Chaipetch,^a Watsa Khongnakorn,^{a,b*} Chaowana Yirong,^a

Jomjai Boonkan,^b Arisa Jaiyu,^c and Marc Heran^d

^aDepartment of Civil and Environmental Engineering, Faculty of Engineering, Prince of Songkla University, Songkhla 90110, Thailand

^bCenter of Excellence in Membrane Science and Technology, Prince of Songkla University, Songkhla 90110, Thailand

^cExpert Center of Innovative Materials, Thailand Institute of Scientific and Technological Research, Khlong Luang 12120, Thailand

^dInstitut Européen des Membranes, IEM, UMR 5635, CNRS, ENSCM, University of Montpellier, Montpellier 34095 Cedex 5 France

*Correspondence: watsa.k@psu.ac.th; Tel.: +66-7428-7122

3 Tables

2 Figures

Table S1 Control hydrodynamic in sAnMBR

Process	Method	Resulted
Recirculate gas (Gas sparking)	<ul style="list-style-type: none"> Gas flow meter 1.25 ± 0.25 L/hr through a gas recirculation from the AnMBR tank Gas pump sucked the produced biogas into the biogas tank 	<ul style="list-style-type: none"> Increase shear force with gas bubbles to help remove scouring
Increasing the flow rate	<ul style="list-style-type: none"> Increasing the feed loading (OLR) Cross-flow 	<ul style="list-style-type: none"> The rate of clogging decreased
Turbulent	<ul style="list-style-type: none"> Electric motor mixer Rotate Speed: 30 rpm Two impellers Timer set to control (second time per days) 	<ul style="list-style-type: none"> Increase shear force

Table S2 The methodology and analyzation of VFA concentration and component

VFA concentration
Collected the sample to analyzed by titration method and calculated as;
$\text{Volatile fatty acid} = \frac{Ax Bx 50x 1000}{\text{Sample volume (ml)}}$
Where; A is The volume of the standard base solution used in the titration to the end point at pH = 7 (ml)
B is NaOH concentration used in titration (0.1 mol/l)
VFA component
Gas chromatography (GC 7820A Agilent Technologies) equipped with thermal conductivity detector (TCD)

Table S3 The concentration of phenolic compound in POME

Phenol	Effect
10 - 24 mg/ L	Toxicity concentrations for humans
9 - 25 mg/L	Toxicity concentrations for fish
Chantho P. et al. shown the phenolic in POME high to 33 to 462 mg/L.	
Discharging POME that untreated or traditionally treated into the rivers could a high environmental risk for the surrounding area.	
Therefore, POME treatments are needed to eliminate the phenols.	

Note: Did not analysis the phenolic compound in current study.

Table S4 Method and analysis of foulant and fouling

Preparation of membrane modules for foulant analyses		
Membrane module was taken out of the sAnMBR and fouled fiber membrane were cut at the end of operate in 90 days, 180days and 270 days, respectively. After cutting the fibers, the fiber sections were closed with an epoxy glue to prevent leakage, and the permeate flow rate was rearranged to maintain the constant flux.		
Type of foulant	Method	Parameters
(i) Foulant particles	<ul style="list-style-type: none"> Physical cleaning by flushing the membrane surface with deionized water until the cake layer was dislodged Take the particles obtained from washing to analysis 	<ul style="list-style-type: none"> MLSS
(ii) Fouling composition and mechanisms	<ul style="list-style-type: none"> Cake layer and bulk suspension were characterized to observe and evaluate the fouling 	<ul style="list-style-type: none"> FTIR CLSM Roughness FESEM-EDS
(ii) Mixed liquor suspended solid in sAnMBR	<ul style="list-style-type: none"> Collected sampling in the sAnMBR after turbulent 	<ul style="list-style-type: none"> MLSS TS
Cleaning method for fouled membrane		
(i) Physical	Cleaning by flushing the membrane surface with deionized water until the cake layer was dislodged (Remove gross solids attached to the membrane surface; reversible or temporary fouling) that SEM allows the observation of surface morphology evolution due to found the thickness layer in term of jel layer.	
(ii) Chemical	<ul style="list-style-type: none"> Cleaning with 1% acetic solution for 2 hours followed by 1% NaOH for 2 hours and 10% sodium hypochlorite (NaClO) for 2 hours. (Remove; irreversible or permanent fouling) 	
Fouling rate		
The permeability is also frequently used as a fouling performance indicator so the fouling rate as;		
$L = \frac{J}{TMP}$		
Where; Permeability (L); LMH/kPa, Flux (J); LMH, Transmembrane pressure (TMP)kPa,		

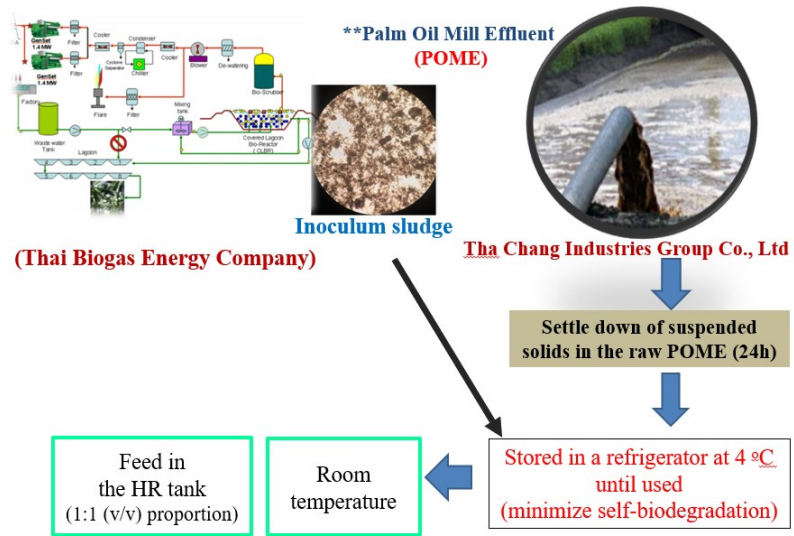


Figure S1 Step of preparation POME and sludge for feed in the two-stage sAnMBR

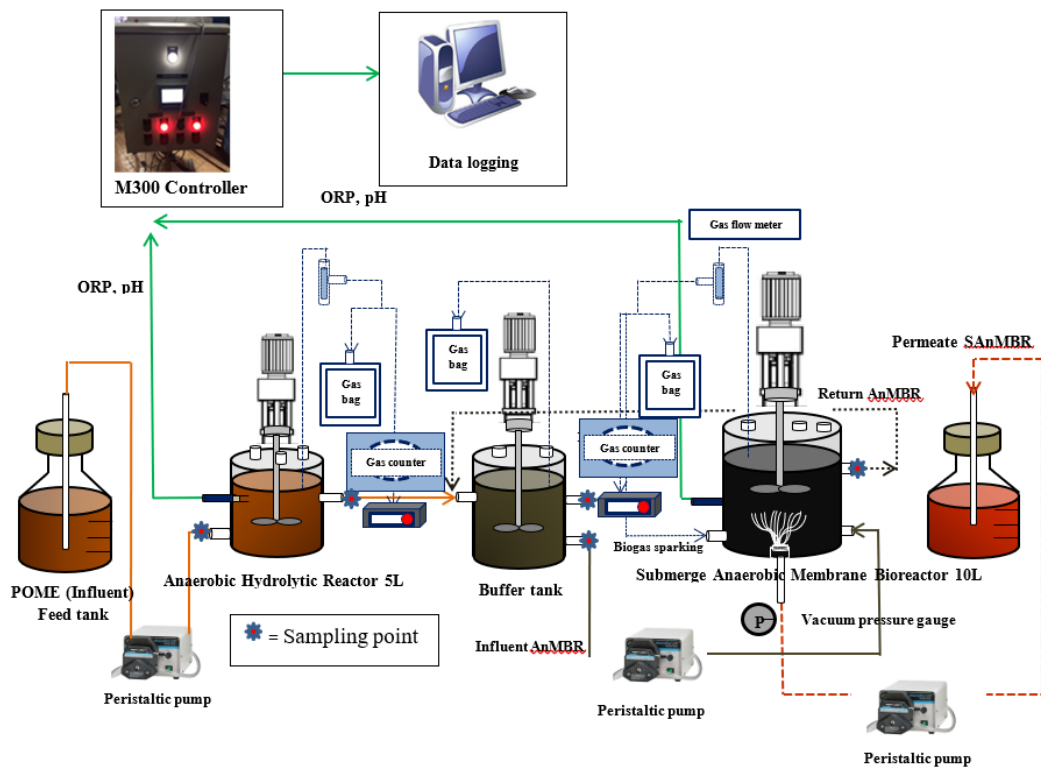


Figure S2 Collection sample in two-stage sAnMBR

Note: The influent of sAnMBR came from the internal recirculation (return AnMBR) and HR effluent that were fed in AnMBR reactor also.

Supplementary Data of paper II

Fouling Behavior in a High-Rate Anaerobic Submerged Membrane Bioreactor (AnMBR) for Palm Oil Mill Effluent (POME) Treatment

Wiparat Chaipetch¹, Arisa Jaiyu², Panitan Jutaporn³,
Marc Heran⁴ and Watsa Khongnakorn^{1,*}

¹Center of Excellence in Membrane Science and Technology, Department of Civil and Environmental Engineering, Faculty of Engineering, Prince of Songkla University, Songkhla 90110, Thailand

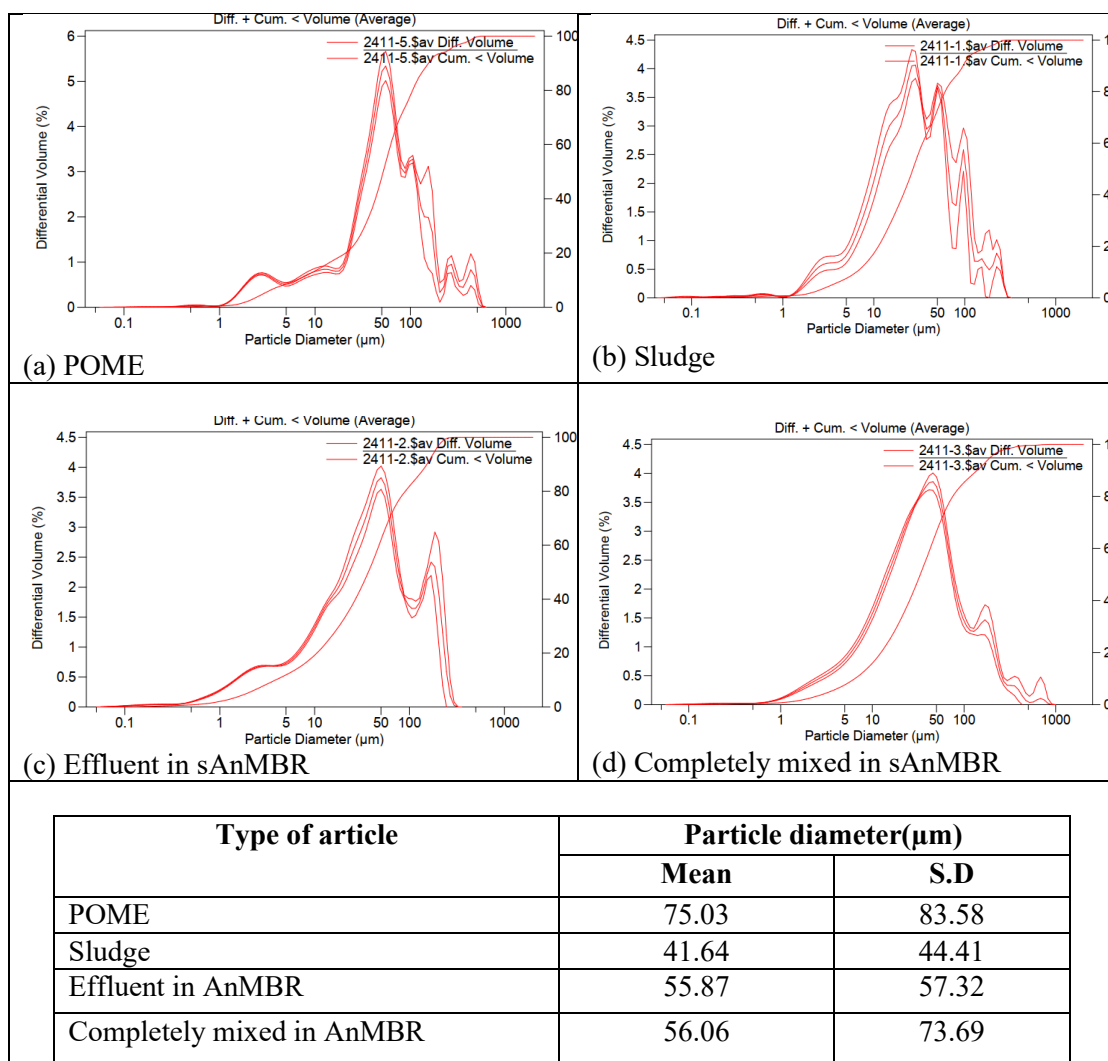
²Expert Center of Innovative Materials, Thailand Institute of Scientific and Technological Research, Khlong Luang 12120, Thailand

³Research Center for Environmental and Hazardous Substance Management (EHSM), Department of Environmental Engineering, Faculty of Engineering, Khon Kaen University, Khon Kaen 40002, Thailand

⁴Institut Européen des Membranes, IEM, UMR 5635, CNRS, ENSCM, University of Montpellier, CEDEX 5, 34095 Montpellier, France

*Correspondence: watsa.k@psu.ac.th; Tel.: +66-7428-7122

3 Figures



Note: Calculation from 0.040 μm to 2000 μm by LS particle size analyzer

Figure S1 The particle size of a) POME, b) Sludge, c) Effluent of HR reactor, d) Effluent of AnMBR and e) Completely mixed in AnMBR

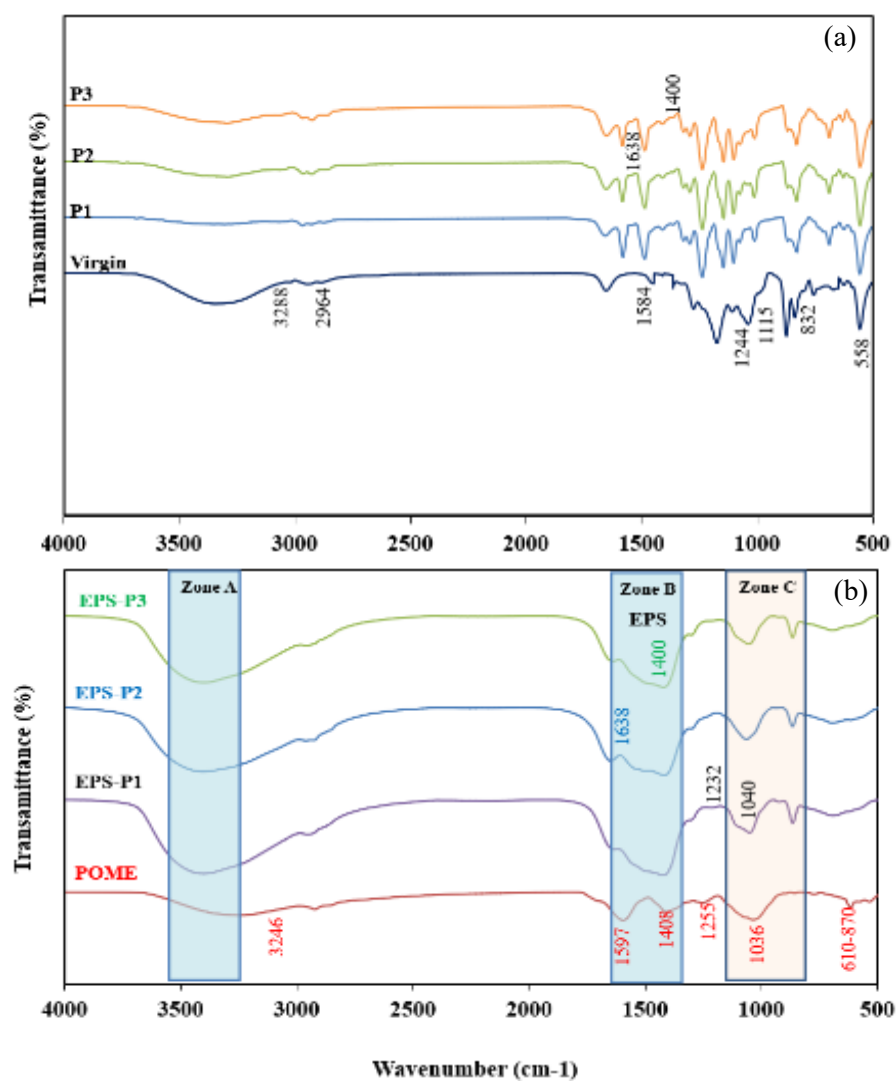


Figure S2 FTIR spectra peak of (a) virgin and fouled membranes and (b) POME and EPS

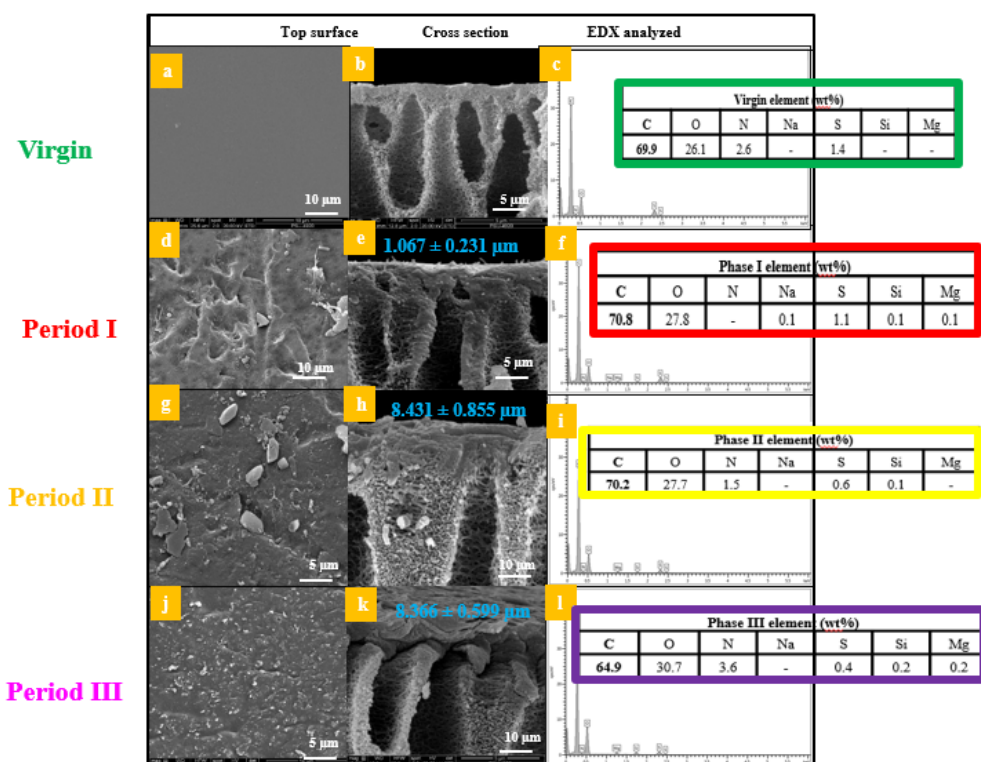


Figure S3 FESEM of the virgin membrane (**a**: top surface, **b**: cross section, **c**: EDX element), fouled membrane in period I (**d**: top surface, **e**: cross section, **f**: EDX element), fouled membrane in period II (**g**: top surface, **h**: cross section, **i**: EDX element), and fouled membrane in period III (**j**: top surface, **k**: cross section, **l**: EDX element) with thickness scales.

APPENDIX I

Performance of a High Rate Two-Stage Anaerobic Membrane Bioreactor (AnMBR) for the Treatment of Palm Oil Mill Effluent

Wiparat Chaipetch,^a Watsa Khongnakorn,^{a,b*} Chaowana Yirong,^a

Jomjai Boonkan,^b Arisa Jaiyu,^c and Marc Heran^d

^aDepartment of Civil and Environmental Engineering, Faculty of Engineering, Prince of Songkla University, Songkhla 90110, Thailand

^bCenter of Excellence in Membrane Science and Technology, Prince of Songkla University, Songkhla 90110, Thailand

^cExpert Center of Innovative Materials, Thailand Institute of Scientific and Technological Research, Khlong Luang 12120, Thailand

^dInstitut Européen des Membranes, IEM, UMR 5635, CNRS, ENSCM, University of Montpellier, Montpellier 34095 Cedex 5 France

*Correspondence: watsa.k@psu.ac.th; Tel.: +66-7428-7122

Performance of a High Rate Two-Stage Anaerobic Membrane Bioreactor (AnMBR) for the Treatment of Palm Oil Mill Effluent

Wiparat Chaipetch,^a Watsa Khongnakorn,^{a,b,*} Chaowana Yirong,^a Jomjai Boonkan,^b Arisa Jaiyu,^c and Marc Heran^d

A two-stage submerged anaerobic membrane bioreactor (2-sAnMBR) was operated to demonstrate the technology concept and to accelerate anaerobic biodegradation of Palm Oil Mill Effluent (POME). Then, the impact of different high organic loading rates (OLR) was investigated with a focus on water quality and biogas production. OLR higher than 50 kg_{COD}.m⁻³.d⁻¹ induced an increase of volatile fatty acids (VFAs). As a consequence, the biogas production decreased from 19.8 to 11.0 L.d⁻¹ and CH₄ yield between 0.23 to 0.38 L_{CH₄}/g_{COD_{removed}}. Nevertheless, the highest OLR (98 kg_{COD}.m⁻³.d⁻¹) made it possible to reach a COD removal effectiveness of 70%, where the membrane contribution was around 23.9% to 34.7%. The ratio of propionic acid/acetic acid appeared to be a key indicator to prevent the AnMBR operation failure. Indeed, as soon as the value of 0.7 has been exceeded, several signs of AnMBR failure appeared. The methanogenic activity in AnMBR was inhibited by a hydrolysis ratio of 13% which transformed to VFA accumulation in system. The 250 mg.L⁻¹ of Phenol concentration in POME was an inhibitory of the microbe in this system. Suspended solids concentration, proteins, polysaccharides, and volatile fatty acids were the substantial parameters that influenced the fouling rate.

DOI: 10.15376/biores.17.2.3398-3412

Keywords: Palm oil mill effluent (POME); Anaerobic membrane bioreactor (AnMBR); High loading rate; Long operation; Methane yield; Volatile fatty acids (VFA)

Contact information: a: Department of Civil and Environmental Engineering, Faculty of Engineering, Prince of Songkla University, Songkhla 90110 Thailand; b: Center of Excellence in Membrane Science and Technology, Prince of Songkla University, Songkhla 90110 Thailand; c: Expert Center of Innovative Materials, Thailand Institute of Scientific and Technological Research, Khlong Luang 12120, Thailand; d: Institut Européen des Membranes, IEM, UMR 5635, CNRS, ENSCM, University of Montpellier, Montpellier 34095 Cedex 5 France; *Corresponding author: watsa.k@psu.ac.th

INTRODUCTION

Anaerobic-aerobic lagoon systems are applied to treat a wide range of pollutants before being discharged into water bodies and lands. Anaerobic digestion (AD) consists of a four-step process involving four different types of microbe groups: hydrolysis, acidogenic, acetogenic, and methanogenic. A high organic loading rate (OLR) in a single-phase reactor may cause inhibitions from, for example, rising VFA and phenols. Therefore, several authors have suggested a two-stage anaerobic process as a solution, which could reduce various inhibitors, e.g., volatile fatty acids (VFAs), phenols, etc. As a result, it increases the treatment capacity and performance. The two-stage AD has been applied for the POME treatment (Mamimin *et al.* 2012; Mota *et al.* 2013; Chaikasem *et al.* 2014; Khan

et al. 2019; Krishnan *et al.* 2019). Palm oil mill effluent (POME) contains high amounts of organic compounds, phenolic compounds, and color, which may cause water pollution. The using of POME for biogas production (CH_4 , CO_2 , H_2S , *etc.*) through AD has widely been reported (Teng *et al.* 2013; Hasanudin *et al.* 2015; Aziz and Hanafiah 2017). In the two-stage AD, POME is first converted to VFAs during the acid-forming stage (commonly referred as hydrolysis, acidogenesis, and acetogenesis). Then, during the second stage, the VFAs are converted into biogas through methanogenesis (Teng *et al.* 2013). However, the operational factors, *e.g.*, OLR, VFAs, pH, *etc.*, must be carefully controlled to ensure good equilibrium between acid formation and methane production *via* effective bacteria diversity and activity to prevent failure from accumulating acids (Cheng *et al.* 2020). Borja *et al.* (1996) conducted a two-stage up flow anaerobic sludge blanket (UASB) for treating POME under mesophilic conditions. The organic loading rate was gradually increased from 2.3 to 17.3 $\text{kgCOD}\cdot\text{m}^{-3}\cdot\text{d}^{-1}$ over 120 days of experiment. The OLR at a level of 16.6 $\text{kgCOD}\cdot\text{m}^{-3}\cdot\text{d}^{-1}$ yielded a high acid concentration, which later induced failure at an OLR of 17.3 $\text{kgCOD}\cdot\text{m}^{-3}\cdot\text{d}^{-1}$. The maximum acid production was found to be 4.1 $\text{kgCOD}\cdot\text{m}^{-3}\cdot\text{d}^{-1}$. Gas production mainly consisted of CO_2 with low methane content. A 1-2% hydrogen gas content was found at higher OLRs, with further reduced methane content (Borja *et al.* 1996). Once the biomass is inhibited, an increase of OLR will decrease the methane production. Mamimin *et al.* (2015) conducted a two-stage (thermophilic and mesophilic) anaerobic sequential batch reactor (ASBR) of POME with an OLR of 60 $\text{kgCOD}\cdot\text{m}^{-3}\cdot\text{d}^{-1}$ under 2-day hydraulic retention time (HRT). Their results showed a 38% COD removal in thermophilic reactor. It can be noted that the limitation of two stage AD is around 20 $\text{kgCOD}\cdot\text{m}^{-3}\cdot\text{d}^{-1}$. The higher OLR of POME leads to the failure of two stage AD. Hence, a two-stage submerged anaerobic membrane bioreactor (2-sAnMBR) was proposed for high OLR and high solid content instead of AD. A high-solid AnMBR has been studied for the benefit of biogas production *via* anaerobic digestion (Cheng *et al.* 2020; Ariunbaatar *et al.* 2021). The operating conditions of both stages must be well controlled for the better effective treatment at high OLRs, especially with the self-inhibiting products such as phenols in POME. At high OLRs, there are many factors affecting filtration performances, *e.g.*, soluble microbial product (SMP), MLSS, viscosity, VFAs, *etc.* (Qiao *et al.* 2013; Li *et al.* 2020).

The aim of this study was to assess the performance of a two-stage anaerobic treatment involving high AnMBR OLR. Afterward, the purpose was focused on the identification of the relevant parameters/elements to be monitored in order to overcome the limiting factors under high OLRs. These inhibiting factors were also analyzed in order to determine the system maximum capacity and to increase and improve the use of AnMBR for high OLR and solids feeding by POME effluent.

EXPERIMENTAL

Palm Oil Mill Effluent (POME) and Inoculum Sludge

The POME wastewater and sludge samples were collected from a covered lagoon bioreactor (CLBR) in the Surat Thani palm oil factory, Thailand. The characteristics of the POME and sludge inoculum were analyzed following the Standard methods outlined by AWWA (2012); the results are presented in Table 1. The POME sample was stored at a temperature of 4 °C until used to minimize self-biodegradation. At the beginning,

wastewater and seed sludge were added to the reactor in a 1:1 (v/v) proportion. Then, this inoculum has been acclimatized after step feeding with 10% of POME concentration during four weeks in order to enhance AnMBR's startup success.

Experimental Setup and Operation of a Two-stage Anaerobic Membrane Bioreactors (AnMBR)

A schematic diagram detailing the set-up of the two-stage anaerobic bioreactor is shown in Fig. 1. It consisted of an anaerobic hydrolytic reactor (HR) and an anaerobic membrane bioreactor (AnMBR) made of polysulfone hollow fibers with a 0.025 m² area, which were fabricated as described in a previous study (Chaipetch *et al.* 2021). The operational conditions are presented in Table 2. The operating pH of the HR and AnMBR were kept constant at 4.5 ± 0.3 and 7.2 ± 0.2 , respectively, with adjustment of 2 M HCl or NaHCO₃ solutions. The reactors were operated until stable COD removal and biogas production were reached.

Table 1. Characteristics of Raw Palm Oil Mill Effluent (POME) and Sludge Inoculum (Mean \pm Standard Deviation)

Parameters	POME	Sludge Inoculum
pH	5.11 ± 0.1	7.73 ± 0.1
Temp (°C)	49 ± 0.5	40 ± 0.5
TCOD (g/L)	190 ± 15	180 ± 15
SCOD (g/L)	120 ± 8	110 ± 5
TS (g/L)	33.6 ± 0.2	41.2 ± 0.2
SS (g/L)	23.3 ± 0.2	32.6 ± 0.3
VS (g/L)	12.8 ± 0.4	11.5 ± 0.4
TKN (g/L)	0.78 ± 0.10	0.25 ± 0.02
Alk (g/L as CaCO ₃)	3.26 ± 0.45	1.62 ± 0.38

Note: TCOD: Total Chemical Oxygen Demand; sCOD: Soluble Chemical Oxygen Demand; TS: Total Solids; SS: Suspended Solids; VS: Volatile Solids; Alk: Alkalinity; TKN: Total Kjeldahl Nitrogen; and Temp: Temperature

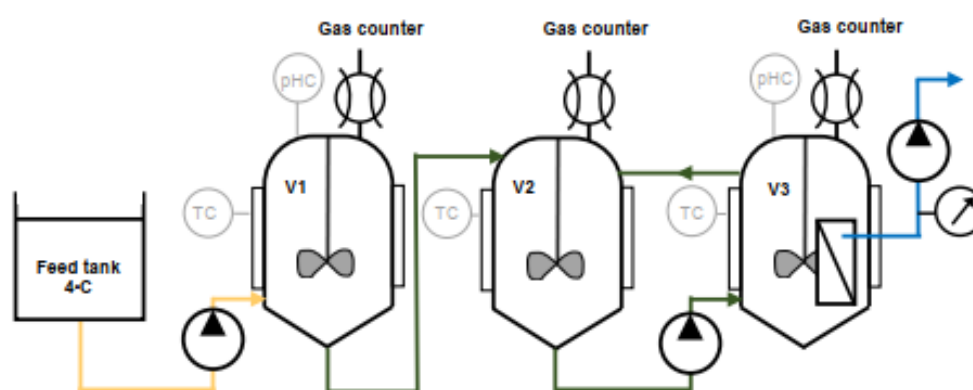


Fig. 1. Lab-scale diagram of two-stage submerged anaerobic membrane bioreactor (sAnMBR). pHC: pH controller, TC: temperature controller, V1: Hydrolytic reactor, and V2&V3: Anaerobic membrane bioreactor

The ORP and pH were recorded daily in both HR and AnMBR tank. Samples were collected three times per week to analyze the TCOD, SCOD, TSS, TS, VS, VSS, and alkalinity, following the Standard methods outlined by AWWA (2012). The VFA components were determined *via* GC/FID (Agilent 7890A, Santa Clara, CA) using a 3 m stainless steel column packed with molecular sieve with 60 mesh to 80 mesh and 100 mesh to 120 mesh. Helium was used as the carrier gas at a flow rate of 35 mL/min. The temperatures of the injection port, oven, and detector were set at 220 °C, 60 °C, and 220 °C, respectively. The volume of biogas production was measured *via* a gas counter, and the composition of the biogas was measured *via* gas chromatography using a Shimadzu GC 8A (Kyoto, Japan), which was fitted with a 2 m stainless steel column packed with molecular sieve 58 (80/100 mesh). Helium was used as the carrier gas at a flow rate of 35 mL/min. The temperatures of the injection port, oven, and detector were set at 100 °C, 40 °C, and 100 °C, respectively. The compositions of the biogas were measured *via* gas chromatography through 0.5 mL gas sample injected in triplicate.

Table 2. Operating Conditions of the Anaerobic Hydrolytic Reactor (HR) and Submerged Anaerobic Membrane Bioreactor (sAnMBR) under Mesophilic Conditions (35 °C ± 5 °C)

Operating Conditions		Phase I (Day 0 to 90)	Phase II (Day 91 to 180)	Phase III (Day 181 to 270)
HR reactor (working volume 5L)	Influent Flow (L/d)	1.5	2	3.3
	HRT (d)	3.33	2.5	1.51
	TCOD _{Influent} (gCOD/L)	189	248	289
	TS (gTS/L)	32.6	35.1	35.7
	OLR (kgCOD.m ⁻³ .d ⁻¹)	57.2	99.2	192.6
AnMBR (working volume 10L)	Influent Flow (L/d)	1.2	1.2	1.2
	HRT (d)	3.3	2.5	1.5
	TCOD _{Influent} (gCOD/L)	142	143	148
	TS (gTS/L)	45.1	47.0	47.1
	OLR (kgCOD.m ⁻³ .d ⁻¹)	42.6	57.2	99.1
	Membrane fluxes (LMH)	2	2.04	2.02
	Internal recirculation (L/d)	1.8	2.8	5.5
	Gas sparging (L/h)	1.25	1.25	1.25

The hydrolysis and acidogenesis ratios in HR were calculated according to Eqs. 1 and 2, respectively,

$$\text{Hydrolysis ratio (\%)} = \frac{(\text{TCOD}-\text{SCOD})_{\text{inf}} - (\text{TCOD}-\text{SCOD})_{\text{eff}}}{(\text{TCOD}-\text{SCOD})_{\text{inf}}} \quad (1)$$

$$\text{Acidogenesis ratio (\%)} = \frac{\text{COD}_{\text{VFA,reactor}} - \text{COD}_{\text{VFA,eff}}}{(\text{TCOD}-\text{COD}_{\text{VFA}})_{\text{inf}}} \times 100 \quad (2)$$

where *inf* is the influent; *eff* is the effluent, and TCOD and COD_{VFA} correspond to the total COD and the COD in term of the volatile fatty acids (VFAs), respectively (Cheng *et al.* 2020).

The acidogenesis and methanogenesis ratios, as well as the observed CH₄ yield in AnMBR, were calculated according to Eqs. 3 and 4, respectively,

$$\text{Methanogenesis ratio (\%)} = \frac{\text{COD}_{\text{CH}_4}}{\text{TCOD}_{\text{inf}}} \times 100 \quad (3)$$

$$\text{Observed CH}_4 \text{ yield} = \frac{\text{Biogas production} \times \% \text{CH}_4}{\left(\frac{\text{SCOD}_{\text{HR,effluent}} - \text{SCOD}_{\text{AnMBR,effluent}}}{x} \right) \times Q} \quad (4)$$

$(L_{\text{CH}_4} / \text{g COD}_{\text{removed}})$

where COD_{CH_4} corresponds to the COD in term of the methane gas, $\% \text{CH}_4$ is the methane content in biogas, and Q is the flowrate of the influent (Sema-Garcia *et al.* 2020).

The impact of the VFAs on the methane yield was determined using SPSS statistical software version 23.0 (IBM, Armonk, NY). The data were analyzed *via* one-way analysis of variance (ANOVA) using the least significant difference (LSD) at a p -value of less than or equal to 0.05.

The membrane filtration was operated under sub-critical and flux constant modes. To prevent fouling, the relaxing conditions and internal recirculation were set to be the same as the previous study (Chaipetch *et al.* 2021). The fouling rate was determined by the ratio of flux obtained per transmembrane pressure. The SMP was quantified from the concentration of proteins and carbohydrates. The supernatant was collected after centrifugation at 8000 rpm for 15 min. The sample was filtrated *via* a 0.45 μm membrane for proteins (PT) and polysaccharides (PS) analysis (Cheng *et al.* 2020). The PT were analyzed *via* a modified Lowry method and the PS were analyzed *via* the phenol sulfuric acid method (Chaipetch *et al.* 2021). The effects of the parameters, *i.e.*, PT, PS, and MLSS, on membrane fouling were analyzed *via* multiple linear regression (ANOVA, p -value of less than 0.05). A stepwise multiple linear regression was performed to determine which variables could be used to estimate the fouling rate based on the obtained data (Mota *et al.* 2013; Navarrete 2020). A 95% confidence level was adopted for all tests. The phenol concentration in the permeate at the end of each phase was analyzed *via* the spectrophotometry method (Merck spectroquant Prove 100, Merck, Kenilworth, NJ).

RESULTS AND DISCUSSION

Hydrolysis Reactor Performance

The hydrolysis reactor was studied in 3 phases, *i.e.*, phase I (day 0 through 90, with an OLR of 57 $\text{kgCOD} \cdot \text{m}^{-3} \cdot \text{d}^{-1}$), phase II (day 91 through 180, with an OLR of 99 $\text{kgCOD} \cdot \text{m}^{-3} \cdot \text{d}^{-1}$), and phase III (day 181 through 270, with an OLR of 192 $\text{kgCOD} \cdot \text{m}^{-3} \cdot \text{d}^{-1}$). According to Fig. 2a, the TCOD of the influent increased in stages, which implied corresponding increases in OLR. In contrast, the SCOD of the influent tended to be slightly increased from phase I to phase III which confirmed the hydrolysis process. In the influent, the averages of the TCOD of phases I, II, and III were 188.7 g/L, 248.4 g/L, and 288.4 g/L, respectively, while the SCOD were 62.93 ± 2.53 g/L, 60.07 ± 3.14 g/L, and 60.30 ± 2.94 g/L, respectively, due to the different batches used in this work. The relative increase in the TCOD were 31.6% and 53.0%, whereas the increases were only 13.2% and 20.7% for the effluent, respectively. In contrast, the relative SCOD increase in the influent from phase I to II, and phase I to III did not vary much (-4.15% for both). However, they were 2.1% and 5.3% for the effluent, respectively. In phase I, the TCOD of the effluent was higher than the TCOD of the influent because of excess TCOD from the inoculum (180 ± 15 g/L TCOD).

In phase II, the TCOD of the effluent was similar to the TCOD of the influent, whereas it was lower in phase III. This could be due to the partial conversion of the TCOD into carbon dioxide and hydrogen *via* anaerobic hydrolysis and acidogenesis as the OLR increases. The microbes in the HR convert the organic compounds into volatile acids, as shown by the increase in the total VFAs. The major species of VFAs (as shown in Fig. 2b) were acetic acid (26%), followed by propionic acid (20.2%), butyric acid (17.4%), i-valeric acid (13.8%), valeric acid (12.1%), and i-butyric acid (10.6%). This finding was aligned with the results of Liu *et al.* (2006). All the VFAs gradually increased during phase I (from 0.4 g/L to 0.8 g/L) and plateaued in phase II (0.6 g/L to 0.7 g/L) before further increasing in phase III, from 0.7 g/L to 1.0 g/L. The higher the OLR, the greater the amount of VFAs. From this experiment, increasing the OLR enhanced the VFA conversion rate, however, with limitations. The VFAs content in phase I linearly increased from the beginning until the 90th day. Increasing the OLR from 57 kgCOD.m⁻³.d⁻¹ to 98 kgCOD.m⁻³.d⁻¹, however, did not lead to a higher VFA content than in phase I. It can be summarized that an OLR between 57 and 98 kgCOD.m⁻³.d⁻¹ was acceptable in the HR in regard to the VFA production. In addition, it was considerably higher than the OLR given in Borja *et al.* (1996), which was 16.6 kgCOD.m⁻³.d⁻¹.

As seen in Table 1, the TS of the POME was 33.6 g/L ± 0.2 g/L and consisted of 69.3% suspended solids. The VS (12.8 g/L ± 0.4 g/L) accounted for 38.1% of the TS, which may have been carbohydrates, fibers, sugars, proteins, and fats (Teoh and Mashitah 2010; Sinnaraprasat and Fongsatitkul 2011). These compounds can be converted to be monomers, *e.g.*, volatile acids and fatty acids. The increasing VFA contents (Fig. 2b) was correlated to the decrease in the SS (Fig. 2c). The VS contents were relatively stable, however, so it can be reasoned that the SS changed to VS, *i.e.*, VFAs. This was confirmed by the stable SCOD in the effluent of the HR. Generally, HR does not remove CODs but converts the polymers into monomers or simpler forms of organic compounds. However, considering the SS, it can be reasoned that the reducing the SS, *i.e.*, fibers, changes them to VS, *i.e.*, VFAs.

The hydrolysis ratio, interestingly, increased as the OLR increased. The hydrolysis ratio was quite scattered in phase I due to the starting up instability. The range of the hydrolysis ratio was between 11.7% to 60.0% (an average of 39.0% ± 13.3%). During phase II and phase III, the hydrolysis ratio was more stable, as well as considerably higher. The percentages increased in phase II to reach 87.1% to 100.0% (an average of 98.4% ± 3.9%). The best hydrolysis ratio belonged to phase III and was equal to 100% for the entire period. The hydrolysis ratio confirmed the previous evidence that a higher OLR yielded greater degradation of complex compounds into simpler compounds, *e.g.*, VFAs. The HR was very effective in converting organic compounds for easier uptake from the methanogens, which were poorly present in this reaction as confirmed by the very low methane content in the produced gas (1.65% ± 0.04%, 1.57% ± 0.1%, and 1.26% ± 0.02% in phase I, II, and III, respectively). Note that Liu *et al.* (2006) found no methane at an OLR of 53 kgCOD.m⁻³.d⁻¹ (or 37.5 kgVS.m⁻³.d⁻¹) (HR) for a household-waste two stage anaerobic digester. Mamimin *et al.* (2015) studied a two-stage anaerobic digester with thermophilic and then mesophilic reactors for POME treatment. At an OLR of 60 kgCOD.m⁻³.d⁻¹ (similar to this study), they obtained a COD removal of 38%, which was 10% in our hydrolytic reactor (during phase III). This could be accounted to the higher temperature when compared with this work.

Anaerobic Membrane Bioreactor (AnMBR) Performance

Chemical oxygen demand (COD) removal

According to Fig. 3, the TCOD in the influent and permeate inclined to increase as the OLR increased.

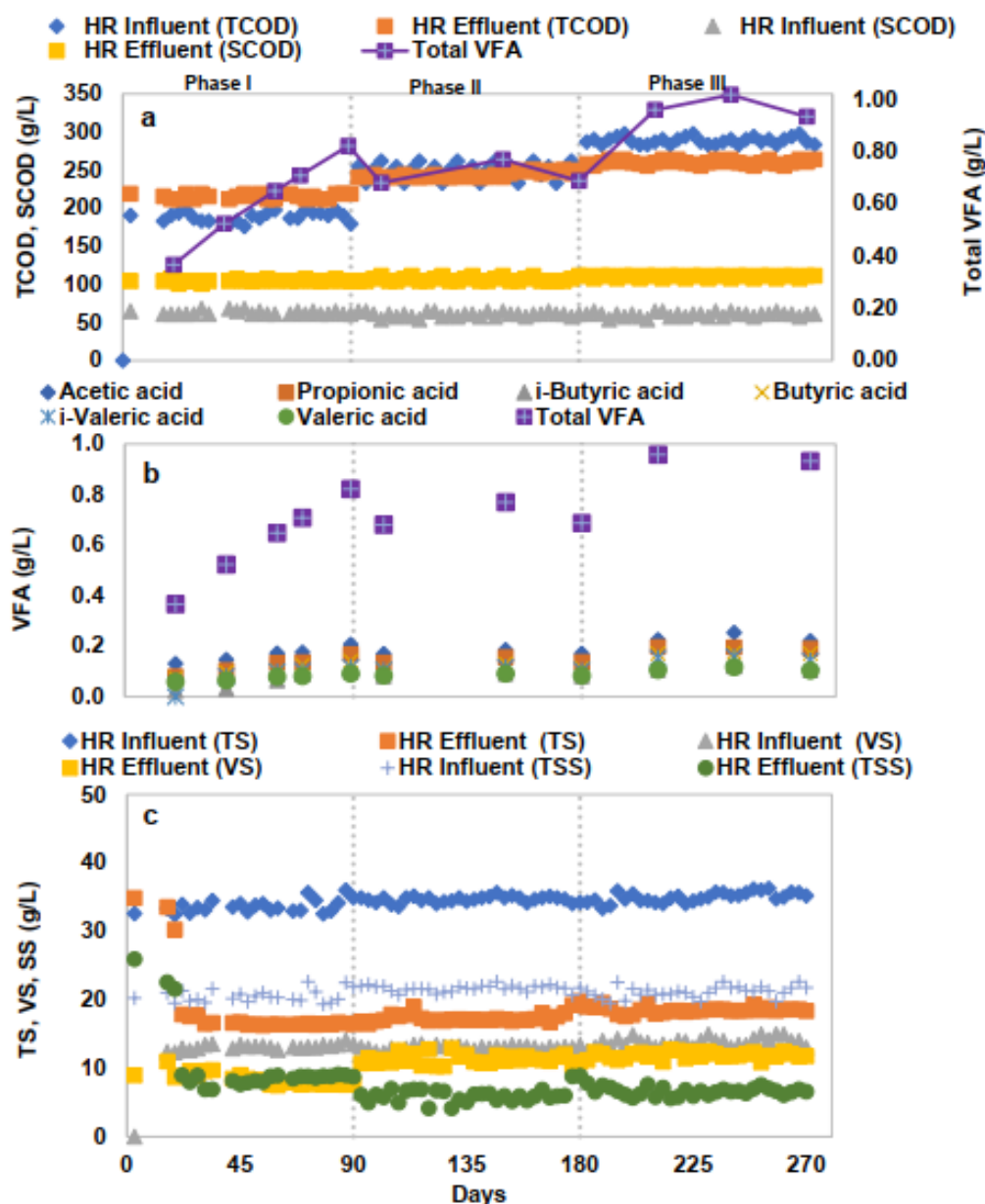


Fig. 2. Performance of the hydrolysis reactors; a) TCOD, SCOD, and total VFA; b) VFAs and pH; and c) TS, VS, and TSS

The average COD removals were 74%, 66%, and 63% for phase I, phase II, and phase III, respectively. Hence, the increasing TCOD or OLR degraded the AnMBR performance following a slight linear trend, as shown in Fig. 3. The COD of the permeate (COD_{per}) was high, *i.e.*, 30 g/L, while the SCOD in the reactor and permeate tended to be stable even though it slightly increased from phase II to III. The COD_{per} and SCOD showed the same stable pattern. Methanogenesis was itself very effective, with a 35% TCOD removal rate. The membrane filtration removed between 23.9% and 34.7% of the TCOD. The COD removal performance was supported by the physical process from the membrane filtration, which accounted for approximately 50% of the overall removal percentage during phase II and phase III. Hu *et al.* (2017) presented a 2% to 21% increasing COD removal rate obtained from membrane filtration.

Stably controlling the pH at neutral pH conditions (7.35 to 7.83) for methanogens, increased the efficiency of the biogas yield (Yu *et al.* 2018). The COD balance in the AnMBR is presented in Fig. 4. The methanogenesis ratio in phase I (53.45%) and phase II (50.18%), were higher than in phase III (40.15%). These results agreed with the COD removal trends presented above. At the beginning of phase II, the COD removal rate gradually decreased and then sharply dropped after 135 d. In phase III, the COD removal and methanogenesis ratios were the lowest, probably due to overloading. The higher OLR was from the incomplete biodegradation of the VFA, which resulted in the hydrolysate being carried to the AnMBR. The increasing OLR in phase III explained the higher hydrolysis ratio (13%) compared to phase I and II (0.87% and 0.72%, respectively). The COD proportions in phase III showed that the acidogenesis ratio and methanogenesis ratio were limited by the residue hydrolysis ratio, as similarly observed by Cheng *et al.* (2020).

Hence, the treatment of POME at a high OLR and high suspended solids content improved the COD removal *via* biological process and membrane filtration of the AnMBR (Mota *et al.* 2013; Cheng *et al.* 2020; Ariunbaatar *et al.* 2021; Chaipetch *et al.* 2021). However, the OLR should not exceed $50 \text{ kgCOD}\cdot\text{m}^{-3}\cdot\text{d}^{-1}$ to prevent process failure.

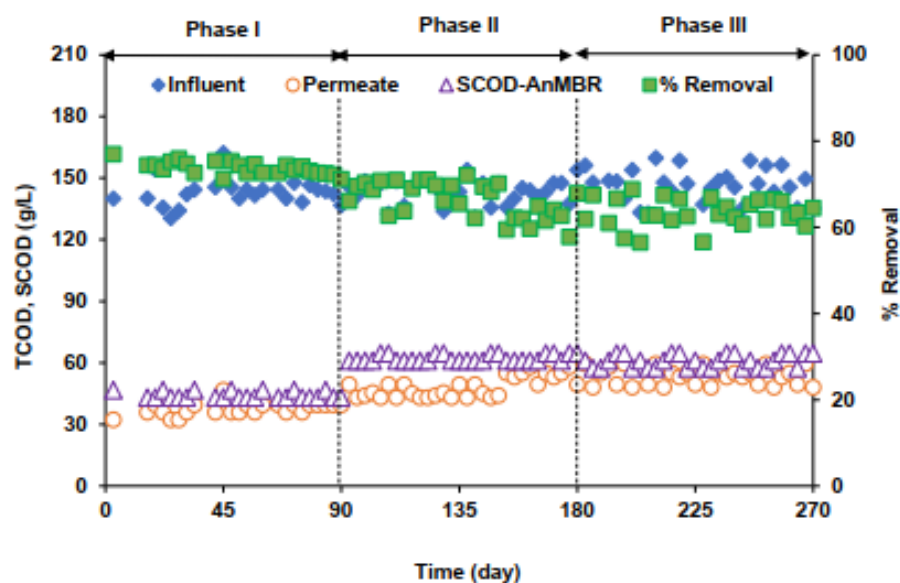


Fig. 3. The COD component in the AnMBR system and the COD removal performance

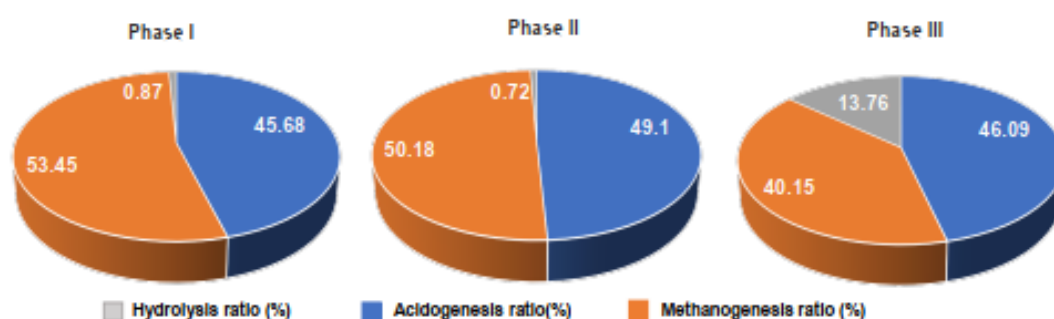


Fig. 4. COD mass balance for hydrolysis, acidogenesis, and methanogenesis ratio in the AnMBR

Volatile Fatty Acid (VFA) and Methane Yield

The average biogas production of the AnMBR in phases I, II, and III were 22.8 L/d, 28.5, and 21.2 L/d, respectively. The biogas production gradually increased in phase I and became more stable in phase II. In phase III, however, it slightly declined due to the higher OLR, which was responsible for the accumulation of VFAs in the system, as shown in Fig. 5. The average methane production increased from 15.4 L/d (66%) to 19.8 L/d (69%) from phase I to phase II. In phase III, the methane production decreased from 19.8 to 16.1 L/d (76%) with an OLR of 99 kg COD.m⁻³.d⁻¹. This result agreed with Cheng *et al.* (2020), which increased the co-digestion of sewage sludge by adding food waste. This upgraded value was also attributed to the improved hydrolysis ratio. In this study the methane yield decreased due to the uncompleted hydrolysis of FOG (fat, oil, and grease) in POME presented as co-digestion from hydrolytic reactor when high OLR. The average methane production seemed to decrease as the VFA production rate increased and the COD removal decreased. The results agreed with previous studies even through the easily biodegradation wastewater such as sugarcane vinasse (Santos *et al.* 2017), food waste (Cheng *et al.* 2020), molasses (Wijekoon *et al.* 2011), *etc.* The decrease in the CH₄ yield as the biogas production, which occurred as OLR increased, are probably due to a threshold VFA effect as the pH was controlled.

The major species of VFAs (as shown in Fig. 5b) were acetic acid (30.7%), followed by propionic acid (18.2%), butyric acid (15.3%), i-valeric acid (12.6%), valeric acid (12.4%), and i-butyric acid (10.8%). The VFA composition in this study was similar to the compositions found in previous studies (Voelklein *et al.* 2016; Krishnan *et al.* 2019). Their findings agreed with this study, *i.e.*, acetic acid being the major component and butyric acid being the minor one, which both positively affected the biogas yield (*p*-value was less than or equal to 0.05). The acetic acid is easily transforming to methane, then presenting a positive effect. Propionic acid presented a negative impact on the biogas yield due the inhibition it causes to acetoclastic methanogens (Voelklein *et al.* 2016). As previously discussed, due to the high hydrolysis ratio in phase III, the VFA was limited at 600 mg/L because the large molecule and LC-VFA increased in the system. The VFA contents were not as high as the contents found in previous studies but were still high enough to negatively impact anaerobic degradation (Wijekoon *et al.* 2011; Chaikasem *et al.* 2014). The propionic acid to acetic acid ratio is a good indicator of approaching failure (Marchaim and Krause 1993). The ratio in this study was higher than 0.7, thus it limited the methane yield in the AnMBR. In addition, the failure of anaerobic degradation also affected the filtration performance, as shown by the higher COD and VFA in the permeate.

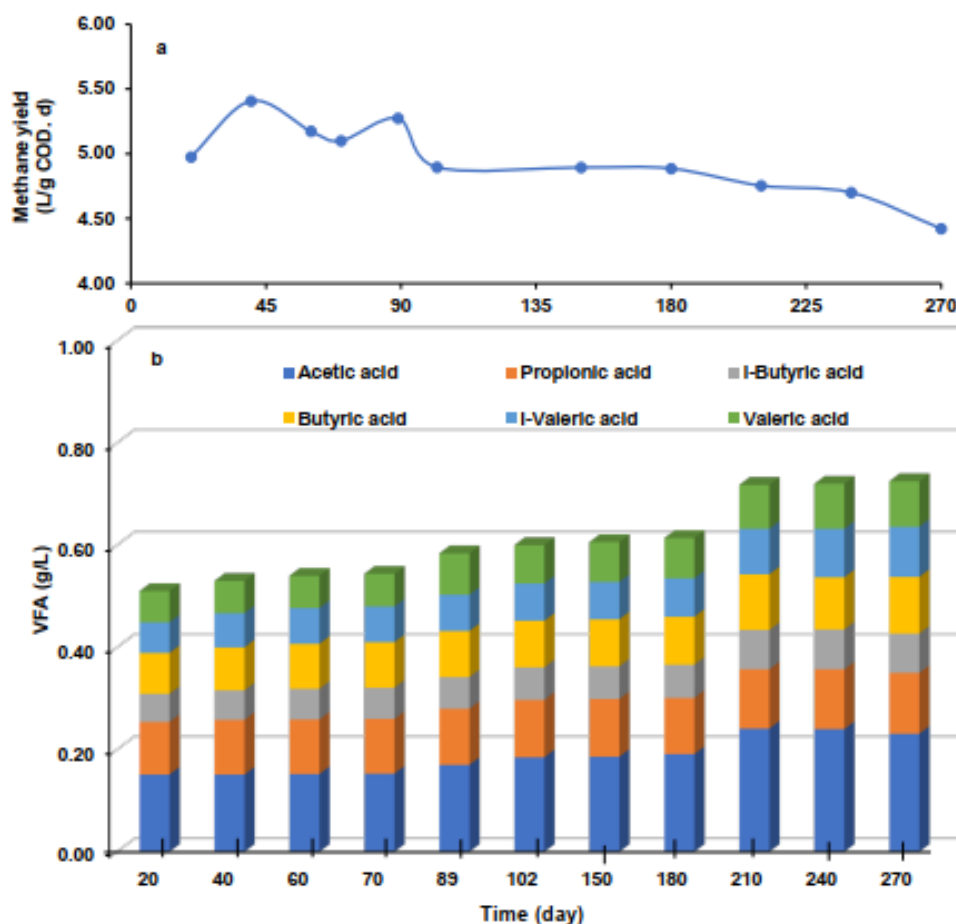


Fig. 5. VFA concentrations and methane yields in AnMBR

Filtration Performance

The internal recirculation and gas sparging were set to prevent fouling due to the high OLRs and high solids contents. In phases I, II, and III, the flux was obtained at 2.00, 2.04, and 2.02 LMH, respectively, which was similar to a previous study by the authors (Chaipetch *et al.* 2021). The average MLSS concentrations in each phase were between 36.7 g/L to 39.5 g/L. The concentrations of biomass decreased during operation. The fouling rate sharply increased in phase I (0.15 kPa/d to 0.19 kPa/d). In phase II and phase III, the fouling rate gradually increased (0.18 kPa/d to 0.22 kPa/d), as shown in Fig. 6. In addition, the fouling rate suddenly increased at the beginning of each phase and stayed constant until the end of operation. The protein concentrations in the supernatant were 6.4, 6.7, and 7.3 g/L for phases I, II, and III, respectively. The polysaccharide concentrations in the supernatant were 9.7, 11.2, and 11.4 g/L for phases I, II, and III, respectively.

These results indicated that polysaccharides leached in the supernatant more easily than proteins. Moreover, the high molecular weight of proteins makes them difficult to degrade, so they can attach to the membrane surface and cause fouling. In this study, the SMP followed the same trend as the fouling rate. The statistical analysis confirmed the impact of all parameters in AnMBR (protein, polysaccharide, MLSS, SCOD, TCOD and

VFA) on the fouling rate. The results showed the impact of those parameters on the fouling rate as follows: in phase I, the statistical analysis showed that only the MLSS significantly affected the fouling rate (a R^2 of 0.50 and a p -value of less than or equal to 0.05). In phase II, the statistical analysis indicated that only the polysaccharide concentration significantly affected the fouling rate (a R^2 of 0.50 and a p -value of less than or equal to 0.05). In phase III, both the protein and VFA concentrations were found to significantly affect the fouling rate (a R^2 of 0.70 and a p -value of less than or equal to 0.05).

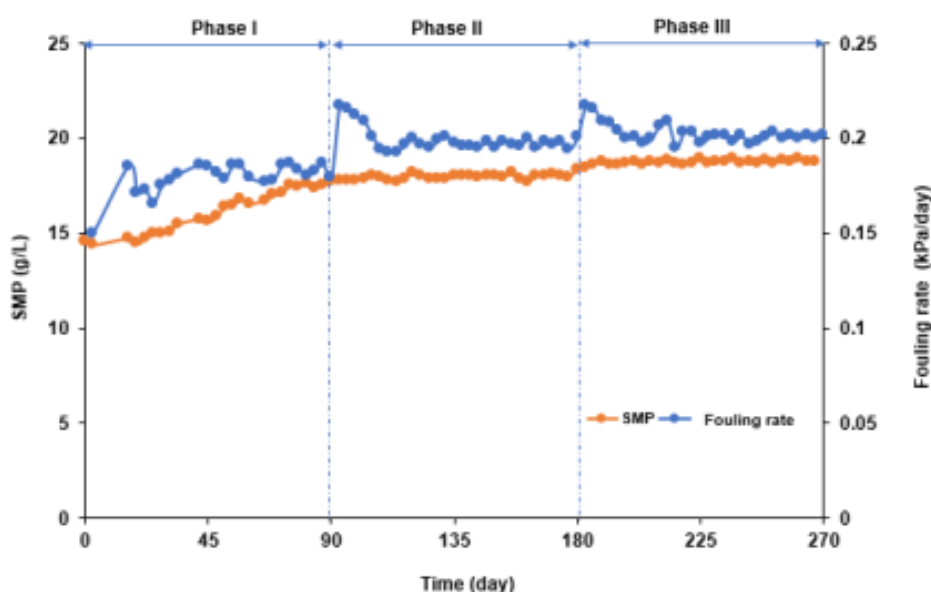


Fig. 6. The fouling rate and SMP concentration in AnMBR

From these statistical results, phase I presented the highest MLSS concentration, although it gradually decreased due to the removal of the membrane for cleaning. In phase II, almost all the polysaccharides detached from the extracellular polymeric substances (EPS), which caused the increased fouling rate (Chaipetch *et al.* 2021). The VFAs in the reactor were not measured in phase III. However, the VFAs in the permeate were measured and their concentration were similar to the HR effluent. This point could be presented as evidence of VFAs in the AnMBR. It could imply a high VFA concentration in the AnMBR, which inhibited the anaerobic degradation and induced the increased fouling rate.

These results are aligned with the research presented by Mota *et al.* (2013). The bulk solution of a high loading in the AnMBR was fouled by protein-like substances, which were released by the acidogens or operated at high VFA conditions. It seems that the AnMBR was unstable, as shown by the high concentration of VFAs and SMP (proteins and polysaccharides that are metabolic products of the microbes under inappropriate environment). This was supported by the high concentration of SCOD and VFAs in the permeate in phase III and presented a linear correlation. Phenol inhibition was reported in previous studies (Chantho *et al.* 2016; Rea *et al.* 2020; Sierra *et al.* 2017). In this study, the phenol contents in the POME and HR were 258 mg/L and 263 mg/L, respectively. The

phenol contents in the permeate were 8.5 mg/L and 5.2 mg/L in phase I and II, respectively. Several studies have reported the low AD performances of wastewater treatment with high phenol and phenolic compounds (Hernandez and Edyvean 2005; Pradeep *et al.* 2015; Chantho *et al.* 2016; Muñoz *et al.* 2017). the anaerobic membrane bioreactors (AnMBR) present seeking solutions for this inhibiting compound (Smith *et al.* 2014; Shin and Bae 2018).

Therefore, it can be concluded that phenols were not inhibiting the HR and AnMBR process because the concentration was lower than the critical value reported by Mamimin *et al.* (2012) and equal to 400 mg/L. However, the phenol in the permeate in phase III was equal to 258 mg/L, which was the same as the POME concentration, which indicated an inhibitor effect, according to VFA accumulation in the system. High VFAs probably inhibited the activity of anaerobes, which affects phenol degradation as well. The results of phenol rejection were small because its molecular weight cut-off (MWCO) was smaller than the membrane pore size. Hence, it is a biological process that removes a considerable portion of the phenols rather than the membrane filtration.

CONCLUSIONS

1. The treatment of palm oil mill effluent (POME) at a high organic loading rates (OLR) via a two-stage anionic membrane bioreactor (AnMBR) presented suitable potential for renewable energy production. The higher the OLRs, the greater the volatile fatty acids (VFA). The chemical oxygen demand (COD) removal performance was 70% higher for the coupling process, *i.e.*, the biological process and membrane filtration. The membrane filtration added a further 23.9% to 34.7% COD removal rate.
2. The AnMBR has the potential to produce a relevant effluent for fertilizer issue, which can be readily concentrated by membrane process.
3. An OLR higher than 50 kgCOD.m⁻³.d⁻¹ induced an accumulation of VFAs, which inhibited the methanogenic activity in the AnMBR in favour of a higher hydrolysis ratio. The ratio of propanoic acid to acetic acid was higher than 0.7, which indicated an approaching anaerobic failure.
4. The MLSS, protein, polysaccharide and VFA contents were the significant observed parameters that influenced the fouling rate.

ACKNOWLEDGMENTS

The research was financially supported by the Thailand Research Fund (TRF) and Tha Chang Palm Oil Industries, Co., Ltd. through a Research and Researcher for industries (RRi) under contract number "PHD58I0056". It was also bilaterally financially supported by the government budget of Prince of Songkla University, under the Integrated Research and Innovation Program 2019, contract number "ENG6201004S".

REFERENCES CITED

- Ariunbaatar, J., Bair, R., Ozcan, O., Ravishankar, H., Esposito, G., Lens, P. N. L., and Yeh, D. H. (2021). "Performance of AnMBR in treatment of post-consumer food waste: Effect of hydraulic retention time and organic loading rate on biogas production and membrane fouling," *Frontiers in Bioengineering and Biotechnology* 8, 1-15. DOI: 10.3389/fbioe.2020.594936
- AWWA (2012). *Standard Methods for Examination of Water and Wastewater*, American Public Health Association, American Water Works Association, and Water Environment Federation, Washington, DC, Denver, CO., and Alexandria, VA.
- Aziz, N. I. H. A., and Hanafiah, M. M. (2017). "The potential of palm oil mill effluent (POME) as a renewable energy source," *Acta Scientifica Malaysia* 1(2), 9-11. DOI: 10.26480/asm.02.2017.09.11
- Borja, R., Banks, C. J., and Sánchez, E. (1996). "Anaerobic treatment of palm oil mill effluent in a two-stage up-flow anaerobic sludge blanket (UASB) system," *Journal of Biotechnology* 45(2), 125-135. DOI: 10.1016/0168-1656(95)00154-9
- Chaikasem, S., Abeynayaka, A., and Visvanathan, C. (2014). "Effect of polyvinyl alcohol hydrogel as a biocarrier on volatile fatty acids production of a two-stage thermophilic anaerobic membrane bioreactor," *Bioresour. Technol.* 168, 100-105. DOI: 10.1016/j.biortech.2014.04.023
- Chaipetch, W., Jaiyu, A., Jutaporn, P., Heran, M., and Khongnakorn, W. (2021). "Fouling behavior in a high-rate anaerobic submerged membrane bioreactor (AnMBR) for palm oil mill effluent," *Membranes* 11(9), 1-15. DOI: 10.3390/membranes11090649
- Chantho, P., Musikavong, C., and Suttinun, O. (2016). "Removal of phenolic compounds from palm oil mill effluent by thermophilic *Bacillus thermoleovorans* strain A2 and their effect on anaerobic digestion," *International Biodeterioration and Biodegradation* 115, 293-301. DOI: 10.1016/j.ibiod.2016.09.010
- Cheng, H., Li, Y., Guo, G., Zhang, T., Qin, Y., Hao, T., and Li, Y.-Y. (2020). "Advanced methanogenic performance and fouling mechanism investigation of a high-solid anaerobic membrane bioreactor (AnMBR) for the co-digestion of food waste and sewage sludge," *Water Research* 187, 1-13. DOI: 10.1016/j.watres.2020.116436
- Hasanudin, U., Sugiharto, R., Haryanto, A., Setiadi, T., and Fujie, K. (2015). "Palm oil mill effluent treatment and utilization to ensure the sustainability of palm oil industries," *Water Science and Technology* 72(7), 1089-1095. DOI: 10.2166/wst.2015.311
- Hernandez, J. E., and Edyvean, R. G. (2005). "Anaerobic treatment of phenol in a two-stage anaerobic reactor," in: *Proceedings of the 7th World Congress of Chemical Engineering: Engineering for Life Incorporating the 5th European Congress*, 10-14 July, Glasgow, England, pp. 1-9.
- Hu, D., Tian, Y., Wang, Z., Wu, P., Wang, P., Chen, Z., Cui, Y., and Ge, H. (2017). "The operational efficiency of a novel AnMBR treating antibiotic solvent wastewater in start-up stage," *Journal of Water Reuse and Desalination* 7(3), 326-337. DOI: 10.2166/wrd.2016.064
- Khan, M. A., Ngo, H. H., Guo, W., Chang, S. W., Nguyen, D. D., Varjani, S., Liu, Y., Deng, L., and Cheng, C. (2019). "Selective production of volatile fatty acids at different pH in an anaerobic membrane bioreactor," *Bioresour. Technol.* 283, 120-128. DOI: 10.1016/j.biortech.2019.03.073

- Krishnan, S., Din, M. F. M., Taib, S. M., Nasrullah, M., Sakinah, M., Wahid, Z. A., Kamyab, H., Chelliapan, S., Rezania, S., and Singh, L. (2019). "Accelerated two-stage bioprocess for hydrogen and methane production from palm oil mill effluent using continuous stirred tank reactor and microbial electrolysis cell," *Journal of Cleaner Production* 229, 84-93. DOI: 10.1016/j.jclepro.2019.04.365
- Li, L., Kong, Z., Xue, Y., Wang, T., Kato, H., and Li, Y.-Y. (2020). "A comparative long-term operation using up-flow anaerobic sludge blanket (UASB) and anaerobic membrane bioreactor (AnMBR) for the upgrading of anaerobic treatment of N, N-dimethylformamide-containing wastewater," *Science of the Total Environment* 699, 1-9. DOI: 10.1016/j.scitotenv.2019.134370
- Liu, D., Liu, D., Zeng, R. J., and Angelidaki, I. (2006). "Hydrogen and methane production from household solid waste in the two-stage fermentation process," *Water Research* 40(11), 2230-2236. DOI: 10.1016/j.watres.2006.03.029
- Mamimin, C., Singkhala, A., Kongjan, P., Suraraksa, B., Prasertsan, P., Imai, T., and O-Thong, S. (2015). "Two-stage thermophilic fermentation and mesophilic methanogen process for biohythane production from palm oil mill effluent," *International Journal of Hydrogen Energy* 40(19), 6319-6328. DOI: 10.1016/j.ijhydene.2015.03.068
- Mamimin, C., Thongdumyu, P., Hniman, A., Prasertsan, P., Imai, T., and O-Thong, S. (2012). "Simultaneous thermophilic hydrogen production and phenol removal from palm oil mill effluent by *Thermoanaerobacterium*-rich sludge," *International Journal of Hydrogen Energy* 37(20), 15598-15606. DOI: 10.1016/j.ijhydene.2012.04.062
- Marchaim, U., and Krause, C. (1993). "Propionic to acetic acid ratios in overloaded anaerobic digestion," *Bioresource Technology* 43(3), 195-203. DOI: 10.1016/0960-8524(93)90031-6
- Mota, V. T., Santos, F. S., and Amaral, M. C. S. (2013). "Two-stage anaerobic membrane bioreactor for the treatment of sugarcane vinasse: Assessment on biological activity and filtration performance," *Bioresource Technology* 146, 494-503. DOI: 10.1016/j.biortech.2013.07.110
- Navarrete, R. P. (2020). *A Statistical Approach to Link Flux and Fouling to Sludge Characteristics for an Anaerobic Membrane Bioreactor Treating Dairy Cheese Wastewater*, Master's Thesis, Delft University of Technology, Delft, Netherlands.
- Pradeep, N. V., Anupama, S., Navya, K., Shalini, H. N., Idris, M., and Hampannavar, U. S. (2015). "Biological removal of phenol from wastewaters: A mini review," *Applied Water Science* 5(2), 105-112. DOI: 10.1007/s13201-014-0176-8
- Qiao, W., Takayanagi, K., Niu, Q., Shofie, M., and Li, Y. Y. (2013). "Long-term stability of thermophilic co-digestion submerged anaerobic membrane reactor encountering high organic loading rate, persistent propionate and detectable hydrogen in biogas," *Bioresource Technology* 149, 92-102. DOI: 10.1016/j.biortech.2013.09.023
- Rea, V. S. G., Sierra, J. D. M., Aponte, L. M. F., Cerqueda-Garcia, D., Quchani, K. M., Spanjers, H., and Lier, J. B. v. (2020). "Enhancing phenol conversion rates in saline anaerobic membrane bioreactor using acetate and butyrate as additional carbon and energy sources," *Frontiers in Microbiology* 11, 1-16. DOI: 10.3389/fmicb.2020.604173
- Santos, F. S., Ricci, B. C., Neta, L. S. F., and Amaral, M. C. S. (2017). "Sugarcane vinasse treatment by two-stage anaerobic membrane bioreactor: Effect of hydraulic retention time on changes in efficiency, biogas production and membrane fouling," *Bioresource Technology* 245, 342-350. DOI: 10.1016/j.biortech.2017.08.126
- Serna-García, R., Zamorano-López, N., Seco, A., and Bouzas, A. (2020). "Co-digestion

- of harvested microalgae and primary sludge in a mesophilic anaerobic membrane bioreactor (AnMBR): Methane potential and microbial diversity," *Bioresource Technology* 298, 1-9. DOI: 10.1016/j.biortech.2019.122521
- Shin, C., and Bae, J. (2018). "Current status of the pilot-scale anaerobic membrane bioreactor treatments of domestic wastewaters: A critical review," *Bioresource Technology* 247, 1038-1046. DOI: 10.1016/j.biortech.2017.09.002
- Sierra, J. D. M., Lafita, C., Gabaldón, C., Spanjers, H., and Lier, J. B. v. (2017). "Trace metals supplementation in anaerobic membrane bioreactors treating highly saline phenolic wastewater," *Bioresource Technology* 234, 106-114. DOI: 10.1016/j.biortech.2017.03.032
- Sinnaraprasat, S., and Fongsatitkul, P. (2011). "Optimal condition of Fenton's reagent to enhance the alcohol production from palm oil mill effluent (POME)," *EnvironmentAsia* 4(2), 9-16. DOI: 10.14456/EA.2011.12
- Smith, A. L., Stadler, L. B., Cao, L., Love, N. G., Raskin, L., and Skerlos, S. J. (2014). "Navigating wastewater energy recovery strategies: A life cycle comparison of anaerobic membrane bioreactor and conventional treatment systems with anaerobic digestion," *Environmental Science and Technology* 48(10), 5972-5981. DOI: 10.1021/es5006169
- Teng, T. T., Wong, Y.-S., Ong, S.-A., Norhashimah, M., and Rafatullah, M. (2013). "Start-up operation of anaerobic degradation process for palm oil mill effluent in anaerobic bench scale reactor (ABSR)," *Procedia Environmental Sciences* 18, 442-450. DOI: 10.1016/j.proenv.2013.04.059
- Teoh, Y. P., and Mashitah, M. D. (2010). "Cellulase production by *Pycnoporus sanguineus* on oil palm residues through pretreatment and optimization study," *Journal of Applied Sciences* 10(12), 1036-1043. DOI: 10.3923/JAS.2010.1036.1043
- Voelklein, M. A., Rusmanis, D., and Murphy, J. D. (2016). "Increased loading rates and specific methane yields facilitated by digesting grass silage at thermophilic rather than mesophilic temperatures," *Bioresource Technology* 216, 486-493. DOI: 10.1016/j.biortech.2016.05.109
- Wijekoon, K. C., Visvanathan, C., and Abeynayaka, A. (2011). "Effect of organic loading rate on VFA production, organic matter removal and microbial activity of a two-stage thermophilic anaerobic membrane bioreactor," *Bioresource Technology* 102(9), 5353-5360. DOI: 10.1016/j.biortech.2010.12.081
- Yu, D., Meng, X., Liu, J., Dian, L., Sui, Q., Zhang, J., Zhong, H., and Wei, Y. (2018). "Formation and characteristics of a ternary pH buffer system for *in-situ* biogas upgrading in two-phase anaerobic membrane bioreactor treating starch wastewater," *Bioresource Technology* 269, 57-66. DOI: 10.1016/j.biortech.2018.08.072

Article submitted: December 1, 2021; Peer review completed: January 15, 2022; Revised version received and accepted: April 13, 2022; Published: April 29, 2022.

DOI: 10.15376/biores.17.2.3398-3412

APPENDIX II

Fouling Behavior in a High-Rate Anaerobic Submerged Membrane Bioreactor (AnMBR) for Palm Oil Mill Effluent (POME) Treatment

Wiparat Chaipetch¹, Arisa Jaiyu², Panitan Jutaporn³,
Marc Heran⁴ and Watsa Khongnakorn^{1,*}

¹Center of Excellence in Membrane Science and Technology, Department of Civil and Environmental Engineering, Faculty of Engineering, Prince of Songkla University, Songkhla 90110, Thailand

²Expert Center of Innovative Materials, Thailand Institute of Scientific and Technological Research, Khlong Luang 12120, Thailand

³Research Center for Environmental and Hazardous Substance Management (EHSM), Department of Environmental Engineering, Faculty of Engineering, Khon Kaen University, Khon Kaen 40002, Thailand

⁴Institut Européen des Membranes, IEM, UMR 5635, CNRS, ENSCM, University of Montpellier, CEDEX 5, 34095 Montpellier, France

*Correspondence: watsa.k@psu.ac.th; Tel.: +66-7428-7122

Article

Fouling Behavior in a High-Rate Anaerobic Submerged Membrane Bioreactor (AnMBR) for Palm Oil Mill Effluent (POME) Treatment

Wiparat Chaipetch ¹, Arisa Jaiyu ², Panitan Jutaporn ³, Marc Heran ⁴ and Watsa Khongnakorn ^{1,*} 

¹ Center of Excellence in Membrane Science and Technology, Department of Civil and Environmental Engineering, Faculty of Engineering, Prince of Songkla University, Songkhla 90110, Thailand; naamaan001@gmail.com

² Expert Center of Innovative Materials, Thailand Institute of Scientific and Technological Research, Khlong Luang 12120, Thailand; arisa@tistr.or.th

³ Research Center for Environmental and Hazardous Substance Management (EHSM), Department of Environmental Engineering, Faculty of Engineering, Khon Kaen University, Khon Kaen 40002, Thailand; panitju@kku.ac.th

⁴ Institut Européen des Membranes, IEM, UMR 5635, CNRS, ENSCM, University of Montpellier, CEDEX 5, 34095 Montpellier, France; marc.heran@umontpellier.fr

* Correspondence: watsa.k@psu.ac.th; Tel.: +66-7428-7122



Citation: Chaipetch, W.; Jaiyu, A.; Jutaporn, P.; Heran, M.; Khongnakorn, W. Fouling Behavior in a High-Rate Anaerobic Submerged Membrane Bioreactor (AnMBR) for Palm Oil Mill Effluent (POME) Treatment. *Membranes* **2021**, *11*, 649. <https://doi.org/10.3390/membranes11090649>

Academic Editor: Petros Samaras

Received: 24 July 2021

Accepted: 22 August 2021

Published: 25 August 2021

Publisher's Note: MDPI stays neutral with regard to jurisdictional claims in published maps and institutional affiliations.



Copyright: © 2021 by the authors. Licensee MDPI, Basel, Switzerland. This article is an open access article distributed under the terms and conditions of the Creative Commons Attribution (CC BY) license (<https://creativecommons.org/licenses/by/4.0/>).

Abstract: The characteristics of foulant in the cake layer and bulk suspended solids of a 10 L submerged anaerobic membrane bioreactor (AnMBR) used for treatment of palm oil mill effluent (POME) were investigated in this study. Three different organic loading rates (OLRs) were applied with prolonged sludge retention time throughout a long operation time (270 days). The organic foulant was characterized by biomass concentration and concentration of extracellular polymeric substances (EPS). The thicknesses of the cake layer and foulant were analyzed by confocal laser scanning microscopy and Fourier transform infrared spectroscopy. The membrane morphology and inorganic elements were analyzed by field emission scanning electron microscope coupled with energy dispersive X-ray spectrometer. Roughness of membrane was analyzed by atomic force microscopy. The results showed that the formation and accumulation of protein EPS in the cake layer was the key contributor to most of the fouling. The transmembrane pressure evolution showed that attachment, adsorption, and entrapment of protein EPS occurred in the membrane pores. In addition, the hydrophilic charge of proteins and polysaccharides influenced the adsorption mechanism. The composition of the feed (including hydroxyl group and fatty acid compounds) and microbial metabolic products (protein) significantly affected membrane fouling in the high-rate operation.

Keywords: anaerobic membrane bioreactor (AnMBR); wastewater; biofouling; protein; EPS

1. Introduction

Alternative energy sources are widely promoted for sustainable development, including in wastewater treatment. The palm oil industry is one of the industries that can practice effective energy recovery from its waste and wastewater [1,2]. Palm oil mill effluent (POME) has a high potential for energy recovery due to its high chemical oxygen demand (COD), which can be converted to biogas by anaerobic digestion [3–5]. POME has high organic content, high organic loading rate (OLR), and high sludge concentration, all of which enhance the potential for methane (CH₄) production. To produce biogas from POME, anaerobic membrane bioreactors (AnMBRs) have been proposed for their high capacity and small footprint; however, membrane fouling, which causes permeate flux decline, is a substantial limitation of the technique [6–8]. An understanding of fouling mechanisms and foulant composition is important to effectively control high-rate AnMBR

operation. Many researchers have studied fouling prevention strategies, such as air sparging [9] and filtration mode (relaxation) [10,11], among others. Fouling in a membrane reactor unit can be categorized as either reversible or irreversible. Reversible foulants include biomass, suspended solids, and inorganic precipitates, which form a cake layer attached at the membrane surface. Reversible fouling can be prevented by controlling hydrodynamic conditions or it can be removed by physical cleaning [11,12]. Irreversible foulants, on the other hand, are produced by microbial products, such as extracellular polymeric substances (EPS) forming a gel layer, and soluble microbial products (SMP) accumulating on the cake layer or in the membrane pores [12,13]. Irreversible fouling can be removed by chemical cleaning [11]. A substantial amount of research has evaluated fouling behavior in AnMBR, with different operational conditions affecting cake layer formation, EPS and SMP, and inorganic precipitates [13–18]. The operational conditions, especially the OLR, can affect microbial production, biomass concentration, and EPS concentration. The fouling of AnMBR in low-strength wastewater and/or at low-rate loading has been observed in many studies. For example, when an AnMBR was operated for a long term in a low-rate condition, the EPS concentration significantly increased with the increase in OLR [15]. High OLR also induced cake layer formation, which increased transmembrane pressure (TMP) due to high filtration resistance. The addition of biochar to reduce fouling propensity has been proposed as a solution. The addition of biochar resulted in less cake layer formation, as confirmed by confocal laser scanning microscopy (CLSM) and energy dispersive X-ray (EDX) analysis [18]. Under medium to high OLR, EPS accumulation in the cake layer has been shown to contribute most to system fouling, as confirmed by scanning electron microscopy (SEM), EDX, Fourier transform infrared (FTIR) spectroscopy, CLSM, zeta potential, roughness, and contact angle [13]. In addition, a higher OLR can cause EPS to be more viscous and hydrophobic, which makes it adhere easily to the membrane surface [14]. The effects of OLR on fouling have also been confirmed when using a ceramic membrane in AnMBR. During high-loading leachate wastewater treatment, fouling was affected by OLR > mixed liquor suspended solids (MLSS) > EPS > SMP [17].

In this study, a fabricated polysulfone (PSf) hollow fiber membrane was used for POME treatment by AnMBR. The cake layer and bulk suspension were characterized by FTIR, CLSM, roughness, and field emission scanning electron microscopy (FESEM) coupled with energy dispersive X-ray spectrometer (EDS) to observe and evaluate the fouling under high-rate conditions to understand the fouling composition and mechanisms over a long operation period.

2. Materials and Methods

2.1. Materials

POME and sludge samples were collected from a palm oil factory in Surat Thani, Thailand. The characteristics of POME, including pH, temperature, total COD (TCOD), soluble COD (SCOD), total solids (TS), volatile solids (VS), suspended solids (SS), and volatile suspended solids (VSS), were analyzed after acid fermentation to remove fat, oil, and grease (FOG) and large particles in wastewater (Table 1). The POME had high organic strength with TCOD and SCOD of 242 and 107 g/L, respectively. The TS was 18.5 g/L, while VS was 10.3 g/L. Thus, a large fraction of the solids was volatile. The SS and VSS were 8.9 and 3.2 g/L, respectively.

Table 1. Characteristics of palm oil mill effluent (POME) after pretreatment.

Parameter	pH	Temp. (°C)	TCOD (g/L)	SCOD (g/L)	TS (g/L)	VS (g/L)	SS (g/L)	VSS (g/L)
Pretreated POME	5.11	35	242	107	18.5	10.3	8.9	3.2

Note: total chemical oxygen demand (TCOD), soluble COD (SCOD), total solids (TS), volatile solids (VS), suspended solids (SS), and volatile suspended solids (VSS).

The inoculum sludge was analyzed following standard methods [19]. The initial concentrations of MLSS and mixed liquor volatile suspended solids (MLVSS) were 32.57 and 26.10 g/L, respectively.

2.2. Membrane Production and Characteristics

Polysulfone resin (19 wt%), polyvinylpyrrolidone K30 (2 wt%), and propylene glycol (PEG, 4 wt%) were dissolved in N-Methyl-2-pyrrolidone (NMP) at approximately 70 °C for about 5 h to form a homogeneous dope solution. Then, the dope solution was transferred into a polymer dope tank and kept overnight at 40 °C to eliminate the air bubbles formed during stirring and pouring. The degassed dope solution was used to fabricate polysulfone hollow fiber membranes (PSf) through a dry-wet spinning process. Distilled water and tap water at room temperature were used as bore fluid and coagulant, respectively. The dope solution and bore fluid (water) were pressurized by nitrogen gas through a spinneret, with an outer tube diameter of 1.06 mm and inner tube diameter of 0.66 mm, to form a coagulation bath of water. After separation and solidification, the membranes were collected by a roller. The obtained membranes were immersed in water over 3 days to completely remove the NMP used in the membrane fabrication. Next, the membranes were immersed in 10% aqueous glycerine solution for 1 h to preserve the pore structure during drying. The fabricated membrane had a molecular weight cut-off (MWCO) of 67 kDa. The virgin membranes were characterized for morphology, chemical composition, and roughness by FESEM with EDS (FEI/Apreo, Eindhoven, Netherlands), FTIR (Vertex 70, Bruker, Germany), and atomic force microscope (AFM; Flex Axiom, Nanosurf, Switzerland), respectively.

2.3. Experimental Setup and Operation of Anaerobic Membrane Bioreactor (AnMBR)

A schematic diagram of the AnMBR setup is presented in Figure 1. The AnMBR consisted of a hollow fiber membrane module with total surface area of 0.025 m² in a 10 L reactor. The module was comprised of 65 membrane fibers, each 24 cm in length, and a fiber outside diameter of 0.1 mm. The fibers were potted in a PVC module with epoxy resin, and the module had a diameter of 0.6 cm. The PSf hollow fibers were fixed only at the bottom. The module was operated in an outside-in flow regime under a vacuum pressure in the range of 0.15–0.25 bar, which was supplied by a peristaltic pump (Masterflex, L/S, Cole-Parmer, Chicago, IL, USA). The TMP at the head of the module was measured by the vacuum pressure gauge, which had a similar set-up to a typical membrane bioreactor operation [7,20]. The reactor was operated under a high OLR for 270 days. The overall operation was broken into three 90-day periods, named periods I, II, and III, during which the OLR was modified. The POME feed rate was controlled with a peristaltic pump at 3, 4, and 6.7 L/d for periods I, II, and III, respectively, which was equivalent to an OLR of 43, 57, and 99 kg COD/m³/d, respectively. At the end of each period, the membrane module was removed and chemically cleaned before the next period. After sludge removal, the fouled membrane from each period was collected for foulant characterization. The physical backwash was set up under 0.5 bar for 1 h followed by the chemical cleaning [11]. The chemical cleaning was achieved by soaking the physically cleaned membrane module in 1% acetic acid solution for 2 h, 1% NaOH for 2 h, and then 10% sodium hypochlorite for 2 h, respectively. The prolonged sludge retention time (SRT) was operated without extraction. However, small samplings were carried out for the purpose of this study.

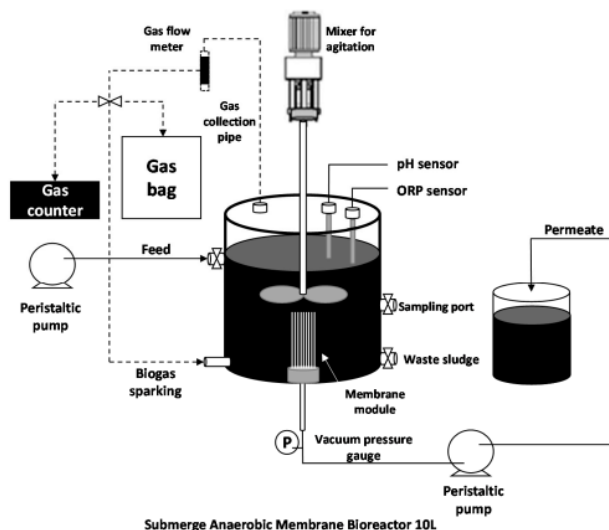


Figure 1. A diagram of the lab-scale submerged anaerobic membrane bioreactor (AnMBR).

2.4. Biomass Analysis

The biomass sample from the AnMBR system was measured for its MLSS, MLVSS, and EPS concentrations. MLSS and MLVSS in the reactor were measured twice a week using standard methods [19]. EPS solution was extracted from the bulk sludge suspension according to Li et al. [21]. EPS samples were analyzed for protein concentration through a modified Lowry method using a BSA standard [22] and for polysaccharide concentration through the phenol sulfuric acid method with glucose as a standard [23].

2.5. Membrane Fouling and Characterization

The membrane filtration was operated under subcritical flux in the TMP constant mode. The permeate flux and permeability rate were measured daily. To minimize physical fouling, gas sparging was added at 1.25 ± 0.25 L/hr through a gas recirculation from the AnMBR tank and internal liquid recirculation. At the end of each period, the foulants in the reactor and at the membrane surfaces were analyzed and characterized, as follows.

- Organic fouling

The hollow fiber membranes in the AnMBR were cut into small pieces of 1 cm length, and the biofilms (attached cells) were dyed with SYTO 9 for 30 min in the dark at room temperature, in order to analyze the distribution of the bacterial cells [24]. Then, the pieces of membrane sample were rinsed with $1 \times$ phosphate buffer saline (PBS) solution to remove excess dye and were incubated for 30 min in the dark, with a mixture of Sypro Orange (green) and Con A Alexa (red). The green represents the total proteins and the red represents polysaccharides, respectively [25]. After that, the membrane samples were rinsed by $1 \times$ PBS solution to remove excess dye from the membrane. The small membrane pieces in the transverse direction (20 mm thick slices) at -20 °C were examined immediately using CLSM (Fluoview FV300/Olympus, Tokyo, Japan). The functional groups of foulants on the membrane surface and the freeze-dried EPS were analyzed with FTIR.

- Inorganic fouling

The membrane preparation was conducted following a procedure reported by Kaya et al. [13]. The membrane morphology and inorganic foulants were characterized by

FESEM (FEI/Apreo) coupled with EDS (Oxford). The roughness of virgin and fouled membranes were analyzed by AFM (Flex Axiom, Nanosurf, Switzerland).

3. Results

3.1. The Relationship of Biomass and EPS

The average of MLSS concentrations during periods I, II, and III were 39.51 ± 2.49 , 38.04 ± 1.12 , and 36.71 ± 1.17 g/L, respectively. As the OLR in each subsequent period was increased by increasing the feed flow rate, higher concentrations of biomass in the reactor were achieved. In this experiment, a small fraction of biomass was lost as the membrane module was removed from the reactor for chemical cleaning between each period of the experiment. The average EPS concentration was around 166.02, 177.27, and 193.15 mg/L for periods I, II, and III, respectively. Protein made up a large fraction of EPS (77–79%), as shown in Figure 2a. The EPS concentration was not correlated to the biomass concentration, but EPS content increased with the increase in OLR in the reactor. The increase in OLR may have promoted sludge aggregation [26,27]. As shown in Figure 2a, high concentrations of protein were produced rather than polysaccharide. Consistent with this result, a previous study reported that protein had a low first-order kinetics constant (k) compared to polysaccharide. Thus, the increase in SRT can promote greater protein concentration in the biomass, rather than polysaccharide [28]. Biomass-associated product (BAP) formation in the EPS was shown [14,29]. From Table 2 and Figure 2b, the specific EPS was correlated to the average HRT, which agreed well with the results obtained by Santos et al. [29]. The increase in HRT enhanced the degradation of persistent organic substances in high OLR. The ratio of polysaccharine/protein (C/P) ratio was between 0.26–0.28, which was in a similar range to previous studies [21,29]. In addition, the specific protein concentration in EPS increased exponentially, while the polysaccharide increased linearly. A previous study has observed this trend [14]. Increasing feed rate and microorganism concentration caused an increase in C/P. The F/M ratio was higher than 2.5 for high OLR—a finding also confirmed in previous research [30], in which the EPS concentration decreased as F/M decreased. The production of EPS from biological metabolism was conclusively dependent on feed condition, F/M ratio, and HRT.

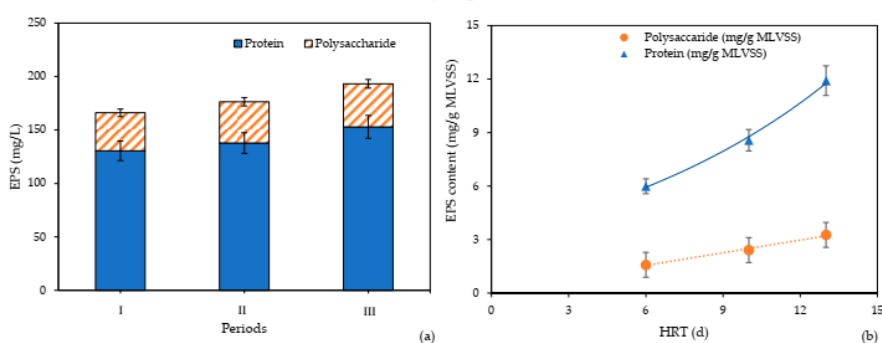


Figure 2. EPS characteristic: (a) composition and (b) specific EPS content as a function of HRT.

3.2. Membrane Filtration Performance

The filtration performance was assessed at different OLRs. Meanwhile, the internal recirculation rate with gas sparging was used to inhibit particle accumulation. According to the operational conditions, the average flux was 2.00, 2.04, and 2.02 L/m²/h during periods I, II, and III, respectively (Figure 3a). The obtained flux slightly fluctuated at the beginning of the experiment with the controlled TMP lower than 0.3 bar to prevent membrane deformation. Then, the TMP and permeability slightly increased in the middle

period and gradually increased until 0.25 bar was reached. The operation of each period was stopped when the final permeate flux was as low as $1.85 \text{ L/m}^2/\text{h}$. Critical flux control and internal recirculation were used to induce shear stress on the membrane surface to minimize particulate fouling. An accumulation of suspended solids in the reactor increased the viscosity of the supernatant. The high rate of recirculation was intended to avoid clogging and accumulation of solids. The control of hydrodynamic conditions by internal recirculation and the critical flux control can prolong the membrane filtration period, resulting in less frequent cleaning [15,31,32].

Table 2. EPS substances and fouling parameters evaluated for each OLR.

Period	OLR ($\text{kgCOD/m}^3 \times \text{d}$)	HRT (d)	EPS (mg/g MLVSS)			CLSM Thickness (μm)		TMP Rate (bar/d)
			Polysaccharide	Protein	C/P	Polysaccharide	Protein	
I	43	13	3.26 ± 0.13	11.91 ± 0.77	0.27	10.16 ± 2.33	10.74 ± 2.91	0.191 ± 0.017
II	57	10	2.41 ± 0.25	8.57 ± 0.94	0.28	15.34 ± 2.97	17.52 ± 3.99	0.195 ± 0.017
III	99	6	1.58 ± 0.17	5.99 ± 0.66	0.26	16.24 ± 2.74	157.56 ± 81.46	0.192 ± 0.016

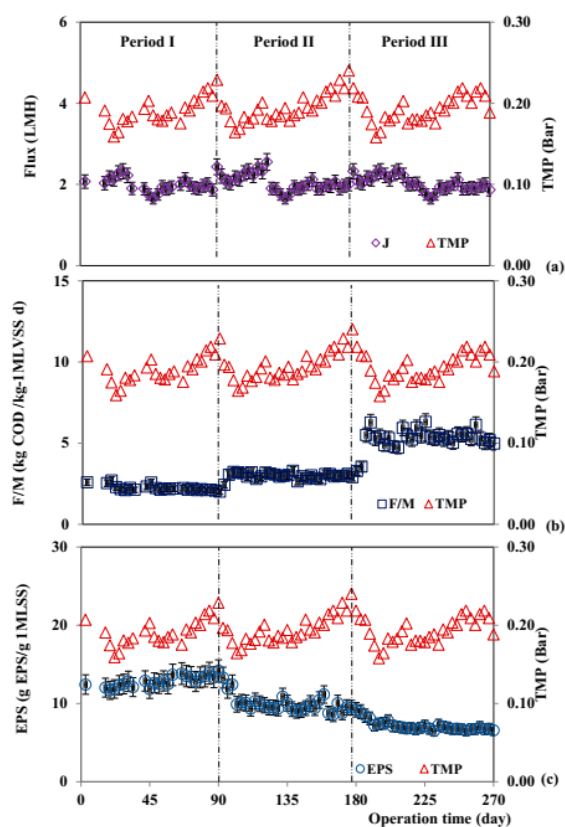


Figure 3. Flux (a), F/M (b), and EPS (c) profiles compared to TMP during operational periods I, II, and III.

OLR increased and HRT decreased from period to period, while TMP rate (dP/dt) was nearly equal (Table 2). Within each period, the TMP increased due to the increase in the resistance of membrane (Figure 3). As TMP increased, the concentration polarization and the number of collisions between particles increased. The increasing pressure also forced the particles to approach the membrane pores, thus inducing pore blocking after cake formation. Also, the EPS accumulation in the cake layer could have been released into the pore, causing pore blocking. High EPS concentration is an indication of biopolymers attached to the membrane surfaces, which also increases membrane resistance [29], especially in period II (Figure 3).

The higher OLR induced an increase in F/M ratio (Figure 3b) and a decrease in specific EPS in the system (Figure 3c). The average F/M ratio was 2.0, 3.2, and 5.5 g COD/g MLVSS/d. The MLSS concentration varied similarly to the F/M ratio and TMP. Once MLSS reached the critical concentration of 40 g/L, it caused TMP to rise rapidly. This jump in TMP was caused by a strongly attached cake layer on the membrane surfaces. On the other hand, for period II, the MLSS concentration did not change, but the TMP jumped at day 159. This result indicated that, not only was TMP affected by MLSS, but also affected by the composition of the colloid or supernatant in the reactor. The TMP result agreed with EPS characterization results (Figure 2), in which the concentration of polysaccharide remained unchanged but proteins increased with time. There is a possibility that the increment of cake layer was related to increasing EPS. The greater protein concentration in the EPS resulted in greater fouling behavior in AnMBR. Many studies have reported that protein, rather than polysaccharide, was the main contributor to membrane fouling [17,18]. In addition, the increase in OLR rather than EPS production significantly affected fouling and was associated with other operational parameters in AnMBR [17]. It should be noted, though, that this study refers to a lab-scale implementation and, therefore, the critical numerical values of MLSS must be verified in pilot- or field-scale plants.

3.3. Organic Foulant

CLSM

As seen in Figure 4, CLSM images illustrated the increasing spatial distribution of a thick cake layer and the accumulation of microorganisms and EPS (in the form of protein and polysaccharide). Moreover, as the OLR of the AnMBR reactor increased, the thickness and the specific EPS also increased (Table 2). The thickness of proteins was higher than that of polysaccharides. The spatial distribution of the protein showed that protein more easily attached on the membrane surface than polysaccharide, due to the charge of the membrane surface [17]. At the beginning, our study observed the attachment of a polysaccharide layer followed by the deposition of protein on the cake layer. Matar et al. [25] observed similar results that indicated that protein is a major biofoulant in EPS, as analyzed by CLSM. The distribution of microbial flocs, mainly protein (green color in Figure 4), was clearly found at the bottom of the membrane fibers. It can be concluded that fouling was caused by adsorption of proteins, followed by a deposition of proteins on the membrane surface that leads to the entrapment of proteins in the pores (as can be called pore blockages). The accumulation of protein EPS in the biomass granule and at the membrane surface can occur even under shear force at the surface due to increased gas sparging, demonstrating the accumulation and attachment was caused by the surface charge interaction [33,34]. The presence of proteins and polysaccharides in the hydrophilic fractions of organic substances resulted in irreversible fouling of different membranes.

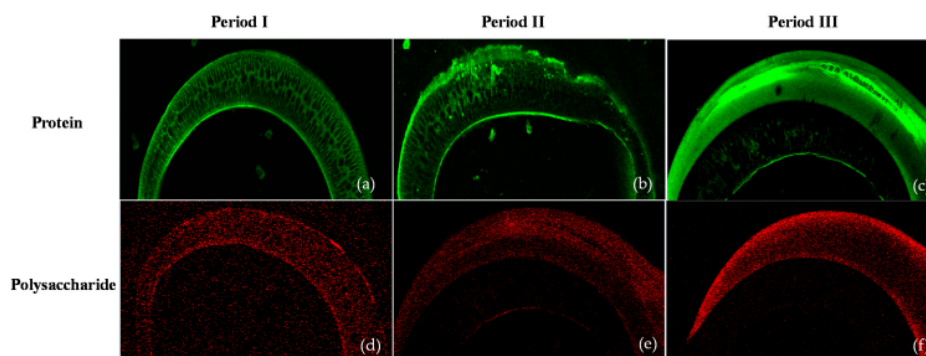


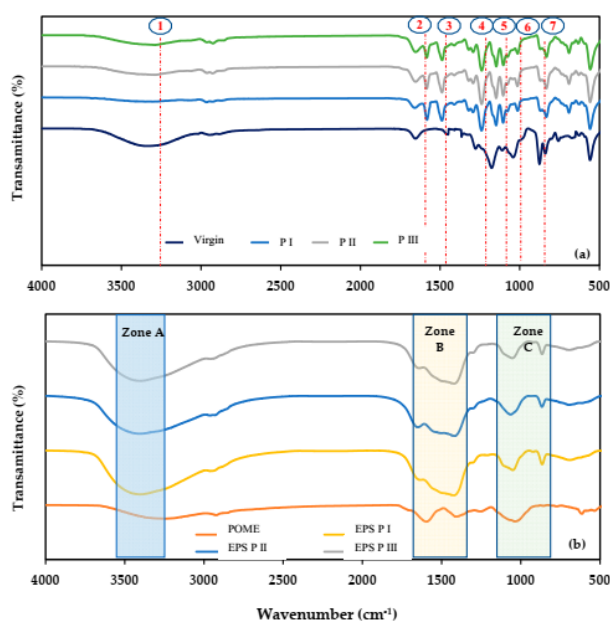
Figure 4. CLSM images of cake layer in AnMBR: period I (a,d), period II (b,e), and period III (c,f).

FTIR

Summary of FTIR spectra peak assigned for the samples is showed in Table 3. The FTIR spectra of the virgin membrane showed peaks at 3288 cm^{-1} , 2964 cm^{-1} , 1584 cm^{-1} , 1244 cm^{-1} , 1115 cm^{-1} , 832 cm^{-1} , and 558 cm^{-1} (Figure 5a). These peaks were attributed to aliphatic amide, O-S-O stretching, C-O-C stretching, C-C aromatic, and C-H stretching of aromatic ring of PSf from the reaction of polymer chain [35]. The fouled membranes had peaks at 1638 cm^{-1} and 1400 cm^{-1} that corresponded to protein EPS in amide I functional group (peak 2) and amide II functional group (peak 3) (Figure 5a), which was also observable in zone B of the EPS (Figure 5b). These peaks were caused by the formation and release of biomass products on membrane surfaces [13]. Strong and high spectra were observed in period II, which correlated to the higher concentration of biomass in the reactor. On the contrary, the high OLR caused a high F/M ratio and induced the excretion of SMP to be higher than EPS, which led to membrane fouling [30]. In addition, the polysaccharides, which contain carbohydrates, presented a peak at 1040 cm^{-1} on fouled membranes. This peak disappeared in EPS but clearly presented in the permeate, suggesting that a fraction of polysaccharides can pass through the membrane. Once the biomass was attached to the membrane surfaces, the cake layer and gel layer were formed, causing biofouling, especially by proteins [25]. The FTIR spectra showed peaks at 3246 cm^{-1} , 1597 cm^{-1} , 1408 cm^{-1} , 1255 cm^{-1} , 1036 cm^{-1} , and $610\text{--}870\text{ cm}^{-1}$ (Figure 5b). These peaks corresponded to hydroxyl ions (O-H stretching), fatty acid and lipids (C-H linkage stretching), aliphatic methylene groups [36], nitrogen compound (C=N stretching), lignin [37], C-O stretching of polysaccharides, phosphorus compounds (P=O stretching), short C chains (humic acids), and inorganics (Si-O complex), respectively [36–38]. Moreover, the peak at 1231 cm^{-1} that was assigned to the stretching vibration of P=O in POME disappeared in EPS, but it was observed at low intensity on the fouled membrane surfaces. The absence of a P=O peak has previously been attributed to mineral complexes and phosphorus precipitation on membrane surfaces [39]. The presence of inorganic peaks, silica complexes, and humic acid formation [36] were found at the membrane surfaces, which will be discussed in the inorganic foulant section. Moreover, the peak at 864 cm^{-1} (peak 7), which was related to the stretching vibration of C–O–C from glycosidic bonds, was found in fouled membranes and Zone C of the EPS.

Table 3. Summary of FTIR spectra peak assigned for the samples.

Sample	Wavelength (cm ⁻¹)
POME	3246, 1597, 1408, 1255, 1036, 610–870
Virgin membrane	3288, 2964, 1584, 1244, 1115, 832, 558
Fouled membrane	1638, 1400, 1231, 1040, 864
EPS	3285, 1638, 1400, 1231, 1040, 864

**Figure 5.** FTIR spectra of (a) virgin and fouled membranes and (b) POME and EPS in each period.

3.4. Inorganic Foulant

FESEM

FESEM images of the top surface (Figure 6a) and cross-section (Figure 6b) of the formed cake layer in the ultrafiltration hollow fibers in AnMBR showed that the top surface of the virgin membrane was smooth and uniform, which indicated good fouling resistance of the membrane [25,40]. The elemental composition of the virgin membrane according to EDX was primarily C, O, N, and S (Figure 6c). Differences in the elemental composition of the virgin and fouled ultrafiltration membranes collected from period I (Figure 6f), period II (Figure 6i), and period III (Figure 6l) were observed. The elements Na, Mg, and Si were present in the fouled membranes. The increase in C and O in the fouled membrane implied that the bio-foulant (EPS) covered and interacted with organic compounds on the membrane surfaces [25]. In addition, inorganic scaling on the fouled membranes showed an increasing signal at Mg and Si peaks caused by the increasing OLR. The increased signal at inorganic peaks can be attributed to the evidence presented in FTIR (Figure 5). In addition to bio-foulants, inorganic scaling also induced fouling behavior in the long-term operation of this lab-scale AnMBR used for POME treatment under high OLR. The thickness of the cake layer formed on the membrane surfaces, which

was calculated using the constant flux rate, differed according to the OLR. The thickness of the cake layer was $1.067 \pm 0.231 \mu\text{m}$ (Figure 6e), $8.431 \pm 0.855 \mu\text{m}$ (Figure 6h), and $8.366 \pm 0.599 \mu\text{m}$ (Figure 6k), respectively, for the three periods. The cake layer seemed to be caused by the accumulation of microorganisms and their products. Microorganism products, especially the inorganic compounds, interacted with increasing biomass on PSf membrane surfaces. With a MLSS of 40 g/L, the morphology signified the most compact cake layer at the highest OLR in period III (Figure 6k). The foulant layer was comprised of both organic and inorganic substances and a dense and compressed sludge deposition. The morphology and thickness of the foulant layer on the membrane surfaces impacted the filtration performance, as a sudden increase in TMP was observed at the end of each period (Figure 3).

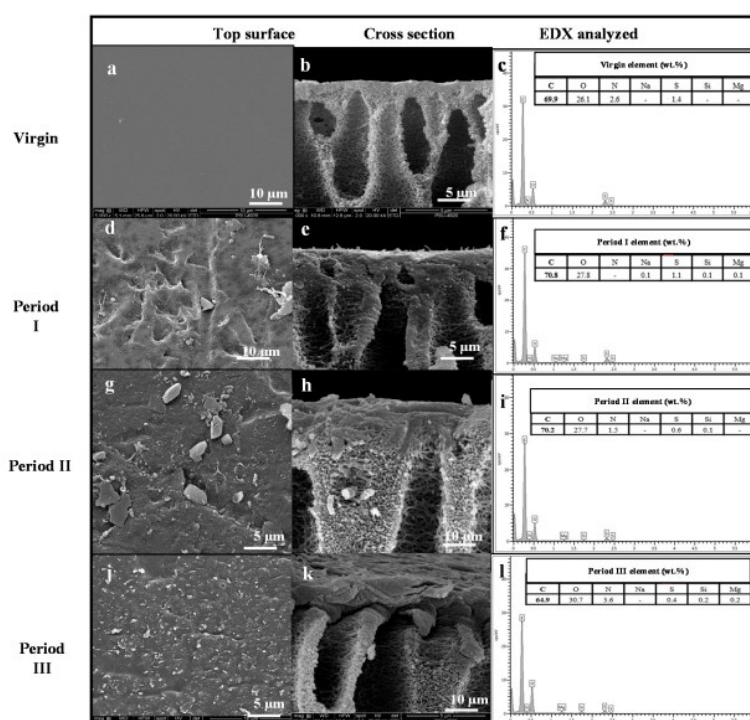


Figure 6. FESEM of the virgin membrane (a): top surface, (b): cross section, (c): EDX element), fouled membrane in period I (d): top surface, (e): cross section, (f): EDX element), fouled membrane in period II (g): top surface, (h): cross section, (i): EDX element), and fouled membrane in period III (j): top surface, (k): cross section, (l): EDX element).

Roughness of the Membrane

The surface probe micrograph (AFM) results indicated a typical morphology (hills and valleys) for membranes (Figure 7). The top surface of the virgin membrane was smooth, which minimized the possibility of solute molecules adhering on the membrane surface and induced less fouling. The average roughness values of the virgin and fouled membranes from period I, II, and III were 44.77, 50.08, 60.58, and 75.80 nm, respectively. The increase in roughness indicated the propensity of pore plugging or fouling of membrane surfaces.

The surface of the fouled membranes after the cake layer was removed showed an increase in roughness with the increase in OLR. The EPS components filled the membrane pores as a result of the increase in OLR [41]. The EPS indicated the release of microorganism products that adhered in the membrane pores even though the cake layer was removed. Furthermore, the hydrophilic property of the membrane surface gave it a tendency to interact and form chemical bonds with EPS [7,14]. The membranes with smoothed surfaces were less prone to fouling; therefore, flux decline over time was not observed in this study. Previous studies [7,21,26,41] also reported that the loosely bound EPS had a large effect on the membrane pores for adsorption and deposition of organic and inorganic compounds. In addition, the EPS formation around the biomass granule induced the surface roughness increase, especially at a high loading rate [33,34].

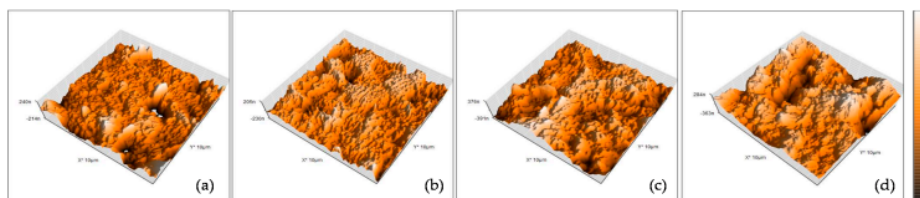


Figure 7. AFM image of the (a) virgin membrane, (b) fouled membrane in period I, (c) fouled membrane in period II, and (d) fouled membrane in period III.

4. Discussion

This study focused on evaluating fouling mechanisms and characterizing the foulants that occurred on a lab-scale AnMBR used to treat POME. We found that the predominant foulant was protein-EPS, which attached on the membrane surfaces through cake layer formation. The FTIR spectra of the cake layer on the fouled membranes showed peaks at 1638 cm^{-1} and 1400 cm^{-1} . The layer had a compact structure and was high in thickness of the protein portion. The increase of surface roughness reduced the membrane hydrophilicity (O-H stretching). The membrane hydrophobicity caused adhesion of protein molecules, adsorption at the membrane surface, and entrapment within membrane pores, respectively. The pore blocking mechanism occurred because of biofouling accumulation. The accumulation of microorganisms and cake layer increased but EPS products decreased due to the lower HRT. On the other hand, polysaccharides easily detached from the membrane as a result of their hydrophilic properties and the control of hydrodynamic conditions with internal recirculation. In addition, on the membrane surfaces, the cake layer was firmly attached, as was scaling by silica complexes combined with humic acid. The scaling on the fouled membrane was confirmed by EDX and FTIR results. These fouling mechanisms and the behavior of foulants can be considered as a progression (Figure 8). The correlation of fouling phenomena with TMP rising occurred over a 90-day period and could be broken into three stages as follows:

- (1) Stage I: initial fouling. The TMP slightly decreased over a short period during days 1 to 20, then a rapid increase of TMP occurred. During the initial decrease of TMP, the flux increased and approached the critical flux ($2.8\text{ L/m}^2/\text{h}$). After that, the cake layer materialized. The flux decreased and reached the local flux instead, causing the TMP to increase from 0.15 bar to 0.18 bar. The organic substances in the bulk feed were the major foulants on membrane surfaces. During this stage, the effect of foulant accumulation in the membrane pores (pore blocking) was minor.
- (2) Stage II: intermediate adsorption fouling. From day 20 to 70, the TMP remained constant at 0.20 bar. The cake layer was attached to the membrane surfaces, for which EPS, especially proteins, was adsorbed on the surfaces. A fraction of EPS

was accumulated in the membrane pores and was entrapped there by the charge adsorption process.

- (3) Stage III: cake and pore blocking. Day 71 onwards, the TMP had risen to 0.25 bar. A dense cake layer accumulated at the surface, and pore blocking occurred simultaneously. In addition, adjacent to the cake layer, the bound EPS released and attached to the membrane.

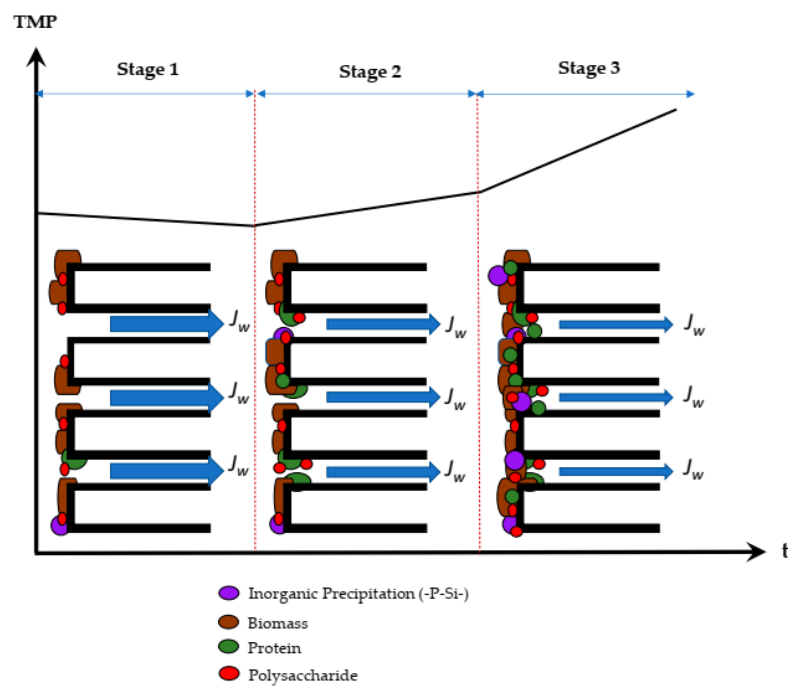


Figure 8. Behavior of foulants in AnMBR for high-rate POME treatment.

Overall, this study presented insight into the effect of operational parameters on fouling behavior in the lab-scale AnMBR during long-term operation. However, in order to commercialize AnMBR for POME treatment in a full-scale operation, the reported design and management results obtained need to be verified on larger-scale systems, and pre-treatment to remove suspended solid may be needed to mitigate membrane fouling.

5. Conclusions

A high organic loading rate anaerobic membrane bioreactor was operated for 270 days (considered a long operation period). Fouling mechanisms were investigated, providing the following conclusion:

- The growing cake layer, which resulted from high OLR and high MLSS, initiated biofilm formation on the membrane surfaces. The biofilm, in turn, bridged across the pores, resulting in increased TMP.
- EPS accumulated on the cake layer and, thus, plugged the membrane pores. The fouling from polysaccharide EPS can be mitigated by control of hydrodynamic conditions using internal recirculation. Due to the charge on the surfaces and the interaction

between proteins and the membrane surface, the removal of protein EPS fouling was more difficult.

- The precipitation of inorganic compounds, silica, and phosphorus, also occurred in the AnMBR system. These compounds were then attached to the cake layer and caused membrane fouling.

Hence, in order for the lab-scale AnMBR to extend its operation time with high OLR, the two following conditions must occur: MLSS must be lower than 40 g/L and the internal recirculation must be higher than 1.25 L/d. High internal recirculation is needed to create violent hydrodynamic turbulence and minimize fouling. Furthermore, to improve the surface charge of the membrane (i.e., for fouling mitigation), future research should focus on the modification of membrane surface properties to reduce the charge interaction between foulants and membrane surfaces.

Author Contributions: Conceptualization: W.K.; investigation: W.C. and A.J.; resources: W.K. and A.J.; data curation: W.K. and W.C.; writing—original draft preparation: W.K. and W.C.; writing—review and editing: W.K., P.J. and M.H.; supervision: W.K. and M.H.; funding acquisition: W.K. and W.C. All authors have read and agreed to the published version of the manuscript.

Funding: The research was financially supported by the Thailand Research Fund (TRF) and Tha Chang Palm Oil Industries, Co., Ltd. through a Research and Researcher for industries (RRI) under contract number “PHD58I0056”.

Institutional Review Board Statement: Not applicable.

Informed Consent Statement: Not applicable.

Data Availability Statement: Not applicable.

Acknowledgments: The authors would like to thank Center of Excellence in Membrane Science and Technology and Department of Civil and Environmental Engineering, Faculty of Engineering, Prince of Songkla University for partial support of this study.

Conflicts of Interest: The authors declare no conflict of interest.

References

1. Krishnan, S.; Md Din, M.F.; Taib, S.M.; Nasrullah, M.; Sakinah, M.; Wahid, Z.A.; Kamyab, H.; Chelliapan, S.; Rezanian, S.; Singh, L. Accelerated two-stage bioprocess for hydrogen and methane production from palm oil mill effluent using continuous stirred tank reactor and microbial electrolysis cell. *J. Clean. Prod.* **2019**, *229*, 84–93. [\[CrossRef\]](#)
2. Abdulsalam, M.; Man, H.C.; Idris, A.I.; Yunus, K.F.; Abidin, Z.Z. Treatment of palm oil mill effluent using membrane bioreactor: Novel processes and their major drawbacks. *Water* **2018**, *10*, 1165. [\[CrossRef\]](#)
3. Teng, T.T.; Wong, Y.-S.; Ong, S.-A.; Norhashimah, M.; Rafatullah, M. Start-up Operation of Anaerobic Degradation Process for Palm Oil Mill Effluent in Anaerobic Bench Scale Reactor (ABSR). *Procedia Environ. Sci.* **2013**, *18*, 442–450. [\[CrossRef\]](#)
4. Tan, S.P.; Kong, H.F.; Bashir, M.J.K.; Lo, P.K.; Ho, C.D.; Ng, C.A. Treatment of palm oil mill effluent using combination system of microbial fuel cell and anaerobic membrane bioreactor. *Bioresour. Technol.* **2017**, *245*, 916–924. [\[CrossRef\]](#) [\[PubMed\]](#)
5. Aziz, N.I.H.A.; Hanafiah, M.M. the Potential of Palm Oil Mill Effluent (Pome) as a Renewable Energy Source. *Acta Sci. Malaysia* **2017**, *1*, 9–11. [\[CrossRef\]](#)
6. Cheng, H.; Li, Y.Y.; Guo, G.; Zhang, T.; Qin, Y.; Hao, T.; Li, Y.Y. Advanced methanogenic performance and fouling mechanism investigation of a high-solid anaerobic membrane bioreactor (AnMBR) for the co-digestion of food waste and sewage sludge. *Water Res.* **2020**, *187*, 116436. [\[CrossRef\]](#) [\[PubMed\]](#)
7. Balcioglu, G.; Yilmaz, G.; Gonder, Z.B. Evaluation of anaerobic membrane bioreactor (AnMBR) treating confectionery wastewater at long-term operation under different organic loading rates: Performance and membrane fouling. *Chem. Eng. J.* **2021**, *404*, 126261. [\[CrossRef\]](#)
8. Li, L.; Kong, Z.; Xue, Y.; Wang, T.; Kato, H.; Li, Y.Y. A comparative long-term operation using up-flow anaerobic sludge blanket (UASB) and anaerobic membrane bioreactor (AnMBR) for the upgrading of anaerobic treatment of N, N-dimethylformamide-containing wastewater. *Sci. Total Environ.* **2020**, *699*, 134370. [\[CrossRef\]](#)
9. Cerón-Vivas, A.; Kalboussi, N.; Morgan-Sagastume, J.M.; Harmand, J.; Noyola, A. Model assessment of the prevailing fouling mechanisms in a submerged membrane anaerobic reactor treating low-strength wastewater. *Bioresour. Technol.* **2018**, *268*, 460–469. [\[CrossRef\]](#)

10. Maaz, M.; Yasin, M.; Aslam, M.; Kumar, G.; Atabani, A.E.; Idrees, M.; Anjum, F.; Jamil, F.; Ahmad, R.; Khan, A.L.; et al. Anaerobic membrane bioreactors for wastewater treatment: Novel configurations, fouling control and energy considerations. *Bioresour. Technol.* **2019**, *283*, 358–372. [[CrossRef](#)]
11. Ruigómez, I.; González, E.; Guerra, S.; Rodríguez-Gómez, L.E.; Vera, L. Evaluation of a novel physical cleaning strategy based on HF membrane rotation during the backwashing/relaxation phases for anaerobic submerged MBR. *J. Memb. Sci.* **2017**, *526*, 181–190. [[CrossRef](#)]
12. Poojammong, K.; Tungsudjawong, K.; Khongnakorn, W.; Jutaporn, P. Characterization of reversible and irreversible foulants in membrane bioreactor (MBR) for eucalyptus pulp and paper mill wastewater treatment using fluorescence regional integration. *J. Environ. Chem. Eng.* **2020**, *8*, 104231. [[CrossRef](#)]
13. Kaya, Y.; Bacaksiz, A.M.; Bayrak, H.; Vergili, I.; Gönder, Z.B.; Hasar, H.; Yilmaz, G. Investigation of membrane fouling in an anaerobic membrane bioreactor (AnMBR) treating pharmaceutical wastewater. *J. Water Process Eng.* **2019**, *31*, 100822. [[CrossRef](#)]
14. Chen, R.; Nie, Y.; Hu, Y.; Miao, R.; Utashiro, T.; Li, Q.; Xu, M.; Li, Y.Y. Fouling behaviour of soluble microbial products and extracellular polymeric substances in a submerged anaerobic membrane bioreactor treating low-strength wastewater at room temperature. *J. Memb. Sci.* **2017**, *531*, 1–9. [[CrossRef](#)]
15. Foglia, A.; Akyol, Ç.; Frison, N.; Katsou, E.; Eusebi, A.L.; Fatone, F. Long-term operation of a pilot-scale anaerobic membrane bioreactor (AnMBR) treating high salinity low loaded municipal wastewater in real environment. *Sep. Purif. Technol.* **2020**, *236*, 116279. [[CrossRef](#)]
16. Anjum, F.; Khan, I.M.; Kim, J.; Aslam, M.; Blandin, G.; Heran, M.; Lesage, G. Trends and progress in AnMBR for domestic wastewater treatment and their impacts on process efficiency and membrane fouling. *Environ. Technol. Innov.* **2020**, *21*, 101204. [[CrossRef](#)]
17. Burman, I.; Sinha, A. Anaerobic hybrid membrane bioreactor for treatment of synthetic leachate: Impact of organic loading rate and sludge fractions on membrane fouling. *Waste Manag.* **2020**, *108*, 41–50. [[CrossRef](#)]
18. Ye, L.; Xia, T.; Chen, H.; Ling, L.; Xu, X.; Alvarez, P.J.J.; Zhu, L. Effect of bamboo charcoal amendment on an AnMBR in the aspect of anaerobic habitat and membrane fouling. *Environ. Sci. Water Res. Technol.* **2018**, *4*, 2058–2069. [[CrossRef](#)]
19. APHA; AWWA; WEF. Standard Methods for examination of water and wastewater. APHA, AWWA, WEF. Standard Methods Exam. *Water Wastewater* **2012**. [[CrossRef](#)]
20. Bae, J.; Shin, C.; Lee, E.; Kim, J.; McCarty, P.L. Anaerobic treatment of low-strength wastewater: A comparison between single and staged anaerobic fluidized bed membrane bioreactors. *Bioresour. Technol.* **2014**, *165*, 75–80. [[CrossRef](#)]
21. Li, Z.; Tian, Y.; Ding, Y.; Wang, H.; Chen, L. Contribution of extracellular polymeric substances (EPS) and their subfractions to the sludge aggregation in membrane bioreactor coupled with worm reactor. *Bioresour. Technol.* **2013**, *144*, 328–336. [[CrossRef](#)]
22. Lowry, O.H.; Rosebrough, N.J.; Farr, A.L.; Randall, R.J. Protein measurement with the Folin phenol reagent. *J. Biol. Chem.* **1951**, *193*, 265–275. [[CrossRef](#)]
23. Dubois, M.; Gilles, K.A.; Hamilton, J.K.; Rebers, P.A.; Smith, F. Colorimetric Method for Determination of Sugars and Related Substances. *Anal. Chem.* **1956**, *28*, 350–356. [[CrossRef](#)]
24. Sun, F.Y.; Wang, X.M.; Li, X.Y. Visualisation and characterisation of biopolymer clusters in a submerged membrane bioreactor. *J. Memb. Sci.* **2008**, *325*, 691–697. [[CrossRef](#)]
25. Matar, G.; Gonzalez-Gil, G.; Maab, H.; Nunes, S.; Le-Clech, P.; Vrouwenvelder, J.; Saikaly, P.E. Temporal changes in extracellular polymeric substances on hydrophobic and hydrophilic membrane surfaces in a submerged membrane bioreactor. *Water Res.* **2016**, *95*, 27–38. [[CrossRef](#)]
26. Chen, L.; Cheng, P.; Ye, L.; Chen, H.; Xu, X.; Zhu, L. Biological performance and fouling mitigation in the biochar-amended anaerobic membrane bioreactor (AnMBR) treating pharmaceutical wastewater. *Bioresour. Technol.* **2020**, *302*. [[CrossRef](#)]
27. Zhang, Z.; Qiu, J.; Xiang, R.; Yu, H.; Xu, X.; Zhu, L. Organic loading rate (OLR) regulation for enhancement of aerobic sludge granulation: Role of key microorganism and their function. *Sci. Total Environ.* **2019**, *653*, 630–637. [[CrossRef](#)] [[PubMed](#)]
28. Cheng, H.; Hiro, Y.; Hojo, T.; Li, Y.Y. Upgrading methane fermentation of food waste by using a hollow fiber type anaerobic membrane bioreactor. *Bioresour. Technol.* **2018**, *267*, 386–394. [[CrossRef](#)]
29. Santos, F.S.; Ricci, B.C.; França Neta, L.S.; Amaral, M.C.S. Sugarcane vinasse treatment by two-stage anaerobic membrane bioreactor: Effect of hydraulic retention time on changes in efficiency, biogas production and membrane fouling. *Bioresour. Technol.* **2017**, *245*, 342–350. [[CrossRef](#)]
30. Liu, Y.; Liu, H.; Cui, L.; Zhang, K. The ratio of food-to-microorganism (F/M) on membrane fouling of anaerobic membrane bioreactors treating low-strength wastewater. *Desalination* **2012**, *297*, 97–103. [[CrossRef](#)]
31. Khongnakorn, W.; Wisniewski, C. Membrane fouling and physical characteristics of sludge in MBR system. *Desalin. Water Treat.* **2010**, *18*, 235–238. [[CrossRef](#)]
32. Wandera, S.M.; Qiao, W.; Jiang, M.; Gapani, D.E.; Bi, S.; Dong, R. AnMBR as alternative to conventional CSTR to achieve efficient methane production from thermal hydrolyzed sludge at short HRTs. *Energy* **2018**, *159*, 588–598. [[CrossRef](#)]
33. Tsui, T.H.; Chen, L.; Hao, T.; Chen, G.H. A super high-rate sulfidogenic system for saline sewage treatment. *Water Res.* **2016**, *104*, 147–155. [[CrossRef](#)]
34. Tsui, T.H.; Ekama, G.A.; Chen, G.H. Quantitative characterization and analysis of granule transformations: Role of intermittent gas sparging in a super high-rate anaerobic system. *Water Res.* **2018**, *139*, 177–186. [[CrossRef](#)] [[PubMed](#)]

35. Singh, K.; Devi, S.; Bajaj, H.C.; Ingole, P.; Choudhari, J.; Bhrambhath, H. Optical Resolution of Racemic Mixtures of Amino Acids through Nanofiltration Membrane Process. *Sep. Sci. Technol.* **2014**, *49*, 2630–2641. [[CrossRef](#)]
36. Huzir, N.M.; Aziz, M.M.A.; Ismail, S.B.; Mahmood, N.A.N.; Umor, N.A.; Faua'ad Syed Muhammad, S.A. Optimization of coagulation-flocculation process for the palm oil mill effluent treatment by using rice husk ash. *Ind. Crops Prod.* **2019**, *139*, 111482. [[CrossRef](#)]
37. Baharuddin, A.S.; Rahman, N.A.A.; Shah, U.K.M.; Hassan, M.A.; Wakisaka, M.; Shirai, Y. Evaluation of pressed shredded empty fruit bunch (EFB)-palm oil mill effluent (POME) anaerobic sludge based compost using fourier transform infrared (FTIR) and nuclear magnetic resonance (NMR) analysis. *Afr. J. Biotechnol.* **2011**, *10*, 8082–8089. [[CrossRef](#)]
38. Ng, K.H.; Cheng, Y.W.; Lee, Z.S.; Cheng, C.K. A study into syngas production from catalytic steam reforming of palm oil mill effluent (POME): A new treatment approach. *Int. J. Hydrog. Energy* **2019**, 20900–20913. [[CrossRef](#)]
39. Bao, P.; Xia, M.; Liu, A.; Wang, M.; Shen, L.; Yu, R.; Liu, Y.; Li, J.; Wu, X.; Fang, C.; et al. Extracellular polymeric substances (EPS) secreted by: *Purpureocillium lilacinum* strain Y3 promote biosynthesis of jarosite. *RSC Adv.* **2018**, *8*, 22635–22642. [[CrossRef](#)]
40. Ni, T.; Ge, Q. Highly hydrophilic thin-film composition forward osmosis (FO) membranes functionalized with aniline sulfonate/bisulfonate for desalination. *J. Memb. Sci.* **2018**, *564*, 732–741. [[CrossRef](#)]
41. Ding, Y.; Tian, Y.; Li, Z.; Zuo, W.; Zhang, J. A comprehensive study into fouling properties of extracellular polymeric substance (EPS) extracted from bulk sludge and cake sludge in a mesophilic anaerobic membrane bioreactor. *Bioresour. Technol.* **2015**, *192*, 105–114. [[CrossRef](#)] [[PubMed](#)]

APPENDIX III

Forward osmosis membrane technology for nutrient removal/recovery from permeates of a two-stage submerged anaerobic membrane reactor (sAnMBR)

1. Introduction

According to one of the major industries in the South of Thailand is Palm oil mill. From 2008 to 2012, the number and size of oil palm plantations was increase for crude palm oil (CPO) production and also the renewable energy as biodiesel boost. The CPO production up to 75% from 2016 to 2022 [1]. However, wastewater (palm oil mill effluent; POME) from CPO production produced 0.77-0.84 m³/ton fresh fruit bunch (FFB) that consisted of high concentration of organic compound (COD and BOD, fat and grease (FOG), and suspended solids (TSS) [2]. The traditional wastewater treatment plant is a waste stabilization pond series including anaerobic ponds, aerobic ponds, and polishing ponds, etc. Since 2001, Thailand participated Kyoto Protocol and concerned about greenhouse gas (GHG) emissions, upgrading of wastewater treatment plants in Palm oil industries was focused and developed for closed system to capture and utilize biogas as renewable energy [3]. According to the residue of organic content and color do not permit to drainage outside. Then the practical for treated POME is used for land application due to the essential of nutrients such as nitrogen (N), phosphorous (P) and potassium (K) for plant outgrowth [2, 4]. Hasanudin et al [2] found 13% of increasing FFB production after utilizing the treated POME as liquid fertilizer for land application. Nevertheless, the limitation of land treatment is not capable of handling high organic content and nutrient to optimize value to meet Thailand's Standards for affluent and Thai regulation for liquid fertilizer regulation. Concentration in term of biochemical oxygen demand (BOD), chemical oxygen demand (COD) and nutrient do not meet the of factory was set the outline value for effluent discharge for COD, BOD and colour is not over 120 mg/L, 20 mg/L, and 300 ADMI, respectively [5]. Many researches are focused on membrane technology for treatment organic content and nutrient in wastewater such as membrane bioreactor [6], anaerobic membrane bioreactor [7], nanofiltration(NF) and reverse osmosis (RO) [8], ultrafiltration couple with adsorption [9], etc. However, Nguyen et al. [10] shown the ammonia (NH₃), phosphorus and total organic carbon (TOC) removal efficiency in Forward osmosis (FO) about 96, 98 and 100%, respectively meanwhile FO capability can recovery of nutrients and reduced chemical cost [10,11]. FO is a challenge membrane technology relying on an osmotic gradient driving force pass through a dense membrane. The advantage of FO process is high rejection, high water recovery, low fouling propensity, requiring low energy for water recovery and lower or no hydraulic pressure [12]. However, the driving force of salt (high concentrate) could lead to salinity accumulation and nitrification. Thus, FO is the great interest for the implementation of water reuse schemes in stand-alone system or when combined with another process [13]. Other studies also demonstrated the potential of FO for the concentration of food and beverages, delivery of pharmaceutical, fertigation, or concentration of complex or highly charged liquids [14]. Many studies favor forward osmosis (FO) used for treat and recover nutrients in wastewater in AnMBR [14,15], enrichment N and P from digested sludge [16]. Phuntsho et al.[17] proposed and

studied pilot-scale fertilizer driven forward osmosis (FDFO) coupled with nanofiltration (NF) system to diluted fertilizer for agricultural for irrigation and obtained 49% recovery rate that fertilizer was used as draw solution (11).

The previous study had referred that FO in the different membrane which are cellulose triacetate (CTA) and thin film composite (TFC) FO membranes, that the water permeability and solute selectivity of in TFC-FO greater than CTA-FO. However, all of the ammonia ($NH_4^+ - N$) and phosphorus (PO_4^{3-}) removal was shown highly than 99% and 98% of TFC and CTA, respectively [10,18, 19, 20, 21, 22, 23 and 24]. The technology of FO has raised interest to the high level as a potential low-fouling contamination on membrane surface and a new approach for nutrient removal/recovery from wastewater [25-28]. Several types of draw solution were development for increased the FO filtration process especially part of osmotic pressure that to provide it high for enhance the water flux. However, the magnesium chloride ($MgCl_2$), potassium nitrate (KNO_3), magnesium sulfate ($MgSO_4$), trimethylamine-carbon dioxide (TMA-CO₂), ammonium bicarbonate (NH_4HCO_3), ammonium hydroxide (NH_4OH) and sodium chloride (NaCl) etc. were used as draw solution in FO process. The lowest of viscosity from NaCl was the best option for select the NaCl for the draw solution in FO [29]. Moreover, the fouling phenomena, concentration polarization, and reverse diffusion of solution from draw solution are challenge in FO operation. The FO was focused on following requirements: (I) low reverse salt diffusion; (II) increase water flux; (III) easy recovery of DS (diluted) and (IV) cost and energy saving to operation. In addition, the main point of DS in FO systems is preferred to be easy to regenerate, non-toxic, and to be economical; while the way of practice for diluted DS would be directly utilized to; fertigation or feed solution in feed solution in desalination plants [30-32]. Therefore, selection of appropriate draw solution or osmotic agent is crucial to achieve high FO membrane performance.

This study treated wastewater in the palm oil mill effluent from permeates of a two-stage submerged anaerobic membrane reactor (T-POME) and tested its performances of TFC membrane and CTA membrane by FO processing with the difference organic loading rate (OLR) for 43, 57 and 99 kgCOD/m³/day in loading 1 (L1), loading 2 (L2) and loading 3 (L3), respectively. The challenge of reverse diffusion of solution from draw solution in three different concentration was 2M, 3M and 4M NaCl was the main important for FO performance. Thus, the objective of this study was to investigate the comparison of the effect of different concentration of NaCl in TFC and CTA membrane when operated with FO process to remove/recover nutrients from T-POME.

2. FO experimental setup and operation conditions

The effluent from two-stage sAnMBR or permeate was used to feed solution in forward osmosis process (FO). FO flat sheet membrane was used in this study with an effective area (A_m) was 50 cm². NaCl was used as draw solution (DS) and finding the optimum condition. A schematic representation of FO process shown in **Figure 1**. FO process was operated by two type of flat sheet membrane as thin film composite (TFC) commercial (Aquaporin Inside™; Steritech, Kongens Lyngby, Denmark) and cellulose triacetate (CTA) commercial (Hydration Technologies, Inc; HTI, Albany, OR, United States). However, normally of the specification of CTA and TFC membrane was shown in **Table 1** [33-38]. The performance of filtration process was compared in both of membrane. The experiment was conducted in co-current mode at room temperature. The membrane module cell (15cmx10cmx0.3cm) was operated by using peristaltic pumps connect to the module. Peristaltic pump (Masterflex L/S, USA) was used for feed solution side and draw solution (DS) side at room temperature (25 ± 0.5 °C). The trans-membrane pressure (TMP) will be monitoring by a pressure gauge in feed line and draw solution line.

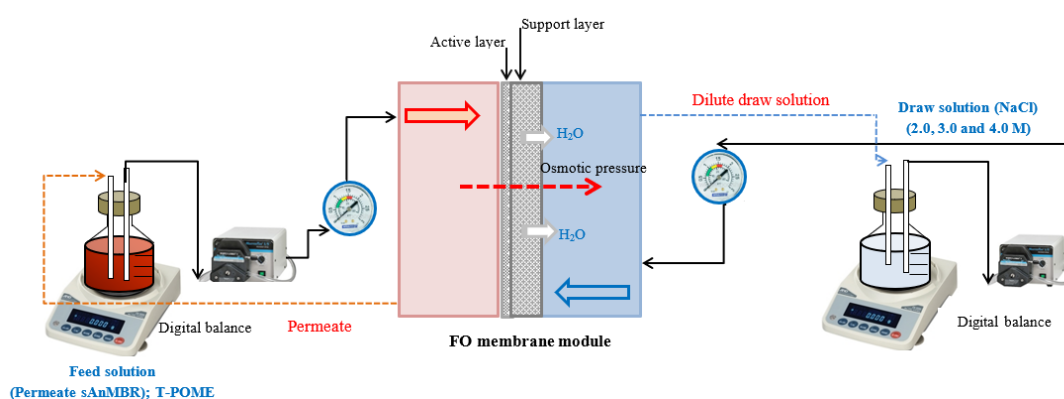


Figure 1 FO system

Table 1 The specification of CTA FO and TFC FO membrane shown in [33-38].

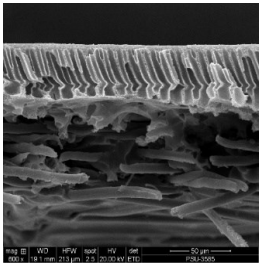
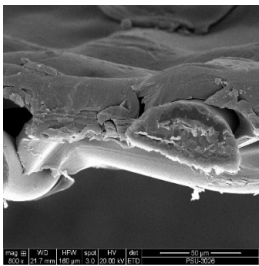
Membrane	Advantage	Disadvantage
TFC 	<ul style="list-style-type: none"> • rejection values higher • pH stability • higher selective water transport (100% selective to water molecules) • reduce internal concentration polarization (ICP) • minimum degradation • satisfy the chemical stability • mechanical strength requires 	<ul style="list-style-type: none"> • salt rejection relies on the surface charges and PA structure

Table 1 (continued) The specification of CTA FO and TFC FO membrane shown in [33-38].

Membrane	Advantage	Disadvantage
CTA 	<ul style="list-style-type: none"> • high water flux • high water permeability • the hydrophilic nature of CTA • better pore wettability and transport properties • pH range 3-7, 3 years of shelf life • maximum chlorine resistance 2 ppm • thin skin layer for salt separation (10-20 μm) • thicker porous scaffold layer (about 100 μm thick) 	<ul style="list-style-type: none"> • get degraded when exposed to an ammonium bicarbonate (DS) • less water permeability • low salt rejection • lacked a thick support layer • poor resistance to biological species, and limited chemical stability

It can be concluded that that TFC membrane exhibited exceptional selectivity and permeability properties with higher water flux and lower fouling tendency and decreased ICP as compared to CTA FO membranes [33-38]. However, TFC FO membrane exhibited good flux performance when operated in active layer on feed side.

2.1 Feed solution

In this work, three feed solutions (FS) were used with various organic loadings from loading 1 (L1) to loading 2 (L2) and loading 3 (L3) in 43, 57 and 99 kgCOD/m³/day, respectively. The operational conditions of this system (two-stage sAnMBR) were as follows: room temperature 35 ± 1 °C, stirring speed 30 rpm with two impellers, hydraulic retention time (HRT) of 3.3, 2.5 and 1.5 day. Three different nutrients in the feed solution (L1, L2 and L3) were 30.49 ± 1.15 , 30.52 ± 3.07 and 81.06 ± 5.10 mg/L of ammonia, 39.37, 35.71 and 42.13 mg/L of magnesium, 6.086, 7.629 and 16.321 mg/L of phosphate, 4.941, 9.315 and 3.55 mg/L of calcium and concentration of COD were 37.52 ± 3.10 , 48.21 ± 4.96 and 55.06 ± 4.15 g/L. Feed solution tank was placed on a digital balance (GF-300, AND, Japan).

2.2 Draw solutions

Three different concentrations of NaCl were used in 2M, 3M and 4M 99.99 Suprapur® were used in this study. DS was prepared by dissolving NaCl in deionized (DI) water. The concentration of NaCl measured by digital balance (GF-300, AND, Japan). For the feed and draw solution was single run with 1L and operated with 420 min. Both solutions were recirculated in a closed-loop system by a batch mode operation. DS tank was placed on a digital scale (GF-300, AND, Japan) and the weight changes were monitored and recorded by manually every 10 mins. interval to determine the water flux. The conductivity sensor (Inpro 7100, Mettler-Toledo, Switzerland) was

used to measure conductivity (reverse salt flux; RSF in the feed and concentration of NaCl).

2.3 Nutrient concentration recovery effect by FO process

Feed solution was is described in section 2.1. and 2.2 flow with co-current mode with 0.1 cm/s of velocity in both side (at room temperature; 25 ± 1). Also, at the end of each filtration run, permeate quality and feed concentration were analyzed. The concentration of sodium (Na^+), calcium (Ca^{2+}), magnesium (Mg^{2+}), potassium (K^+) and phosphate (PO_4^{3-}) were digested HNO_3 (5%) and determined by inductively coupled plasma–optical emission spectroscopy analysis (Avio 500 ICP-OES, PerkinElmer, USA). All of the experimental data were collected after 1 h filtration passed for prevent the adsorption of ions on the membrane surface that it has influencing in the FO performances.

2.4 FO test

The FO mode was carried with lab scale process and co-current flow. Water flux was analyzed with DI water at 0.10 cm/s in the feed side and peristaltic pump (EYELA MP-3N, Japan) controlled a velocity at 0.70 cm/s for draw solution flow rate. The pressure was monitored by a pressure transducer (TR-PS2W, Lutron, Taiwan) in both sides.-The previous work [39] had been presented-terms of water permeance (A , LMH/Bar), salt rejection (R , %) and salt permeability (B , LMH) were tested with RO mode. Measured the permeance of DI water as the feed that using the cross-flow filtration method to evaluate the separation efficiency of TFC FO membrane and CTA FO membrane which calculated by Eqs. (1) and (2). Salt rejection and salt permeability were measured by utilizing NaCl as the feed solution, and were calculated by Eqs. (3) and (4). In addition, these tests were performed each experiment by also carried out after each experiment for recheck the membrane performance.

$$J_v = \frac{\Delta v}{A_m \cdot \Delta t} \quad (1)$$

$$A = \frac{J_v}{\Delta P} \quad (2)$$

$$R = \left(1 - \frac{C_p}{C_f}\right) \times 100 \quad (3)$$

$$\frac{1-R}{R} = \frac{B}{A(\Delta P - \Delta \pi)} \quad (4)$$

Where A_m , is the effective FO membrane surface area (50 cm^2), ΔV (L) is the permeate volume change from the feed solution to the draw solution over a determined testing time Δt (h). A and J_v are water permeability and water flux (in $\text{Lm}^{-2}\text{h}^{-1}\text{bar}^{-1}$ referred to $\text{LMH}\cdot\text{bar}^{-1}$). The solute rejection is calculated follow Eqs. (3) where C_p (mg/L) and C_f (mg/L) are salt concentration of the permeate solution and feed solution, respectively. R is a salt rejection (%), ΔP and $\Delta \pi$ are the applied different pressure and osmotic pressure of the feed respectively. Osmotic pressure, π , is the

pressure that would control the passage of FS across the membrane when applied with DS. The difference of osmotic pressure determines generally with the transport of water and transport salt through the membrane from FS to DS for FO processes. The effect of osmotic pressure gradient from lower concentration of DS to higher concentration of FS.

2.5 Surface properties for the fouling particles and the membrane morphology

The fouling layer of fouled and pure membrane (flat sheet) were analyzed the membrane foulants. Membrane surface characterization of was performed by selected and cut membrane after the end of operation period (L1, L2 and L3), soaking them in DI water for a few seconds to remove FS and DS, and then make it dried with desiccator for 1 day. The surface and cross-sectional morphologies and inorganic foulants of the fouled membrane were observed and characterized by scanning electron microscopy (SEM-Quanta, FEI Quanta 400) coupled with energy dispersive X-ray spectroscopy (EDX; Oxford) following the procedures in Woo et al. [40].

3. Results and discussion

3.1 Water permeability and membrane wettability

Contact angle is the physical characteristic that describing wettability of a surface membrane. It is the primary data which as to indicated the ability of surface of wetting and spreads over the surface. While the hydrophilic of the membrane with different thin active layers was studied by measuring the contact angle value. In this case found top surface contact angle in CTA FO commercial and TFC FO commercial were summarized 64 and 75°, respectively. The specification of TFC flat sheet aquaporin was NaCl reverse flux was less than 2 gm⁻²h⁻¹ and the active layer made from polyamide as flat sheet aquaporin. The water permeability coefficient of CTA flat sheet (HTI) was 2.1x10⁻¹² ms⁻¹Pa⁻¹ while found 88% of salt rejection while the salt reverse flux was 0.027 mol. GMH. Xiao M. et al. [41] found that contact angle data in dry and wet membranes closely correlates with surface porosity and porous membrane swelling. In addition, the water contact angle higher that shown the higher selective water transport that some case reported 100% selective to water molecules. Although TFC FO membrane higher water permeability but more loss of water flux when comparison with CTA FO membrane.

3.2 Effect of different concentration NaCl on water flux

Two types of membranes include a commercial TFC and a commercial CTA. The results showed that TFC membrane exhibited higher water permeability but more loss of water flux in comparison with CTA. The long term (420 mins) of water flux was observed that both of membrane at all NaCl concentration shown the flux decreases in

Figure 2. The operation time at 120 mins obviously shown the water flux in TFC membrane slightly decreased while drastically reduced in CTA membrane. In generally, the reduction of water flux in membrane because of the viscosity's effect of the draw solution and thickness layer form on surface FO membrane [42]. Wang et al. [43] illustrated the effected of increasing DS concentration (ranged from 0.5 to 5 M) to water fluxes increased with FO process that can supported in NaCl (higher 2.0 to 4.0 M) which enhancing water flux (CTA: 9.2, 11.5 and 17 LMH) and (TFC: 9.8, 16.2 and 14.1 LMH) **Figure 2.** Higher salinity DS source (4M) in **Figure 2c** can efficiently improve the water flux of TFC and CTA in FO membrane also has greater potential flux with higher operation temperature. These results supported the high-water flux came from high concentration of DS which as a larger osmotic pressure. The highest of flux in TFC FO membrane found at loading1 that was closely to loading2 and highest at loading3 for CTA FO. Although, the increasing in loading 1 to 3 was not associated with increasing the DS concentration because of it did not enhance the flux efficiency in FO process. [42] reported that CTA membrane had lower water permeability and water flux when compared with TFC. However, the reduction effective of osmotic pressure in FO membrane came from the activity of accumulated salinity in the feed (salts can flow backward from DS to FS by diffusion process) let to reducing the water flux [44]. The reverse salt flux (RSF) phenomenon was affected to the decrease of water flux because it causes of internal concentration polarization (ICP) from FS to DS [44] The main reason of the increasing water flux is the upper flow rate (L1-L3) of DS (NaCl) can collected more effective osmotic pressure at the support layer because of permeate dilution quickly [10]. However, TFC-FO in 4M of L3 received gradually declined at 14.1 LMH with the salt concentration increasing.

After 240 mins of filtration, the FO membrane appeared the trend of permeate fluxed of CTA and TFC in different loading rate (43, 57 and 99 kgCOD/m³/day) was gradually declined as expected from increased osmotic pressure and high driving force from salt concentrate [39]. However, the permeate flux of loading 1 to loading 2 on three concentrated DS (NaCl; 2M, 3M and 4M) CTA membrane was slowly decreased about 0.31 LHM but increased in loading 3 that more than 0.70 LHM. On the other hand, the permeate flux of TFC membrane in loading 3 of all NaCl intensity has the most negligible value that less than the lowest loading 1 to 0.35, 0.81 and 1.25 LMH in 2M-4M NaCl, respectively. Thus, the rising DS concentrate in L1-L3 led to a stronger effect for both permeates water flux and reverse draw solute fluxes to increase.

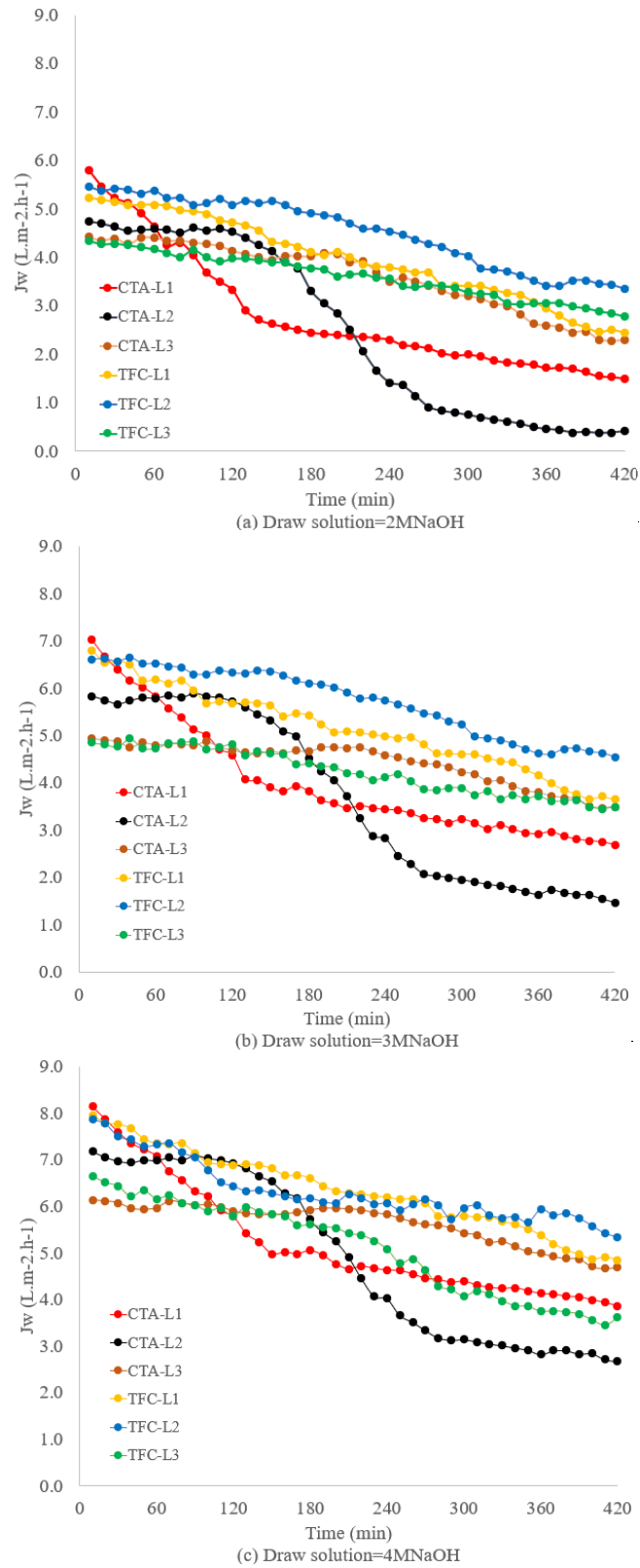


Figure2 The permeate flux versus TFC and CTA in FO filtration process for T-POME treated in different concentration of draw solution (a) 2M NaOH (b) 3M NaOH and (c) 4M NaOH

3.3 Nutrient concentrating effect by FO membrane

The increasing of draw solution concentration (2M, 3M and 4M) led to the gradual salinity increase in the DS to FS that show negative impact on nutrient removal because of it can be dispersed to the FS. Moreover, the increasing loading in the feed side of the FO operation showed the percentage of nutrient removal (calcium, magnesium, potassium, phosphorus and ammonia etc.) in FO process for CTA FO and TFC FO membrane was decreased in loading 1 to loading 2 and increasing in loading 3 in **Figur3**. Apart from trend of water flux up on the increasing of NaCl concentration, Liu et al. [45] reported the effect of concentration in draw solution can indicate the leakage rate of TOC, TN and $\text{NH}_4^+\text{-N}$ in FS also. Nitrogen and phosphorus are essential consideration for the nutrients due to important roles in metabolism as microorganisms from wastewater that as T-POME in this case. Nutrients removal efficiency achieved in this study is consistent with those reported in the literature (**Table3**) as high nitrogen removal (>95%) and phosphorus removal (>95%) were presented in [43 and 45-48]. For this case obvious that the removal of all nutrients (especially phosphate) was high to 100% in POME treatment by two-stage sAnMBR integrated with co-current flow mode in FO process by using TFC FO and CTA FO (flat sheet). In addition to surface adsorption, the uptake rate of phosphate also greatly depends on various factors, such as phosphorus deficiency [43].

The operated under 420 min, the two-stage AnMBR was started to feed solution (FS) with permeate AnMBR. The details of feed characteristics in the FO process were operating conditions in each experiment (L1, L2 and L3) are shown in **Table2**. Moreover, only a few hundred percent in evaluations of FO membrane for rejection efficiency and reverse salt flux (reverse ions transfers from the DS and FS) [11, 41]. However, the nutrient removal/recovery that came from permeate AnMBR (POME and sludge treated with two-stage AnMBR). The COD, ammonia (NH_4^+), and phosphorus concentration of the influent varies from 37.52-55.06, 30.49-81.06, 6.086-16.321 mg/L, respectively at different phases (L1 to L3) in **Table2**. **Figure 3** shown the COD removal efficiency in form of TFC-FO higher than CTA-FO that could be varied from 53%, 62% and 73% and 20%, 20% and 39% (L1, L2 and L3). Also, the same effected for the increased loading with high concentration DS was the removal efficiency increase in both membranes. The ammonia removal efficiency of TFC-FO and CTA-FO found the same at one hundred percent of removal in L2 and after that slowly down to 78% and 91% in L3, respectively which might be possibility that the salinity was sodium ions (Na^+) leaked from the draw solution [43]. Driver et al. and Loeb et al. [48,49] found the increase of pH (8.0-9.5) and Ca/P ratio in FO process is the one cause which led to the enhance precipitation of the form of amorphous calcium phosphate (ACP) from PO_4^{3-} , calcium (Ca^{2+}), magnesium (Mg^{2+}), NH_4^+ . However, the increasing of Ca^+ and Mg^+ salts were relatively with collected phosphate salts in **Table2** that would reduce the effective osmotic pressure and led to decreasing the water flux [50-52]. The rejection of the FO membrane led to potassium ion (K^+) in the feed being enriched because

positive charge of K^+ may also diffuse into the DS [43]. On the other hand, found the phosphorus concentrate gradually increased when the influent loading higher but can maintain the efficiency removal to 100% in L1 and L3 of TFC-FO and 99%, 100% and 88% in L1-L3 of CTA-FO, respectively which can regard as very high phosphorus removal. In other words, the effect from FO membrane size sieving is suitable for most organic and phosphate rejection [53 and 54]

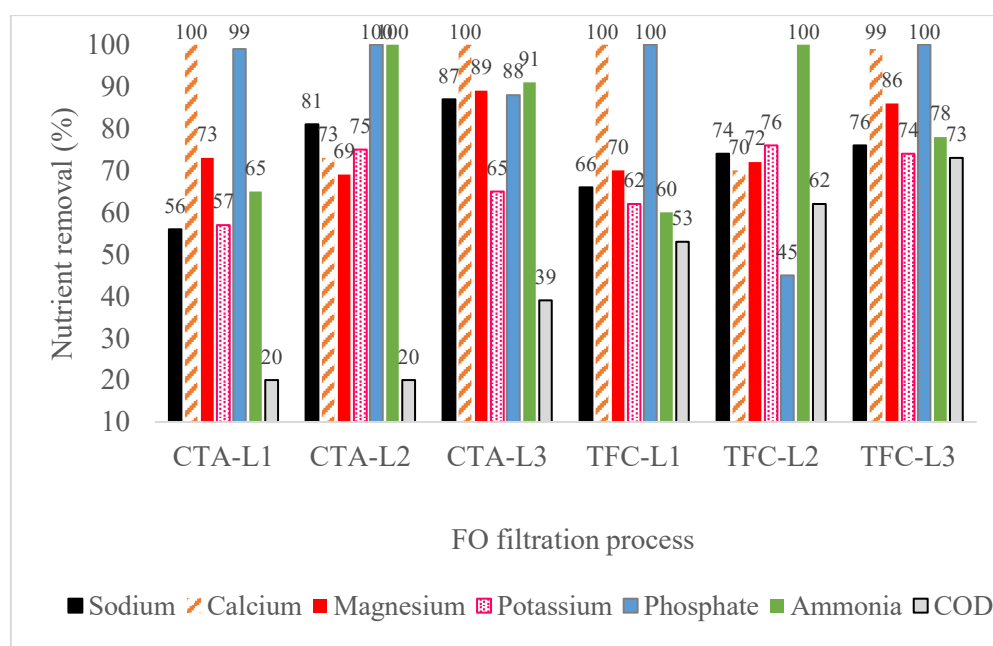


Figure 3 Nutrient removal efficiencies in FO filtration process with TFC membrane and CTA membrane in loading 1 (L1), loading 2 (L2) and loading 3 (L3)

Previous studies in **Table 3** have shown the nutrient removal efficiency and water flux in CTA-FO membranes are less than TFC-FO membranes. Jafarinejad et al. [26] shown that membrane surface charges holds the key to this contaminant rejection. For instance, highly negatively charged in TFC-FO membrane was higher the nitrate rejection ratio. Whereas, CTA-FO membrane was better of ammonia rejection ratio because of CTA has a slight negative charge [55]. In addition, FO process of T-POME with aquaporin membrane (TFC-FO) using sodium chloride as the DS reported an average water flux of 5.9 LMH over 24 h. Also, recovery of phosphate and NH_3 were highly to 99-100% and 60-100%, respectively. In other works, Luo et al. [56] observed that ammonia nitrogen, TN and PO_4^{3-} removals of >90%, 60-80% and >90%, respectively meanwhile Schneider et al. [27] and Camilleri-Rumbau et al. [46] using the aquaporin Inside™ TFC-FO membranes reported >95.5% rejection of total ammonia nitrogen (TAN). The nutrient removal efficiency accomplished in this study has in line with **Table 3** reported of literature review where high of nitrogen and phosphorus removal by TFC-FO membrane

Table 2 Characteristics for FO experiment

Parameter	Feed solution			TFC FO membrane			CTA FO membrane		
	Load 1	Load 2	Load 3	Load 1	Load 2	Load 3	Load 1	Load 2	Load 3
COD (g/L)	37.52±3.10	48.21±4.96	55.06±4.15	25.25±5.10	38.21±10.25	48.56±8.59	9.24±2.05	11.70±5.89	26.49±2.15
Alkalinity(g/L)	3.3±0.10	4.38±0.12	5.45±0.08	25.42	21.78	23.18	18.37	22.48	25.91
Acidity(g/L)	2.49±0.59	3.65±0.50	4.48±0.13	19,999±256	19,596±128	19,999±374	16,789±165	19,482±229	19,779±896
Conductivity(mS/cm)	12.67	18.00	18.03	13.5	10.4	10.6	11.0	9.8	9.8
TDS (mg/L)	11,493±23.5	16,218±78.9	16,235±58.6	23.24±2.12	41.02±4.15	76.66±7.52	24.10±5.2	49.00±1.51	91.58±4.68
Salinity (ppt)	12.3	10.1	10.5	3,635	2,520	2,265	2,945	2,600	2,658
Ammonia (mg/L)	30.49±1.15	30.52±3.07	81.06±5.10	9.439	8.294	4.257	8.954	8.156	5.660
Na⁺ (mg/L)	4,337	2,679	2,446	35.39	32.93	44.09	35.16	29.65	46.58
Ca⁺ (mg/L)	4.941	9.315	3.55	2,234	2,301	2,233	1,954	2,155	2,005
Mg⁺ (mg/L)	39.37	35.71	42.13	8.386	4.394	20.862	7.355	9.725	17.935
K⁺ (mg/L)	2,797	2,382	2,478	25.25±5.10	38.21±10.25	48.56±8.59	9.24±2.05	11.70±5.89	26.49±2.15
PO₄³⁻ (mg/L)	6.086	7.629	16.321	25.42	21.78	23.18	18.37	22.48	25.91

*ICP-OES AVIO500 (detection limit of Na = 3 ppb, Ca = 0.02ppb, Mg = 0.1 ppb, K = 20 ppb and PO₄³⁻ =30 ppb)

The ion fluxes for the FO membrane tested revealed the following trend: K and salt concentration Na (CTA:1,954-2,155mg/L and 2,600-2,945mg/L; TFC: 2,233-2,301mg/L and 2,265-3,635mg/L) higher ions than Mg, Ca, PO₄³⁻ and ammonia due to the accumulation of salinity from leaked of Na⁺ ions from draw solution led to high salinity. However, the phosphate recovery efficiencies were minimally affected by the form of sludge (flocculated or granular)

Table 3 Comparative analysis of nutrient concentration (Na^+ , Ca^{2+} , Mg^{2+} , K^+ and PO_4^{3-} with various studies related to Forward Osmosis

Study	Membrane	Feed/Draw solution	Flux (LMH)	Final nutrient removal efficiency (Na^+ , Ca^{2+} , Mg^{2+} , K^+ , PO_4^{3-} , NH_3 and COD; %)
Current study	CTA (HTI)	T-POME /NaCl	5.19	56, 100, 73, 57, 99,65 and 20
			4.89	81, 73, 69, 75, 100,100 and 20
			5.62	87, 100, 89, 65, 88, 91 and 39
	TFC(Aquaporin)		6.33	66, 100, 70, 62, 100, 60 and 53
			6.31	74, 70, 72, 76, 45, 100 and 62
			5.08	76, 99, 86, 74, 100, 78 and 73
[28]	TFC-PA (HTI), TFC(Aquaporin)	Digested manure centrate/ NaCl	17.5	40% $\text{NH}_4\text{-N}$
[42]	CTA (HTI)	Municipal wastewater/NaCl	6	99.7% TP, 67.8% TN, 48% NH_3 and 99.8%COD
[44]	CTA (HTI)	Human urine/NaCl	6	95% TN, >99% $\text{NH}_4^+\text{-N}$ and >98% TOC
[45]	CTA (HTI) and TFC(Aquaporin)	Synthetic wastewater/NaCl	TFC=15 CTA=5	>90% NH_4 , 60-80% TN and >90% PO_4^{3-}
[46]	TFC(Aquaporin)	Cow digestate liquid fraction from a biogas plant /NaCl	4.4, 8.5 and 8.5	>95.5% $\text{NH}_4^+\text{-N}$
[47]	TFC (Toray Industry Inc)	Central Park WWTP / NaCl	19.92	COD, TP, $\text{NH}_4^+\text{-N}$, TN, of >97%, >98%, 70-73% and 73-76%, respectively
[57]	CTA (HTI)	Sewage from the aeration grit chamber of a municipal WWTP /NaCl	-	COD, $\text{NH}_4^+\text{-N}$, TN, TP of 18, 2.5, 2.8, 0.4 mg/L, respectively
[58]	TFC (Porifera Inc. California, USA)	Activated sludge from the aeration tank at Aalborg West WWTP/NaCl	1.7-20	P > 40 mg/L

3.4 Membrane fouling

SEM micrographs imaging in the top-surface and cross-section modes in TFC and CTA after filtration (fouled membrane) shown in **Figure 4-9**. A finger-like morphology area most of the polysulfone (PSf) support layer thickness, but the higher magnification micrograph (50 μ m) in **Figure 4b, 5 and 6** exposes a thin layer 1- to 2- μ m. A dense sponge-like morphology layer area found near the top surface of TFC membrane. **Figure 4a, 8 and 9** presents the specific structure of the CTA (HTI) in the cross-section that shows the area to be like a woven mesh embedded in a continuous polymer layer. The unique CTA FO is that lack of a thick support layer in structure. The RO test with DI water found no change of morphology of TFC FO and CTA FO membrane the was observed with SEM micrographs imaging.

SEM micrographs imaging in the top-surface and cross-section modes in TFC and CTA after filtration (fouled membrane) shown the top layer was arrangement of nutrients clusters and EDX analysis confirms that the recovered solids contain phosphorus, potassium and magnesium (TFC: 13.3, 5.1 and 10.7; CTA: 4.3, 0.1 and 1.5, respectively) **Figure5-8**. The foulant of sludge found in the active layer meanwhile also found NaCl (DS) in support layer [10]. The identification of carbon, oxygen, and magnesium in the solids on the top-surface membrane can be indicated by the incorporation of organic matter, covering the precipitation of magnesium in the solids on the surface membrane. The possibility of diffusion of organic matter from the feed side to DS thus led to a slightly fouled in the draw side of the membrane. The accumulation of salinity from leaked of Na⁺ ions from draw solution led to high salinity **Figure5-8** at the same time affected to the resistance water was increased then caused to fouling [39]. The positive charge of potassium ion in L1, L2 and L3 of TFC and CTA shown 2,234, 2,301 and 2,233 and 1,954, 2,155 and 2,005 mg/L, respectively (**Table2**) may be spread into the DS also indicated the propensity of pore plugging or fouling of membrane surfaces [44, 49 and 50] **Figure5-8**. Otherwise, the membrane fouling layer and accumulated salinity in the mixed liquor since 180 min up reduced adequate osmotic pressure and increased the resistance for water passage. The thicker cake layer of CTA membrane fouling in **Figure6** related to Cartinella et al. [46] reported the negative charge in CTA membrane caused to easily attached ammonia ion on the surface membrane that higher fouling layer than TFC membrane.

Nevertheless, carbon, oxygen and sodium peaks were detected on the surface of the virgin membrane (**Figure5 and 7**) which related in Li et al. [28]. As **Figure6 and 8** illustrates, show the resulted of foulant after long term operation in form element component; C, O, P, Mg, Na, K, Cl, S, Si appeared on the fouled membrane surface. The strong phosphorus and magnesium peaks were found in TFC while phosphorus and calcium peaks were found in CTA surface membrane. The concentrated diffusion of cations, especially Ca₂⁺, enhanced the overpass for EPS network, a cake layer formed on the membrane's active layer [59-60].

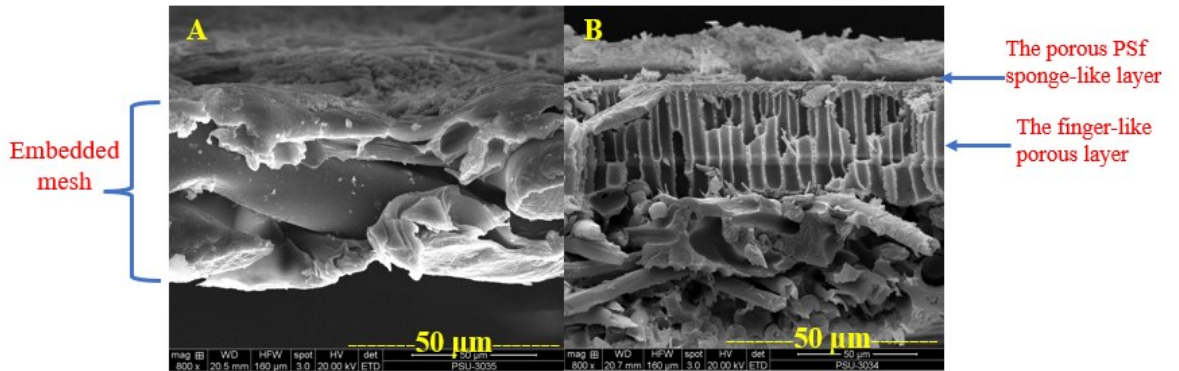


Figure 4 Cross-section SEM micrographs of (A) CTA-HTI fouled membrane and (B) TFC aquaporin fouled membrane

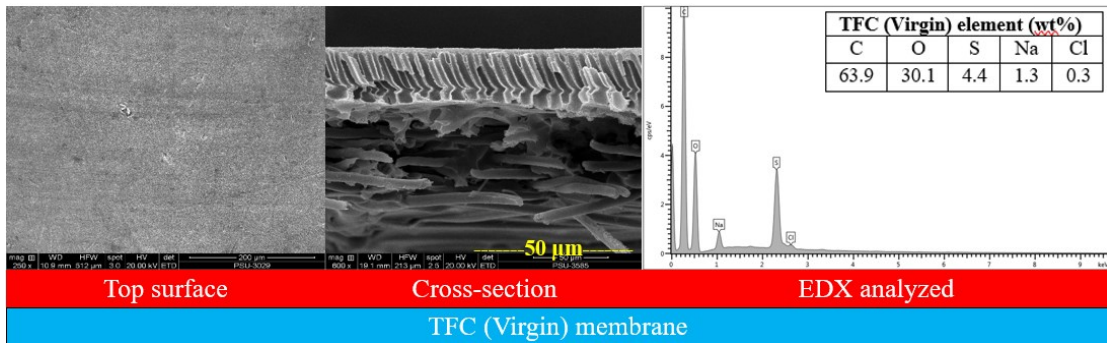


Figure 5 SEM micrographs of the top-surface and cross-section modes for TFC virgin membrane and the element component by EDX of membrane

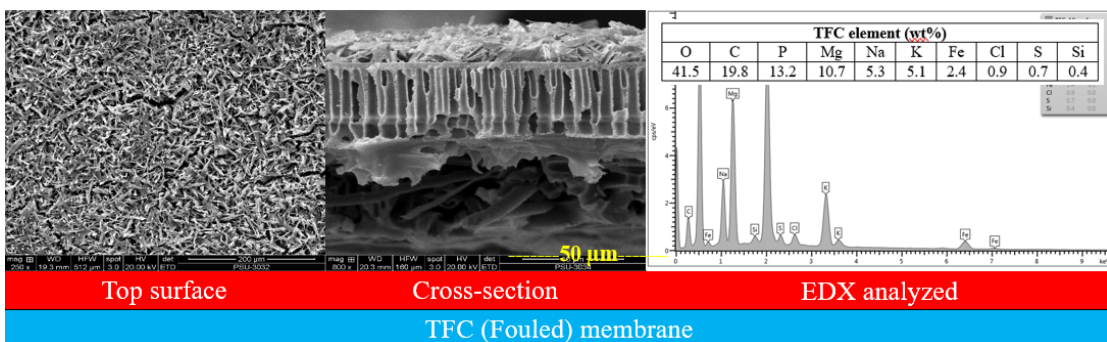


Figure 6 SEM micrographs of the top-surface and cross-section modes for TFC fouled membrane and the element component by EDX of membrane

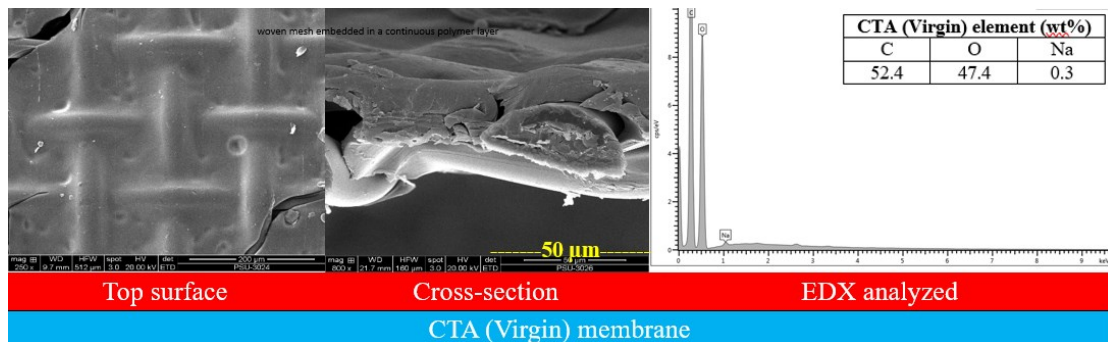


Figure 7 SEM micrographs of the top-surface and cross-section modes for CTA virgin membrane and the element component by EDX of membrane

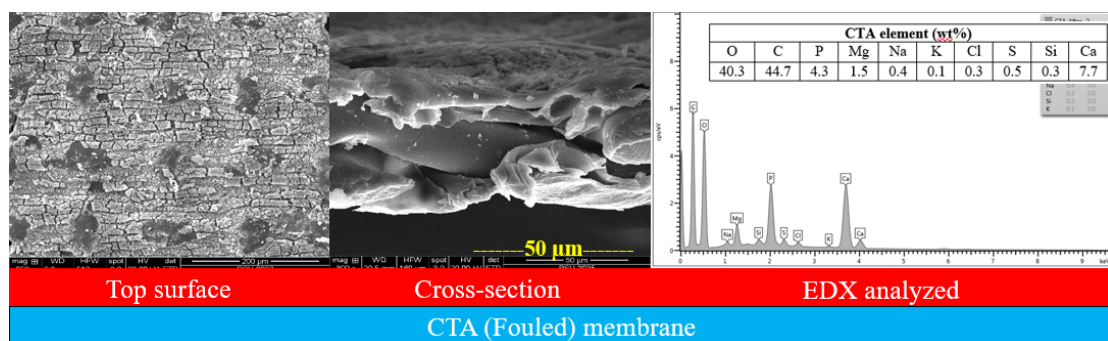


Figure 8 SEM micrographs of the top-surface and cross-section modes for CTA fouled membrane and the element component by EDX of membrane

4. Conclusion

1. The increase of organic loading rate led to high concentrate salinity because its accumulation and effected to nitrification process.
2. The PO_4^{3-} and ammonia removal is effective in TFC-FO and CTA-FO up to 90-100% thus FO capability can recovery nutrient and reduced chemical cost.
3. The leaked Na^+ ions from the draw solution led to high salinity that increased the resistance water and caused fouling.
4. The concentrated diffusion of Ca_2^+ ion in CTA, enhanced the overpass for EPS network; a cake layer formed on the membrane's active layer.
5. Two main mechanisms to cause of FO membrane fouling are cake layer formation from nutrient and accumulation of salinity especially draw solution diffusion.
6. The complex composition of wastewater (POME) may be cause of increasing fouling mechanism (nutrient, organic, etc.) or differentiation chemical reaction in fouling (sludge).

The efficient removal of nutrients with two-stage sAnMBR and FO treatment depends on the properties of the compounds of wastewater (POME) and the operational parameters of both system (**Figure9**)

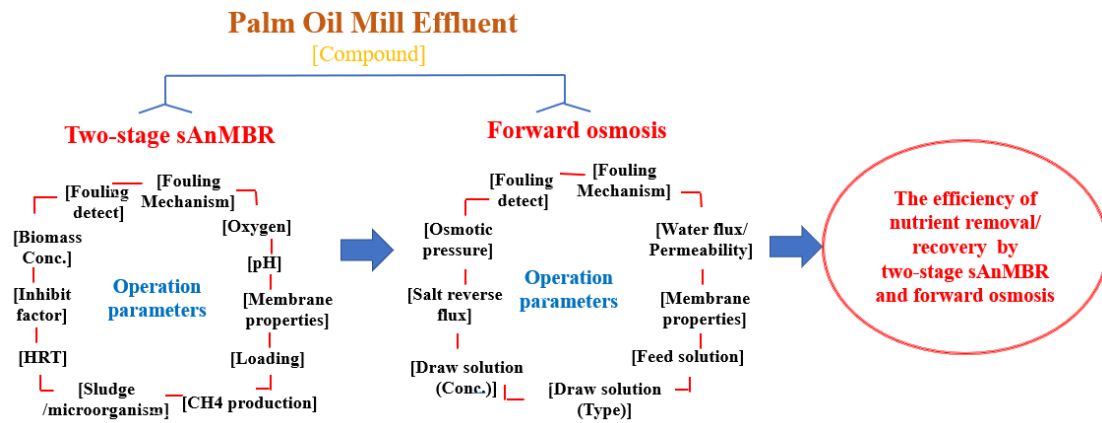


Figure9 The most important factors affecting the nutrient removal in the FO process

Acknowledgement

The research was financially supported by the Thailand Research Fund (TRF) and Tha Chang Palm Oil Industries, Co., Ltd. through a Research and Researcher for industries (RRi) under contract number "PHD58I0056". The authors would like to thank Center of Excellence in Membrane Science and Technology and Department of Civil and Environmental Engineering, Faculty of Engineering, Prince of Songkla University for partial support of this study.

References

- [1] R. Dusseldorp, Industry outlook, *Des. Eng.* 63 (2017) 30–31.
- [2] U. Hasanudin, R. Sugiharto, A. Haryanto, T. Setiadi, K. Fujie, Palm oil mill effluent treatment and utilization to ensure the sustainability of palm oil industries, *Water Sci. Technol.* 72 (2015) 1089–1095. <https://doi.org/10.2166/wst.2015.311>.
- [3] R. Kaewmai, A. H-Kittikun, C. Suksaroj, C. Musikavong, Alternative technologies for the reduction of greenhouse gas emissions from palm oil mills in Thailand, *Environ. Sci. Technol.* 47 (2013) 12417–12425. <https://doi.org/10.1021/es4020585>.
- [4] W.P. Wah, N.M. Sulaiman, M. Nachiappan, B. Varadaraj, Pre-treatment and membrane ultrafiltration using treated palm oil mill effluent (POME), *Songklanakar J. Sci. Technol.* 24 (2002) 891–898.
- [5] Department of Industrial Works, Standards for effluent of factory wastewater, Ministry of Industry announcement, (2018) 11–15. <http://www.diw.go.th/hawk/news/11.PDF>.
- [6] M. Abdulsalam, H.C. Man, A.I. Idris, K.F. Yunos, Z.Z. Abidin, Treatment of palm oil mill effluent using membrane bioreactor: Novel processes and their major drawbacks, *Water (Switzerland)*. 10 (2018). <https://doi.org/10.3390/w10091165>.
- [7] S.P. Tan, H.F. Kong, M.J.K. Bashir, P.K. Lo, C.D. Ho, C.A. Ng, Treatment of palm oil mill effluent using combination system of microbial fuel cell and anaerobic membrane bioreactor, *Bioresour. Technol.* 245 (2017) 916–924. <https://doi.org/10.1016/j.biortech.2017.08.202>.
- [8] W. Xue, T. Tobino, F. Nakajima, K. Yamamoto. Seawater-driven forward osmosis for enriching nitrogen and phosphorous in treated municipal wastewater: effect of membrane properties and feed solution chemistry, *Water Resour.* (2015). 69, 120-130.
- [9] N.S. Azmi, K.F.M. Yunos, Wastewater Treatment of Palm Oil Mill Effluent (POME) by Ultrafiltration Membrane Separation Technique Coupled with Adsorption Treatment as Pre-treatment, *Agric. Agric. Sci. Procedia.* 2 (2014) 257–264. <https://doi.org/10.1016/j.aaspro.2014.11.037>.
- [10] N.C.Nguyen, S.S.Chen, H.Y.Yang, N.T. Hau, Application of forward osmosis on dewatering of high nutrient sludge, (2013). *Bioresour. Technol.* 132, 224-229
- [11] F.Volpin, H. Heo, J. Hasan, M.A. Cho, J. Phuntsho, S. Shon, H.K, Techno-economic feasibility of recovering phosphorous, nitrogen and water from diluted human urine via forward osmosis. (2019). *Water Res.* 150, 47-55.
- [12] S. Jafarinejad, A framework for the design of the future energy-efficient, costeffective, reliable, resilient and sustainable full-scale wastewater

- treatments plants, (2020). *Curr. Opin. Environ. Sci. Health*. 13, 91-100.
- [13] W. Jiang, L. Lin, S.M.H. Gedara, T.M. Schaub, J.M. Jarvis, X. Wang, X.Xu, N. Nirmalakhandan, P. Pei Xu, Potable-quality water recovery from primary effluent through a coupled algal-osmosis membrane system, (2020). *Chemosphere* 240, 124883.
- [14] L. Li, W. Shi, S. Yu, Research on forward osmosis membrane technology still needs improvement in water recovery and wastewater treatment, *Water (Switzerland)*. 12 (2020) 1–27. <https://doi.org/10.3390/w12010107>.
- [15] Y. Ding, Y. Tian, Z. Li, F. Liu, H. You, Characterization of organic membrane foulants in a forward osmosis membrane bioreactor treating anaerobic membrane bioreactor effluent, *Bioresour. Technol.* 167 (2014) 137–143. <https://doi.org/10.1016/j.biortech.2014.06.033>.
- [16] M. Xie, H.K. Shon, S.R. Gray, M. Elimelech, Membrane-based processes for wastewater nutrient recovery: Technology, challenges, and future direction, *Water Res.* 89 (2016) 210–221. <https://doi.org/10.1016/j.watres.2015.11.045>.
- [17] S. Phuntsho, J.E. Kim, M.A.H. Johir, S. Hong, Z. Li, N. Ghaffour, T.O. Leiknes, H.K. Shon, Fertiliser drawn forward osmosis process: Pilot-scale desalination of mine impaired water for fertigation, *J. Memb. Sci.* 508 (2016). <https://doi.org/10.1016/j.memsci.2016.02.024>.
- [18] L. Huang, D.J. Lee, J.Y. Lai, Forward osmosis membrane bioreactor for wastewater treatment with phosphorus recovery, (2015). *Bioresour. Technol.* 198, 418-423.
- [19] G. Qiu, Y.M. Law, S. Das, Y.P. Ting. Direct and complete phosphorus recovery from municipal wastewater using a hybrid microfiltration-forward osmosis membrane bioreactor process with seawater brine as draw solution. (2015). *Environ. Sci. Technol.* 49 (10), 6156-6163.
- [20] T. Husnain, B. Mi, R. Riffat. A combined forward osmosis and membrane distillation system for sidestream treatment. (2015). *Water Resour. Protect.* 7, 1111-1120.
- [21] S. Jafarinejad and S.C. Jiang. Current technologies and future directions for treating petroleum refineries and petrochemical plants (PRPP) wastewaters. (2019). *Environ. Chem. Eng.* 7 (5), 103326.
- [22] M.A. Hafiz, A.H. Hawari, A. Altaee. A hybrid forward osmosis/reverse osmosis process for the supply of fertilizing solution from treated wastewater. (2019). *Water Process Eng.* 32, 100975.
- [23] C. Schneider, R.S. Rajmohan, A. Zarebska, P. Tsapekos, C. Helix-Nielsen. Treating anaerobic effluents using forward osmosis for combined water purification and biogas production. (2019). *Sci. Total Environ.* 647, 1021-1030.
- [24] Y. Li, Z. Xu, M. Xie, B. Zhang, G. Li, W. Luo. Resource recovery from

- digested manure centrate: comparison between conventional and aquaporin thin-film composite forward osmosis membranes. (2020). *Membr. Sci.* 593, 117436.
- [25] J.L. Soler-Cabezas, J.A. Mendoza-Roca, M.C. Vincent-Vela, M.J. Luján-Facundo, L. Pastor-Alcaniz. Simultaneous concentration of nutrients from anaerobically digested sludge centrate and pretreatment of industrial effluents by forward osmosis. (2018). *Separ. Purif. Technol.* 193, 289-296.
- [26] S. Jafarinejad, H. Park, H. Mayton, S.L. Walker, S.C. Jiang. Concentrating ammonium in wastewater by forward osmosis using a surface modified nanofiltration membrane. (2019). *Water Res. Technol.* 5, 246-255.
- [27] C. Schneider, R.S. Rajmohan, A. Zarebska, P. Tsapekos, C. Helix-Nielsen. Treating anaerobic effluents using forward osmosis for combined water purification and biogas production. (2019). *Sci. Total Environ.* 647, 1021-1030.
- [28] Y. Li, Z. Xu, M. Xie, B. Zhang, G. Li, W. Luo. Resource recovery from digested manure centrate: comparison between conventional and aquaporin thin-film composite forward osmosis membranes. (2020). *Membr. Sci.* 593, 117436.
- [29] L.A. Handojo, K. Khoiruddin, A.K. Wardani, A.N. Hakim, I G. Wenten. Advancement in forward osmosis (FO) membrane for concentration of liquid foods. (2019) *IOP Conf. Ser.: Mater. Sci. Eng.* 547 012053.
- [30] Q. Ge, M. Ling, T.S. Chung. Draw solutions for forward osmosis processes: Developments, challenges, and prospects for the future. (2013). *Membr. Sci.*, 442, 225–237.
- [31] S. Phuntsho, H.K. Shon, S. Hong, S. Lee, S. Vigneswaran. A novel low energy fertilizer driven forward osmosis desalination for direct fertigation: Evaluating the performance of fertilizer draw solutions. (2011). *Membr. Sci.*, 375, 172–181.
- [32] F. M. Munshi, J.-H. Hwang, S. Stoll and W.H. Lee. Reverse Salt Flux Effect on Dewatering *Chlorella vulgaris* in a Forward Osmosis System. (2023). *Water*, 15(8), 1462; <https://doi.org/10.3390/w15081462>
- [33] W. Ye, H. Madsen, J. Lin, E. G Sogaard. Enhanced performance of a biomimetic membrane for Na_2CO_3 crystallization in the scenario of CO_2 capture. (2016). *Membrane Sci.* 498, 75–85.
- [34] W. Y. Chia, K. S. Khoo, S. R. Chia, K. W. Chew, G. Y. Yew, Y.-C. Ho, P. L. Show and W.-H. Chen. Factors Affecting the Performance of Membrane Osmotic Processes for Bioenergy Development. (2020). *MDPI-Energies*, 13, 481.
- [35] Y. Zhao, X. Li, J. Wei, J. Torres, A.G. Fane, R. Wang, C.Y. Tang. Optimization of Aquaporin Loading for Performance Enhancement of Aquaporin-

- Based Biomimetic Thin-Film Composite Membranes. (2022) *Membranes*, 12, 32.
- [36] Z. Li, R. V. Linares, S. Bucs, L. Fortunato, C. H.-Nielsen, J. S. Vrouwenvelder, N. Ghaffour, T. O. Leiknes, G. Amy. Aquaporin based biomimetic membrane in forward osmosis: Chemical cleaning resistance and practical operation. (2017). *Desalination*, 420, 208-215.
- [37] M. P. Ayach, Empresa. Comparison of CTA and TFC FO-membranes for water recovery. Institució: Laboratori d'Enginyeria Química i Ambiental. Data de dipòsit de la memòria a secretaria de coordinació: Dimecres, 19 de Juliol de 2017.
- [38] W. Suwaileha, N. Pathakb, H. Shonp, N. Hilala. Forward osmosis membranes and processes: A comprehensive review of research trends and future outlook College of Engineering, Swansea University, Swansea, SA1 8EN, UK. (2020). *Desalination* 485(7).
- [39] W. Maknakorn, P. Jutaporn, W. Khongnakorn, Coagulation and adsorption as pretreatments of thin-film composite-forward osmosis (TFC-FO) for ink printing wastewater treatment, *Water Sci. Technol.* 79 (2019) 877–887.
- [40] Y.C. Woo, Y. Kim, W.-G. Shim, L.D. Tijing, M. Yao, L.D. Nghiem, J.-S. Choi, S.-H. Kim, H.K. Shon, Graphene/PVDF flat-sheet membrane for the treatment of RO brine from coal seam gas produced water by air gap membrane distillation, *Journal of Membrane Science*, 513 (2016) 74-84.
- [41] M. Xiao, F. Yang, S. I'm, D. S. Dlamini, D. Jassby, S. Mahendra, R. Honda, E. M.V. Hoek, Characterizing surface porosity of porous membranes via contact angle measurements, *Membrane Science Letters*. 2(1), (2022), 100022.
- [42] H. T. Nguyen, N. C. Nguyen , S.-S. Chen, H. H. Ngo, W. Guo, C.-W. Li. A new class of draw solutions for minimizing reverse salt flux to improve forward osmosis desalination. (2015). *Science of The Total Environment*. 538, 129-136.
- [43] Q. Wang, Z. Zhou, J. Li, Q. Tang, Y. Hu, Modeling and measurement of temperature and draw solution concentration induced water flux increment efficiencies in the forward osmosis membrane process, 452 (2019). *Desalination* 75–86.
- [44] J.Y. Li, Z.Yi Ni, Z.Y. Zhou, Y.X. Hu, X.H. Xu, L.H. Cheng, Membrane fouling of forward osmosis in dewatering of soluble algal products: Comparison of TFC and CTA membranes, 552, (2018), *Membrane Science*. 213-221.
- [45] Q. Liu, C. Liu, L. Zhao, W. Ma, H. Liu, J. Ma. Integrated forward osmosis membrane distillation process for human urine treatment. (2016). *Water Res.* 91,45-54.
- [46] M.S. Camilleri-Rumbau, J.L. Soler-Cabezas, K.V. Christensen, B. Norddahl,

- J.A. Mendoza-Roca, M.C. Vincent-Vela. Application of aquaporin-based forward osmosis membranes for processing of digestate liquid fractions. (2019). *Chem. Eng. J.* 371, 583-592.
- [47] J.E. Kim, J. Kuntz, A. Jang, I.S. Kim, J.Y. Choi, S. Phuntsho, H.K. Shon. Technoeconomic assessment of fertiliser drawn forward osmosis process for greenwall plants from urban wastewater. (2019). *Process Saf. Environ. Protect.* 127, 180-188.
- [48] J. Driver, D. Lijmbach, I. Steen. Why recover phosphorus for recycling, and how? (1999). *Environ. Technol.* 20, 651–662.
- [49] S. Loeb, L. Titelman, E. Korngold, J. Freiman. Effect of porous support fabric on osmosis through a Loeb-Sourirajan type asymmetric membrane. (1997) *Member. Sci.* 129, 243–249.
- [50] B. Kim, S. Lee, S. Hong, A novel analysis of reverse draw and feed solute fluxes in forward osmosis membrane process, 352 (2014), *Desalination* 128–135.
- [51] S. Jafarnejad, Forward osmosis membrane technology for nutrient removal/recovery from wastewater: Recent advances, proposed designs, and future directions. (2021) *Chemosphere*, 128116.
- [52] X. Lu, C. Boo, J. Ma, M. Elimelech. Bidirectional diffusion of ammonium and sodium cations in forward osmosis: role of membrane active layer surface chemistry and charge. (2014). *Environ. Sci. Technol.* 48, 14369–14376.
- [53] E. Desmidt, K. Ghyselbrecht, Y. Zhang, L. Pinoy, B. Van der Bruggen, W. Verstraete, K. Rabaey, B. Meesschaert. Global phosphorus scarcity and full-scale P-recovery techniques: A review, (2015). *Crit. Rev. Environ. Sci. Technol.* 45, 336–384.
- [54] G. Qiu, Y.M. Law, S. Das, Y.P. Ting. Direct and complete phosphorus recovery from municipal wastewater using a hybrid microfiltration-forward osmosis membrane bioreactor process with seawater brine as draw solution. (2015). *Environ. Sci. Technol.* 49, 6156–6163.
- [55] F. Kong, L. Dong, T. Zhang, J. Chen, C. Guo. Effect of reverse permeation of draw solute on the rejection of ionic nitrogen inorganics in forward osmosis: comparison, prediction and implications. (2018). *Desalination* 437, 144-153.
- [56] W. Luo, M. Xie, X. Song, W. Guo, H.H. Ngo, J.L. Zhou, L.D. Nghiem. Biomimetic aquaporin membranes for osmotic membrane bioreactors: membrane performance and contaminant removal. (2018). *Bioresour. Technol.* 249, 62-68.
- [57] Y. Gao, Z. Fang, P. Liang, X. Huang. Direct concentration of municipal sewage by forward osmosis and membrane fouling behavior. (2018). *Bioresour. Technol.* 247, 730-735.
- [58] M.K. Jørgensen, J.H. Sørensen, C.A. Quist-Jensen, M.L. Christensen. Wastewater treatment and concentration of phosphorus with the hybrid osmotic microfiltration bioreactor. (2018). *Membr. Sci.* 559, 107-116.

- [59] Z. Wang, J. Zheng, J. Tang, X. Wang, Z. Wu. A pilot-scale forward osmosis membrane system for concentrating low-strength municipal wastewater: performance and implications. (2016). *Sci. Rep.* 6, 21653.
- [60] X. Bao, Q. Wu, W. Shi, W. Wang, H. Yu, Z. Zhu, X. Zhang, Z. Zhang, R. Zhang, F. Cui. Polyamidoamine dendrimer grafted forward osmosis membrane with superior ammonia selectivity and robust antifouling capacity for domestic wastewater concentration. (2019). *Water Res.* 153, 1-10.

VITAE

Name Miss Wiparat Chaipetch

Student ID 6310130011

Educational Attainment

Degree	Name of Institution	Year of Graduation
Bachelor of science (Industrial Environmental Management)	Prince of Songkla University	2006
Master of science (Environmental Management)	Prince of Songkla University	2008

Scholarship Awards during Enrolment

The research was financially supported by the Thailand Research Fund (TRF) and Tha Chang Palm Oil Industries, Co., Ltd. through a Research and Researcher for industries (RRi)

List of Publication and Proceeding

Publication

- W. Chaipetch, W. Khongnakorn, C. Yirong, J. Boonkan and M.Heran. (2022) Performances of High Rate Two-Stage AnMBR for Palm Oil Mill Effluent Treatment. *BioResource*,17(2), 3398-3412.
<https://doi.org/10.15376/biores.17.2.3398-3412>
- W. Chaipetch, A. Jaiyu, P. Jutaporn, M. Heran and W.Khongnakorn. (2021) Fouling Behavior in a High-Rate Anaerobic Submerged Membrane Bioreactor (AnMBR) for Palm Oil Mill Effluent (POME) Treatment. *Membrane*,11, 649.
<https://doi.org/10.3390/membranes11090649>